An Experimental Investigation of the Influence of Mechanical Damage and Rust on the Ability of Flame Gaps to Prevent Hydrogen Gas Explosion Transmission

Linn Ringdal

A thesis submitted in partial fulfillment of the requirements
for the degree of Master of Science in the subject of Physics;
Process Safety Technology

Department of Physics and Technology
University of Bergen
Bergen, Norway
June 2012

Preface

This thesis is a mandatory part that must be completed to obtain a Master of Science degree at the University of Bergen. The thesis is based on experimental research carried out in the Gas Explosion Laboratory at the Department of Physics and Technology, University of Bergen (UoB).

The experimental work requires that all equipment must be available and that the various components of all devices must operate at the desired time of use. The Mechanical workshop has designed special slits for the experimental apparatus, and also created other special parts in order to implement the experiments as realistic as possible. A special thanks to Leif Egil Sandnes, who has the honor of providing optimal corrosion conditions for the slits over the desired time period.

A big thank you also goes out to Werner Olsen (Chief Engineer at the Department of Physics and Technology) for his technical computer knowledge that contributed to the setup of temperature measurement in LabView, which made it possible to perform temperature measurements. I will also express my appreciation to Professor Harald Høiland who have contributed with chemical information and helped me understand the chemistry around the issues this thesis covers.

I want to express my gratitude to those persons who have guided and motivated me throughout the work in this thesis. First of all I want to thank my supervisor Associate Professor Bjørn J. Arntzen for support and interesting discussions of the work, and Professor Rolf K. Eckhoff for his enthusiasm and interest in the field, and also for the educational discussions. I am also grateful for the talented and helpful fellow students of mine, especially Marianne Winnes Steiner, who are always ready for a discussion. Thanks to former master students who introduced me to the topic this thesis concerns.

I also want to thank my friends and my training environment, which made it possible for me to take my mind away from schoolwork when it was needed. Thanks to Truls who is such a caring person for my mother and I. I will also give a special thanks to my dear Petter Tresselt Iversen for his encouragement through my whole studies.

Finally I must thank my mother Nina Ringdal who has always supported me, always wanted the best for me, and always been present when it was most important. Her fantastic being, hilarious humor, and great cooking make my everyday life easier and better. She is my biggest inspiration in life.

Bergen 1. June 2012

Linn Ringdal

Department of Physics and Technology
University of Bergen
Norway

Abstract

The present work investigates the influence of rusted and mechanical damaged flame gaps, and the ability of these flame gaps to prevent a hydrogen gas explosion transmission between an inner and outer explosion chamber. An explosion chamber intended for preventing such an explosion transmission between an inner and outer explosive atmosphere is called an Ex'd' enclosure. In the industry there are many potential ignition sources that could be a threat in an explosive atmosphere, as an explosion may occur if being ignited. Ex'd' enclosures are designed to surround the potential ignition sources and to protect a possible internal explosion from spreading to the outer environment.

Ex'd' enclosures have certain design requirements specified in the international standards IEC. The design criteria that was examined in this work is (IEC 2007a)'s requirement which states that the mean surface roughness of the flame gap opening shall be less than 6.3 µm. The international standards also require that any damaged flame gap surface must be restored to the original state. However, the standards have no definition of what damages are considerable large enough for having to be restored to the original quality. As a result of this lack of guidance, even minor rust or mechanical damage of the flame gap surfaces must be repaired, which is a time consuming and expensive procedure.

The purpose of the present research is, due to the lack of damage ranking definition, to examine what effect different damages have on the safe gap. To be able to conclude about the importance and effect of the damage, one must have a characteristic value for each slit to compare the results. The characteristic value used in this work is the maximum experimental safe gap, MESG, which is a measure of the largest gap opening that does not generate a re-ignition on the outside of the Ex'd' enclosure. An increase in MESG value does therefore imply an increased efficiency of the safe gap. The MESG value is individual for each explosive gas, and will vary as the surfaces of the flame gaps are changed. Similar experiments have previously been performed with propane as the explosive gas, but the present work is carried out with hydrogen as the explosive gas.

The present work has also considered the effect of different time periods of rust formation. Six slits were set at sea side for one month and six others for two months. Rusted slits shall, according to the stardards, be restored to the initial state. But results show that corrosion

actually increases the efficiency of the safe gap. The efficiency of the safe gap also increases with increased rust formation on the slit's surfaces.

The mechanical damaged flame gaps were applied grooves of various depths and various widths to their surfaces. All grooves were crosswise, thus in the opposite direction of the gas flow that was being pushed through the opening by the internal explosion. The MESG values of the mechanical damaged slits turned out to be larger than the undamaged slits' MESG values, which refers to an increased efficiency of the safe gap.

The overall conclusion from this investigation is that damaged surfaces of flame gaps do not reduce the efficiency of the safe gap. Neither rusted nor significant mechanical damaged flame gap surfaces reduce the efficiency of the safe gap. In fact, improvements are observed in all cases. This indicates that the surface roughness requirements of the international standards which states that the mean surface roughness must be less than 6.3 µm, is an arbitrarily chosen value. It is also shown in this study that the temperature of the hot combustion gases is lower after they have penetrated through flame gaps with grooves, rather than after penetrating through an undamaged flame gap. The probability of generating a re-ignition in the secondary chamber through flame gaps with grooves is then decreased as a result of the lower temperature.

Table of Contents

1 Introduction

1.1 Background

Accidental explosions are the worst outcome for an industry where an explosive atmosphere may occur. Examples of these industries where explosion hazards have to be taken into special consideration include:

- Oil and natural gas industries: production on and offshore, refineries, transportation
- Petrochemical, chemical, and metallurgical process industries
- Mechanical processing
- Special processing: storage and handling of explosives, pyrotechnics, and propellants

An explosion can cause major equipment damage and injury, maybe even death, to humans. Focusing on safety in these industries is very important, not only with regard to the life and health of the employees, but also with regard to the finances of the company. Shutting down a manufacturing plant can cost several million per day, and is therefore an act that will be avoided if possible. Such an accidental explosion may also cause damage to the environment and to surrounding buildings and areas.

High safety standards were established all the way from the start of the development of oil and natural gas industry on the Norwegian continental shelf, but in 1988, the Piper Alpha catastrophe struck. Piper Alpha was an oil platform, and became well known for the catastrophic accident that killed 169 people in the UK North Sea. The reason was mainly human error. After this tragic incident, these strict security procedures in Norway gained wide international acceptance.

Understanding the process of the outcomes that lead to an accident is an important part of process safety technology. To achieve high safety standards and a low explosion risk, two terms are particularly important: probability and consequence. Risk is usually defined as the product of probability and consequence, and it is therefore of great interest to minimize both the probability that an accident will occur, and the consequence if the accident should occur.

One type of safety equipment for preventing accidental explosions is flameproof enclosures, with the abbreviation Ex'd'. This Ex'd' equipment is designed to hold potential ignition sources, among electrical equipment, so that if an explosion occur, the enclosure should be strong enough to withstand the explosion pressure built up inside it. Any holes or cracks in the enclosure are designed so that the explosion will not propagate any further into the plant.

1.2 Motivation

In year 1815, Sir Humphrey Davy started his research to create an explosion proof lamp for use in coal mines, where he knew explosive atmospheres could be formed. Since 1815, research on explosion safety has continued. About 100 years ago, research on explosion safe electrical equipment, such as Ex'd' flameproof enclosures, started. The concept of flameproof enclosures, Ex'd' equipment, is one of the oldest explosion protection methods for electrical apparatuses. It has constantly been improvements in safety methods for electric apparatuses, but there has also been an increase of potential hazards in the industry worldwide.

Figure 1.1 shows the hydrocarbon leaks on Norwegian installations the last years, and it can be seen that a great amount of hydrocarbon leakages above 0.1 kg/s did occur. (Vinnem 2006) writes in his research paper that each year there are about 5-6 hydrocarbon leaks in the Norwegian offshore industry at least the size of the Piper Alpha catastrophe. Prevention of accidental explosions as a result of leaks can be strengthened through both improved and better inspections and equipment. It is important for the process industry to implement good routine checks and maintenance on the electrical equipment, among them Ex'd' equipment, in process plants.

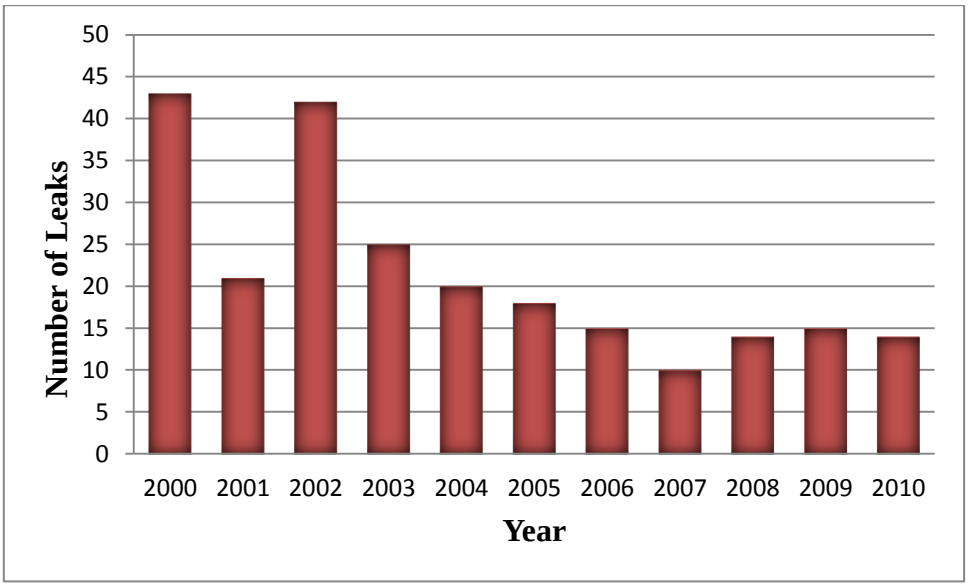

Figure 1.1 : *Hydrocarbon leaks on Norwegian installations in the period of 2000 to 2010. All leaks are above 0.1 kg/s. Based on values from (Petroleum Safety Authority Norway 2010).*

A great deal of the potential ignition sources in the industry are electrical apparatuses. In areas where an explosive atmosphere can occur, electrical apparatuses have to be isolated to avoid an ignition. One of these isolation methods is the flameproof enclosure, Ex'd', which prevents transmission of the explosion from the inside of the enclosure and to the surrounding atmosphere.

The international IEC standards are valid for Ex'd' equipment, and contains requirements for design and maintenance. When it comes to the joint surface, the only requirement is that the average surface roughness shall be less than 6.3μm. Since Ex'd' equipment often is used in

the offshore industry with a highly corrosive environment, rust is likely to be formed and thus be a potential damage on the apparatus. Damages on the joints can also occur during inspection by use of tools and poor handling by employees. This means that even the thinnest rust coating or the slightest damage leads to repair or overhaul of the flameproof enclosure. If these repair actions are unnecessary, major economic costs could be spared.

The aim of the experimental research in the present work has been to investigate the influence of highly rusted and severe damaged flame joints, and what affect this has on the ability to prevent transmission of an explosion. Similar work has previously been performed by (Opsvik 2010), (Grov 2010), and (Solheim 2010), who all studied how different damages on flame gap surfaces affected the safety of the flameproof enclosure. Various results and conclusions from previous work have contributed to make this extremely interesting research, and is a great motivation for more research on this topic.

2 Review of Relevant Literature

This chapter contains relevant and basic theory on topics that this thesis concerns. It also gives a review on important literature of previous work, and similar previous investigations are summarized.

2.1 Gas explosion

An explosion is defined in many different ways. (Eckhoff 2005) has a possible definition: "*An explosion is an exothermal chemical process that, when occurring at constant volume, gives rise to a sudden and significant pressure rise*". The fact that it is an exothermal reaction implies that it is a chemical reaction that generates and releases heat to the surroundings.

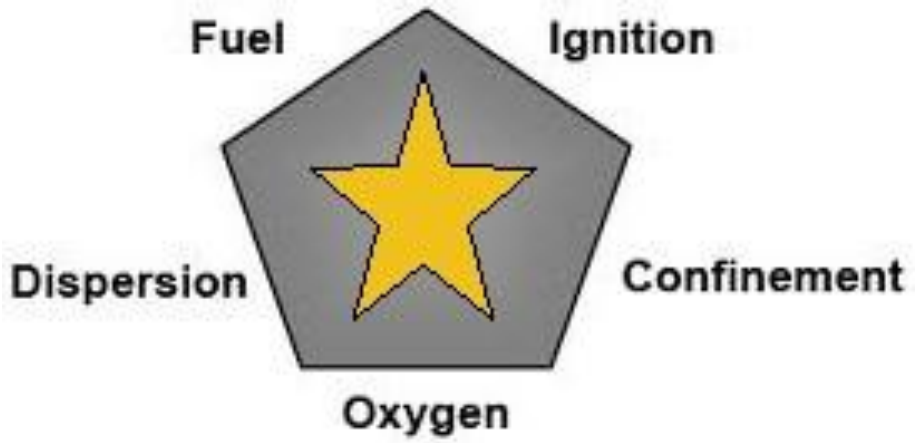

Figure 2.1 : *The explosion pentagon. From (Safety-Instruction 2010).*

As shown in Figure 2.1 all five factors fuel, ignition, confinement, oxygen, and dispersion have to be present for an explosion to take place. There is a real hazard connected to leakage of gas in the process industries, and this may lead to the formation of an explosive atmosphere. The key to avoid an explosion is to eliminate at least one of the five factors. If it is unlikely to avoid any of the five factors to occur, a method for preventing the explosion to spread should be used. One of these preventing methods is flameproof enclosure Ex'd', see Section 2.2.2.

All gases also have a certain concentration interval, known as the explosive range, within where they will explode. These limits are called LEL (Lower Explosion Limit) and UEL (Upper Explosion Limit). If the fuel with respect to oxygen ratio is too high (above UEL), combustion will not take place. The same principle applies below LEL, but in this region the fuel with respect to oxygen ratio is too low to be ignited.

Table 2.1: *Combustibility and ignitability parameters of some combustible gases and vapors in the air at atmospheric and normal temperature. From (Eckhoff 2005).*

Fuel	Flammable limits [vol. % in air]		Min. ign. temp.
	Lower	Upper	[°C]
Methane	5.0	15.0	540
Ethane	3.0	12.4	515
Propane	2.1	9.5	493
Ethylene	2.7	36.0	425
Acetylene	2.5	100	305
Hydrogen	4.0	75.0	560

Typical ignition sources can, as (Eckhoff 2005) states, be:

- Open flames
- Glowing or smoldering particles
- Hot surfaces
- Burning metal particles and “thermite” reactions
- Electrical and electrostatic sparks
- Jets of hot combustion gases
- Adiabatic compression
- Light radiation

The most hazardous explosion will occur at what is called the stoichiometric mixture. A stoichiometric mixture is where all the fuel is consumed upon the reaction.

The present work investigates re-ignitions ignited from a jet of hot combustion gases.

2.1.1 Physical and chemical properties of hydrogen

Hydrogen is the first element of the periodic system with atomic number 1, and is thus the lightest atom there is today. The gas is colorless, odorless, tasteless, non-toxic, and highly flammable. The fact that hydrogen atoms are small and light makes them highly diffusive,

which causes them to rapidly mix with other gases, for example air. Hydrogen has low viscosity and can therefore leak through minor holes and gaps.

Table 2.2 : *Viscosity and diffusivity of different gases at 1 atm and 0 °C. From (Air-Liquide 2009), (Energy 2009), and (Cussler 1997).*

Gas	Viscosity [cP]	Diffusivity [m^2/sec] x10^5
Hydrogen	0.0087	6.11
Ethylene	0.0095	3.00
Propane	0.0097	1.00
Methane	0.0103	1.60

Table 2.2 shows that hydrogen has the lowest viscosity value, and is therefore the most volatile gas. In addition to having the lowest viscosity value, it also has the smallest molecule size, which causes hydrogen to penetrate easily through small cracks and holes. Hydrogen's diffusivity value is also significantly higher compared to the other gases in Table 2.2, which describes how fast the hydrogen molecules mix with air.

A stoichiometric hydrogen-air mixture contains about 29.6 vol% hydrogen:

$$2H_2 + O_2 + \frac{79}{21}N_2 \xrightarrow{yields} 2H_2O + \frac{79}{21}N_2$$

$$Mol\ air\text{:}\quad 1molO_2 + \frac{79}{21}mol\ N_2 \approx 4.76\ mol\ air$$

$$Total\ mol\text{:}\quad 2molH_2 + 1mol\ O_2 + \frac{79}{21}mol\ N_2 \approx 6.76\ mol$$

$$Vol\% = mol\% = \frac{\#\ mol}{total\ \#\ mol} \cdot 100\%$$

$$Vol\%\ H_2 = \frac{2mol}{6.76mol} \cdot 100\% \approx 29.6\%$$

As shown in Table 2.1, hydrogen has a flammability range in air between 4 and 75 vol%. The flammability range for hydrogen is even wider in pure oxygen: from 4 to 95 vol%.

Hydrogen is highly reactive and is able to react with most other elements. The highly reactive factor causes the minimum ignition energy (MIE) of hydrogen to be 0.02 mJ, which is extremely low compared to other combustible gases.

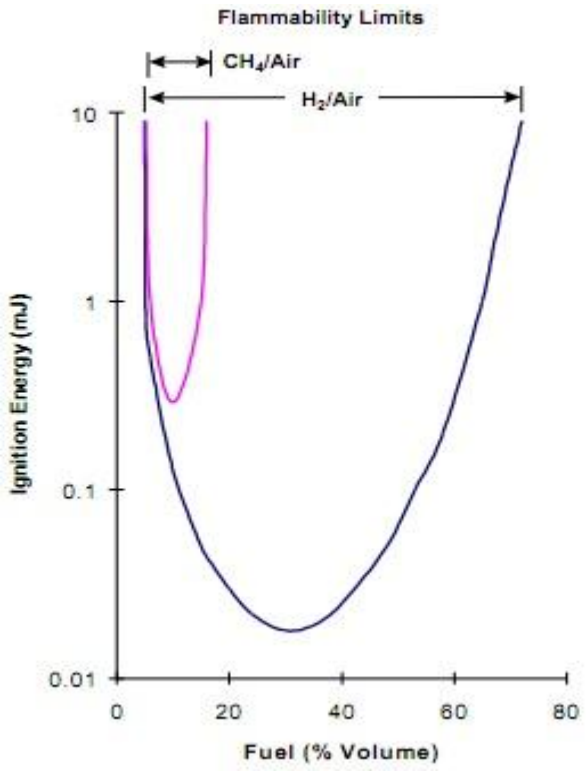

Figure 2.2 : *Minimum ignition energies. From (Alcock 2001).*

According to (M. Kröner 2003), the burning velocity of hydrogen in air in stoichiometric conditions is 2.55 m/s. The burning velocity reaches its maximum of 3.2 m/s at a hydrogen concentration of 40.1 % in air. This is shown in Figure 2.3, where λ is the vol% hydrogen divided by vol% air. λ is thus reaching its highest point at 0.67.

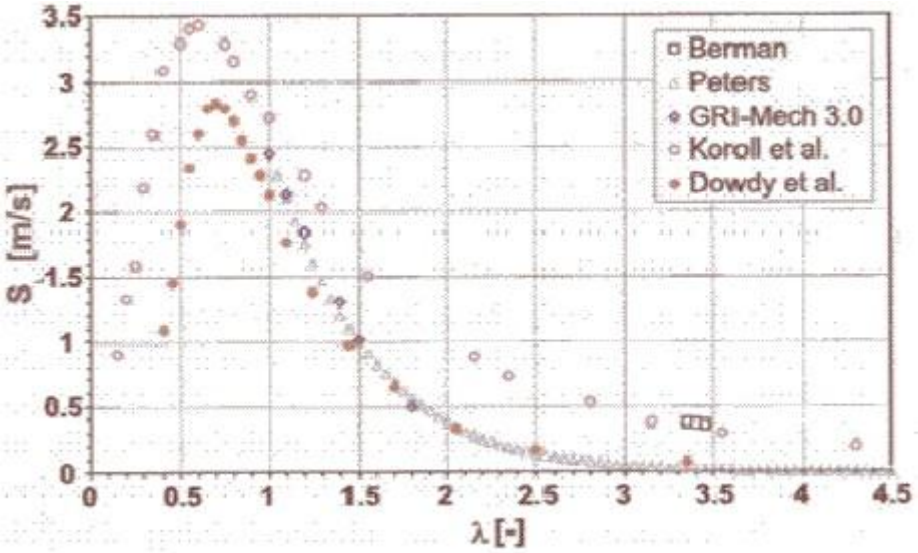

Figure 2.3 : *Burning velocities in hydrogen-air mixture. From (M. Kröner 2003).*

A chemistry calculator, made by (Dandy 2012), has been used for calculations of temperature values at given concentrations. Figure 2.4 shows a comparison of temperature and burning velocity, both as a function of hydrogen concentration in air. The temperature reaches its maximum value just above a concentration of 30 % hydrogen in air, while the burning velocity reaches its maximum at a concentration of 40 % hydrogen in air. The burning velocity depends on, among other factors, the diffusivity of the gas, which is the reason for hydrogen's high burning velocity, as the diffusivity of hydrogen is six times larger than the diffusivity of propane.

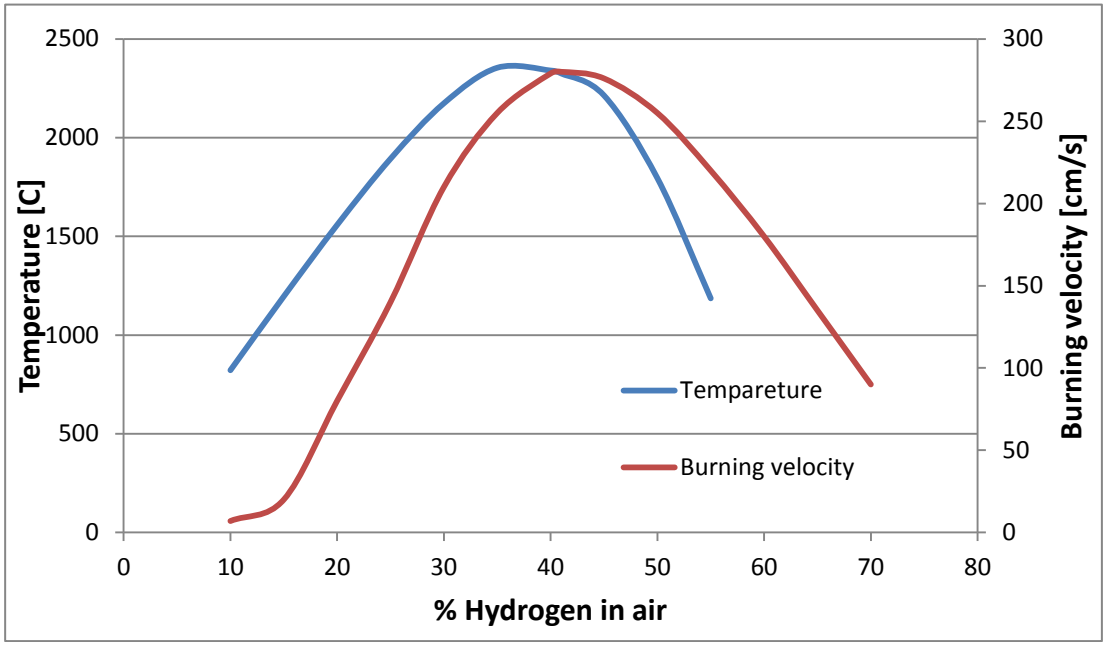

Figure 2.4 : *Temperature and burning velocity as a function of hydrogen concentration in air.*

The amount of hydrogen gas mixed in air also affects the explosion pressure ratio. (Cashdollar 2000) presented the data, see Figure 2.5, for initially quiescent hydrogen-air mixtures with spark ignition in a 120 L chamber. The explosion pressure ratios of pressure rise are plotted as a function of hydrogen concentration in air. The pressure ratio increases as the hydrogen concentration in air increases up to about the stoichiometric ratio, and then it starts to decrease. The pressure ratio can also be interpreted as a measure of how much the gas expands.

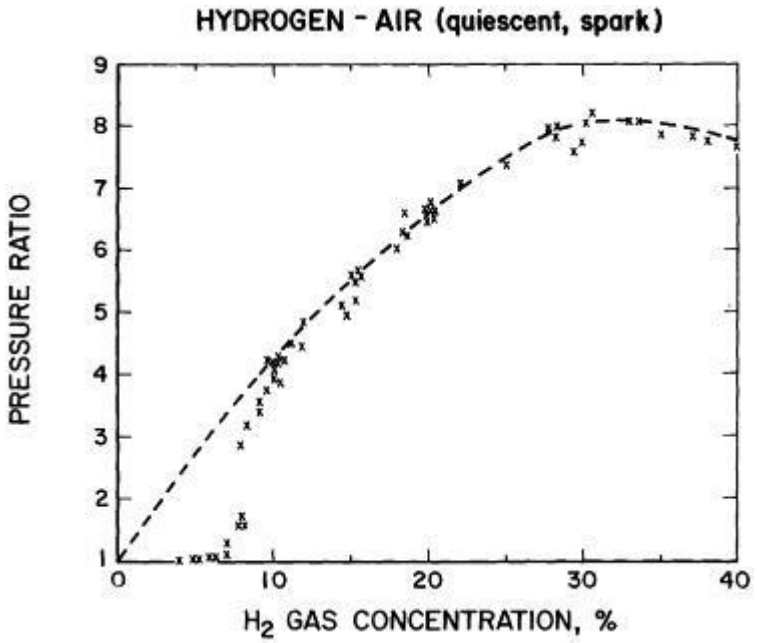

Figure 2.5 : *Flammability data for quiescent mixtures of hydrogen in air in a 120 L chamber, compared to dashed curve for calculated adiabatic values. From (Cashdollar 2000).*

Summarized comparison of hydrogen and propane

All previous research in the same detailed field as this thesis deals with, has been carried out with propane as the explosive gas. The present work is to be carried out with hydrogen as the explosive gas. It is therefore important to compare some key factors that may affect the results and conclusions of the present thesis. Table 2.3 shows some physical and chemical values of hydrogen and propane that may be of importance when the results shall be compared and discussed.

Table 2.3 : *Comparison of some physical and chemical properties of hydrogen and propane.*

	Hydrogen	**Propane**
Viscosity [cP]	0.0087	0.0097
Diffusivity [m^2/s] x 10^5	6.11	1.00
Minimum Ignition Energy [mJ]	0.02	0.3
Maximum Laminar Burning Velocity, S_u [cm/s]	325	40
Flammable Limits [vol% in air]	4.0 – 75.0	2.1 – 9.5

Table 2.3 provides a good overview of how much more reactive and thus how much more violent hydrogen gas can be compared to propane.

2.1.2 Area classification

Area classification is a term introduced to minimize the probability of accidental ignition of explosive atmospheres. The main philosophy is that there shall be stricter requirements for the safety equipment used in areas where the probability for an explosive atmosphere to occur is high, than for the equipment in areas where this probability is low.

(Eckhoff 2005) describes different zones or areas based on the probability of an explosive atmosphere to occur and the duration of the explosive atmosphere's presence. These are defined as follows:

- Zone 0:
  The part of a hazardous area in which a flammable atmosphere is continuously present or present for long periods

- Zone 1:
  The part of a hazardous area in which a flammable atmosphere is likely to occur in normal operation

- Zone 2:
  The part of a hazardous area in which a flammable atmosphere is not likely to occur in normal operation and, if it occurs, will exist only for a short period

- Non-hazardous areas:
  Areas that do not fall into any of the above zones are non-hazardous

2.2 Flameproof enclosures, Ex'd'

2.2.1 Historical review

The first case histories of accidental gas explosions took place during the 17th and 18th centuries as coal mining developed. The hazardous mixture of both methane gas and coal dust lead to explosions in the mines. As a light source they used an open flame, which of course ignited the explosive mixture, also called firedamp.

In 1815, Sir Humphrey Davy was asked to implement a research on the cause of ignition and flame propagation of the explosive mixture. Six months later, after having completed a comprehensive research of the chemical composition of the firedamp and after countless experiments, the "Davy lamp" was invented. The concept of the "Davy lamp" is that the lamp screen acts as a flame arrestor; the grid is so fine that it will not allow flames to propagate through it, but air can pass through the grid to continuously maintain combustion in the chamber.

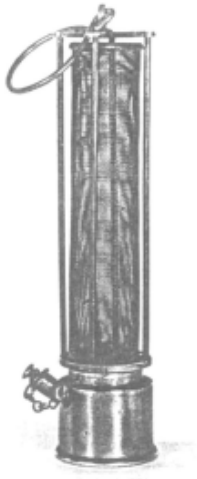

Figure 2.6: *Early version of the coal mine lamp developed by Sir Humphrey Davy about 1815. From (Eckhoff 2005).*

During the 19th century the development of electrical equipment and appliances increased rapidly, but this was not yet enough to manage to avoid explosions. Sparks from the electrical equipment was in fact a hazardous ignition source. To eliminate electric spark as an ignition source, electrical equipment was totally enclosed. This was the first step in the development of flameproof enclosures.

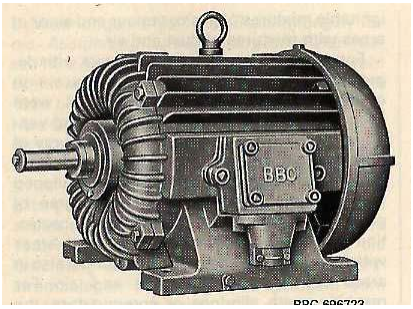

Figure 2.7: *An illustration of an early version of an enclosed electrical motor.*

To make sure that all Ex'd' equipment are within the required safety limits, an International Electrotechnical Commission, IEC, was established in 1906. The IEC is the world's international organization in its field. In 1973 Europe founded its own committee called European Committee for Electrotechnical Standardization, CENELEC (French: *Comité Européen de Normalisation Électrotechnique*). CENELEC is in charge of the European standardization. A Norwegian committee called Norsk Elektroteknisk Komite, NEK, was established in 1912. NEK is responsible for the electro technical standardization operations in Norway and is a member of both IEC and CENELEC.

2.2.2 Flameproof enclosures – an introduction of the concept

In the process industries there are a great number of electrical apparatuses to be used. All electrical apparatuses can be a possible ignition source for an explosive atmosphere. It is therefore very important to separate these potential ignition sources from the explosive gas clouds to avoid violent explosions.

(IEC 2011) defines a flameproof enclosure 'd' as an: "*enclosure in which parts which can ignite an explosive atmosphere are placed and which can withstand the pressure developed during an internal explosion of an explosive mixture and which prevents the transmission of the explosion to the explosive atmosphere surrounding the enclosure*".

As we can read from the definition of flameproof enclosures, the concept is to prevent an internal explosion from propagating to an external explosive atmosphere. The flameproof enclosure must therefore be strong enough to withstand the pressure rise caused by the internal explosion and prevent the explosion to be transmitted to the external atmosphere. According to (Eckhoff 2005) there are three main requirements the flameproof enclosure must satisfy:

- The gap widths have to be smaller than the MESG (maximal experimental safe gap, see Section 2.3.2) at actual conditions

- The enclosure must be able to withstand the maximum internal overpressure that an internal gas explosion can produce at actual conditions

- The temperature of the external enclosure surface must be below the minimum ignition temperature at actual conditions

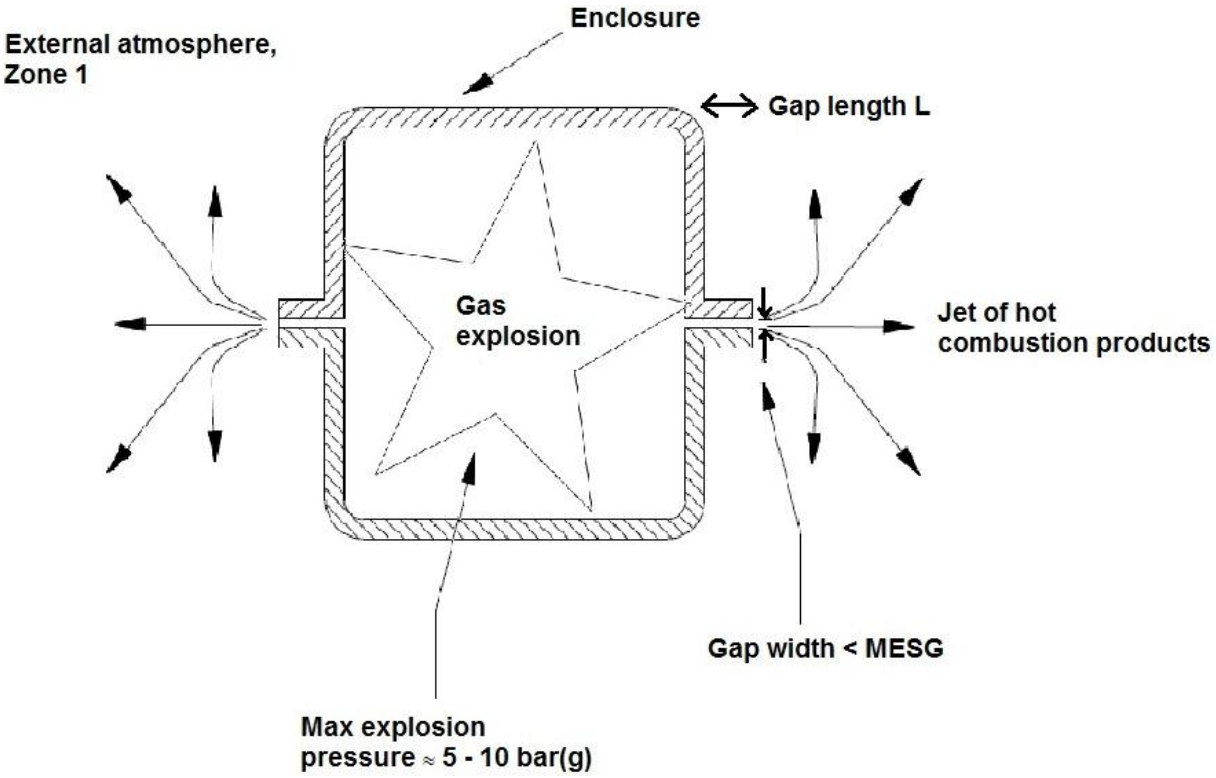

Figure 2.8: *Illustration of flameproof enclosure Ex'd' with an internal explosion.*

Flameproof enclosures are approved and may be used for both Zone 1 and Zone 2 areas. The equipment protection Ex'd' is used in for example:

- Transformers
- Motors
- Heating equipment
- Switchgear
- Light fittings etc.

The criteria the flameproof enclosure must achieve are described in detail and have to be in accordance to IEC requirements (IEC 2007a). One of the requirements is that joints shall have an average roughness less than 6.3 μm, see Figure 2.11.

Type of joint		Minimum width of joint *L* mm	Maximum gap mm											
			For a volume cm³ $V \leq 100$			For a volume cm³ $100 < V \leq 500$			For a volume cm³ $500 < V \leq 2\,000$			For a volume cm³ $V > 2\,000$		
			I	IIA	IIB	I	IIA	IIB	I	IIA	IIB	I	IIA	IIB
Flanged, cylindrical or spigot joints		6	0,30	0,30	0,20	–	–	–	–	–	–	–	–	–
		9,5	0,35	0,30	0,20	0,35	0,30	0,20	0,08	0,08	0,08	–	–	–
		12,5	0,40	0,30	0,20	0,40	0,30	0,20	0,40	0,30	0,20	0,40	0,20	0,15
		25	0,50	0,40	0,20	0,50	0,40	0,20	0,50	0,40	0,20	0,50	0,40	0,20
Cylindrical joints for shaft glands of rotating electrical machines with:	Sleeve bearings	6	0,30	0,30	0,20	–	–	–	–	–	–	–	–	–
		9,5	0,35	0,30	0,20	0,35	0,30	0,20	–	–	–	–	–	–
		12,5	0,40	0,35	0,25	0,40	0,30	0,20	0,40	0,30	0,20	0,40	0,20	–
		25	0,50	0,40	0,30	0,50	0,40	0,25	0,50	0,40	0,25	0,50	0,40	0,20
		40	0,60	0,50	0,40	0,60	0,50	0,30	0,60	0,50	0,30	0,60	0,50	0,25
	Rolling-element bearings	6	0,45	0,45	0,30	–	–	–	–	–	–	–	–	–
		9,5	0,50	0,45	0,35	0,50	0,40	0,25	–	–	–	–	–	–
		12,5	0,60	0,50	0,40	0,60	0,45	0,30	0,60	0,45	0,30	0,60	0,30	0,20
		25	0,75	0,60	0,45	0,75	0,60	0,40	0,75	0,60	0,40	0,75	0,60	0,30
		40	0,80	0,75	0,60	0,80	0,75	0,45	0,80	0,75	0,45	0,80	0,75	0,40
NOTE Constructional values rounded according to ISO 31-0 should be taken when determining the maximum gap.														

Figure 2.9: *Minimum width of joint and maximum gas opening for enclosures of groups I, IIA, and IIB. From (IEC 2007a).*

Electrical equipment is also classified in terms of the violence of the explosive atmosphere. The equipment is divided into two groups; Group I and Group II. Group II has three subgroups. These subgroups are divided relating to the energy required for ignition to occur. Hydrogen belongs to group IIC, which indicates that it is easily ignitable, and hence one of the most dangerous gas to handle in areas where an explosive atmosphere may occur.

Table 2.4 : *Classification of electrical equipment. Based on (Geoffrey Bottrill 2005) and (R.Stahl 2007).*

Apparatus Group	Representative Gas	Maximum Experimental Safe Gap	Energy Band [µJ]
I	Methane		200
IIA	Propane	> 0.9	>180
IIB	Ethylene	0.5 – 0.9	>60
IIC	Hydrogen	< 0.5	>20

2.2.3 Typical damages on Ex'd' safety equipment

There are two main reasons for damages on Ex'd' safety equipment. The first and most common one is corrosion. Figure 2.41 shows that the "droplet zone" is the environment where the corrosion rate is at its highest, and this is where large parts of the offshore equipment is located, thus also where many of the Ex'd' equipments are installed.

The second main reason for damage is related to the human factor. These errors can be such as welding, cutting, rough handling during inspections, and poor maintenance, which all can result in a greater roughness than required (>6.3 μm).

2.2.3.1 Inspection and maintenance

Inspection and maintenance are two important factors for avoidance of an explosion. Figure 2.10 shows the three basic principles of explosion protection.

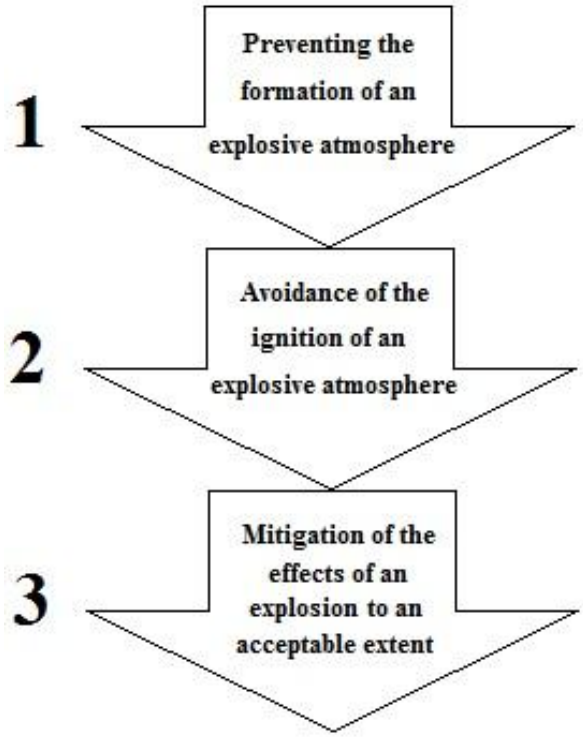

Figure 2.10 : *Basic principles of explosion protection. Based on (R.Stahl 2007).*

The following theory is based on (Geoffrey Bottrill 2005):

To ensure that all equipment is functioning as optimally as possible, inspections must be performed. The inspection procedures may vary from one location to another, as it is the owner of the plant who is responsible for the safety.

There are three types of inspection:

- Visual:
  An inspection by the use of human senses as vision, hearing, touch, and smell. No use of other equipment and tools

- Close:
  An inspection that identifies defects only by the use of access equipment and tools

- Detailed:
  An inspection in which one must open the enclosure to detect defects. Test equipment and tools may be necessary

After the installation of safety equipment is completed, it is required to perform a detailed inspection.

An inspection schedule is given in (IEC 2007):

Table 2.5 : *Inspection schedule for Ex'd' installations (D = Detailer, C = Close, V = Visual). Based on (IEC 2007).*

Check that:		Ex'd' Grade of inspection		
		D	**C**	**V**
A	**EQUIPMENT**			
1	Equipment is appropriate to the EPL/Zone requirements of the location	X	X	X
2	Equipment group is correct	X	X	
3	Equipment temperature class is correct	X	X	
4	Equipment circuit identification is correct	X		
5	Equipment circuit identification is available	X	X	X
6	Enclosure, glass parts and glass-to-metal sealing gaskets and/or compounds are satisfactory	X	X	X
7	There are no unauthorized modifications	X		
8	There are no visible unauthorized modifications		X	X
9	Bolts, cable entry devices (direct and indirect) and blanking elements are of the correct type and are complete and tight			
	- physical check	X	X	
	- visual check			X
10	Flange faces are clean and undamaged and gaskets, if any, are satisfactory	X		
11	Flange gap dimensions are within maximal values permitted	X	X	
12	Lamp rating, type and position are correct	X		
13	Motor fans have sufficient clearance to enclosure and/or covers	X		
14	Breathing and graining devices are satisfactory	X	X	
B	**INSTALLATION**			
1	Type of cable is appropriate	X		
2	There is no obvious damage to cables	X	X	X
3	Sealing of trunking, ducts, pipes and/or conduits is satisfactory	X	X	X

Maintenance is also important, in addition to inspections, to retain an item in conditions so it is able to perform its required functions. Tasks that shall be maintained on the protection concept Ex'd' are as follows:

- Prevent clearance gaps from becoming excessive
- Keep all joint surfaces clean
- Ensure that all bolts, screws, and nuts are present, tight, and secured against working loose

2.2.3.2 Repair of Ex'd' equipment

When it comes to the issue of when it is necessary to repair an Ex'd' safety apparatus, the answer is unclear. The only requirement that currently exists (IEC 2007b) for an Ex'd' apparatus, is that the average roughness of the gap opening should not be larger than 6.3 μm.

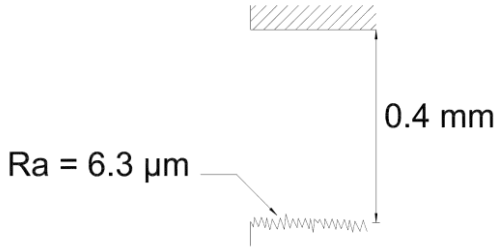

Figure 2.11: *The maximum allowable roughness of the joint/flame gap surface (average depth of 6.3 μm) compared with the maximum allowable flange gap (0.4 mm). From (Opsvik 2010).*

If the surface of the flame opening has a higher roughness than the requirement, is must either be repaired or replaced. For example corrosion, which makes the roughness of a surface to increase, leads to large sums of money being spent on the repair.

2.3 Basic Theory

2.3.1 Quenching distance, Q_D

The quenching distance becomes an important parameter in terms of flame propagation through small/narrow openings. For the flame to be able to propagate through an opening, the heat generation has to be greater than the heat loss due to the walls, see Section 2.3.5 and Section 2.3.6.

Q_D is defined as "*the smallest tube diameter through which a laminar flame can propagate*". (Eckhoff 2005) states that there is a correlation between the quenching distance and the maximum experimental safe gap. A rough rule is that $Q_D \approx 2 \cdot MESG$ (see Section 2.3.2 for a detailed explanation of the term MESG).

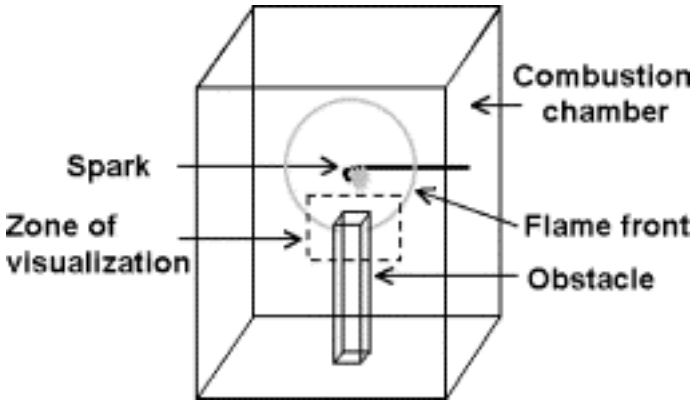

Figure 2.12: *One out of many test apparatuses for determination of Q_D. From (Bellenoue, Kageyama et al. 2003).*

Figure 2.12 illustrates an experimental set-up for determination of quenching distances. The explosive mixture in the combustion chamber is ignited by spark electrodes. The flame front, drawn as a sphere, reaches the obstacle at a time of 18 to 23 ms after being ignited, depending on the value of the initial pressure. When the flame front comes in contact with the obstacle, the pressure will increase as the obstacle prevents the penetrating gases from further expansion. Windows are located on all sides of the combustion chamber, allowing observers to observe if the flame is being quenched or not.

2.3.2 Maximal experimental safe gap, MESG

When an explosion occurs inside a vented chamber, hot combustion gases will be pushed through the vent, which is a gap smaller than the quenching distance. Although this opening is $< Q_D$, it may still cause a re-ignition on the outside. This means that not only flames can re-ignite an explosive atmosphere, but also hot combustion gases can cause re-ignition. It is therefore important to define the smallest gap where the hot combustion gases will not re-ignite the explosive mixture outside the gap, and this value is called the minimum experimental safe gap, MESG.

(IEC 2010) has defined the term MESG as follows: "*maximum gap between the two parts of the interior chamber which, under the test conditions specified below, prevents ignition of the external gas mixture through a 25 mm long flame path when the internal mixture is ignited, for all concentrations of the tested gas or vapor in air*".

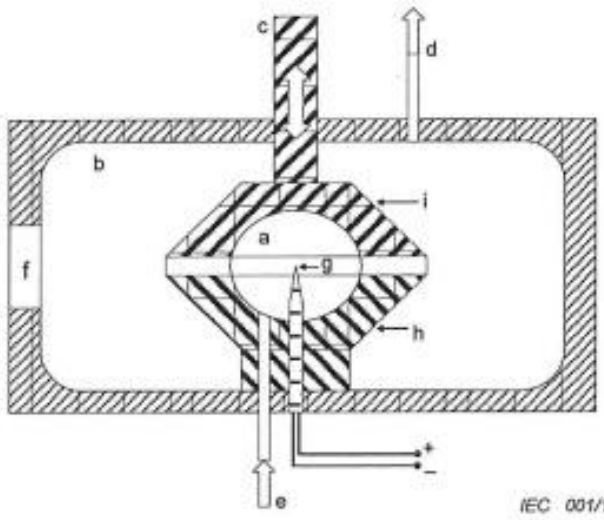

Key

a interior spherical chamber
b exterior cylindrical enclosure
c adjustable part
d outlet of mixture
e inlet of mixture
f observation windows
g spark electrode
h lower gap plate, fixed
i upper gap plate, adjustable

Figure 2.13: *Standard IEC apparatus used for determination of MESG values. From (IEC 2010).*

A common way to determine the MESG value was developed and used to classify gases by their sensitivity and reactivity. The apparatus in Figure 2.13 is the standard apparatus used for determination of MESG values. The interior chamber, a, is a sphere with volume 20 cm^3, and the exterior cylindrical enclosure, b, has a diameter of 200 mm and a height of 75 mm, which gives a volume of 2356 cm^3. The interior and exterior chambers are filled with a known mixture of the gas in air under normal conditions. These normal conditions of temperature[1] and pressure are respectively 20 °C and 100 kPa. The mixture in the interior chamber is then ignited and a re-ignition, if any, can be observed from the observation window.

However, as (Eckhoff 2003) points out, MESG values are not specific for each gas cloud. It depends on the length of the slot, the explosion pressure inside the chamber, and the volume of the chamber. But MESG values are still important in practice and must be determined.

MESG is always the parameter used as a measure of the gap for flameproof enclosures. There will be a safety factor included when the maximum allowable gap opening for Ex'd' safety equipment is found.

[1] An exception is made for substances with vapor pressures which are too low to permit mixtures of the required concentrations to be prepared at normal ambient temperatures. For these substances, a temperature 5 K above that needed to give the necessary vapor pressure or 50 K above the flash point is used. From IEC (2010).

Table 2.6 : *MESG values of hydrogen, ethylene, propane, and methane. From (Engineering 2011).*

Gas or Vapor	Optimum Mixture [vol % in air]	MESG [mm]
Hydrogen	29.6	0.29
Ethylene	6.5	0.65
Propane	4.2	0.92
Methane	8.2	1.14

2.3.3 Ignition point's influence on burning velocity

The ignition point in a ventilated container affects the flow of the unburnt gases. Figure 2.14 illustrates an idealized adiabatic (no heat loss) laminar combustion of premixed explosive gas and air in a one end open tube.

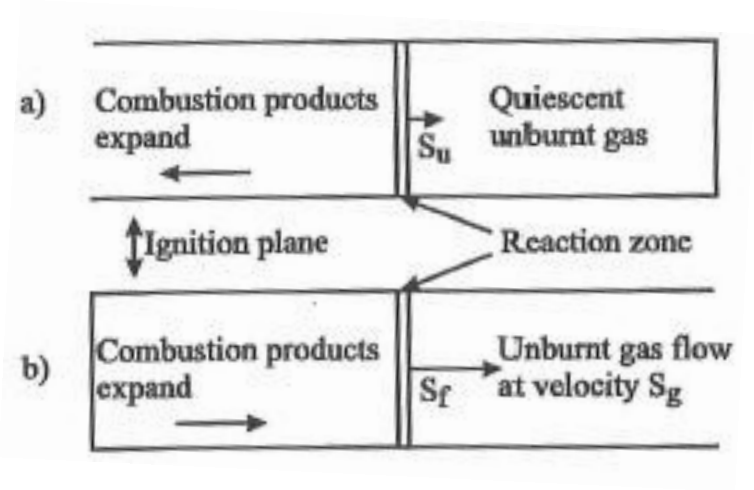

Figure 2.14 : *Premixed fuel gas/air burning at constant pressure with a plane, laminar flame in a one-end-open tube. a) ignition at open tube end. b) ignition at closed tube end. From (Eckhoff 2005).*

If the gas mixture is ignited in the open end of the tube, as shown in Figure 2.14 a), the combustion products will expand freely to the surroundings, while the unburnt gases in the closed end of the tube will remain quiescent. If the ignition takes place in the closed end of the tube, the combustion products will be forced to expand in the same direction as the flame propagation. The unburnt gases ahead of the combustion products will then be pushed towards the tube's opening, see Figure 2.14 b).

In reference to (Eckhoff 2005), one must note that there is a difference between the term *burning velocity* and *flame speed*. The burning velocity is the relative linear velocity, S_u, equivalent to the velocity the combustion reaction "eats" itself into the unburned mixture. The flame speed, however, is the linear velocity, S_f, of the observable flame front.

Figure 2.15 illustrates an ideal laminar spherical combustion of a premixed explosive atmosphere, where the unburned gases will be pushed in the direction of the flame propagation.

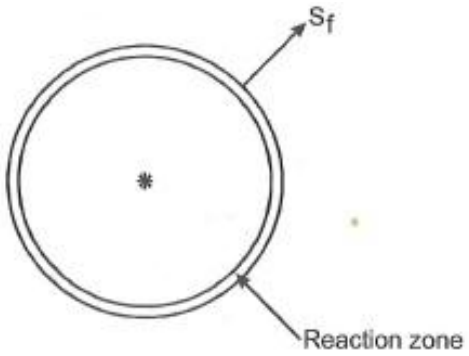

Figure 2.15 : *Ideal laminar spherical burning of quiescent premixed fuel gas/air, following ignition at a point. From (Eckhoff 2005).*

2.3.4 Radical chain reaction

Radicals are highly reactive atoms, molecules, or ions. The reason why they are so reactive is because they have unpaired electrons in their outer shell. These types of radical chain reactions are what form the basis of combustion processes. From (J. Warnatz 2006), an example of a radical chain reaction is demonstrated by using the hydrogen – oxygen system, where the dots illustrate radicals:

Table 2.7: *Most important reactions with respect to ignition in the hydrogen - oxygen system. From (J. Warnatz 2006).*

(1)	Chain initiation:	H_2	+	O_2	=	2 OH•				
(2)	Chain propagation:	OH•	+	H_2	=	H_2O	+	H•		
(3)	Chain branching:	H•	+	O_2	=	OH•	+	O•		
(4)	Chain branching:	O•	+	H_2	=	OH•	+	H•		
(5)	Chain termination:	H•			=	½ H_2				
(6)	Chain termination:	H• + O_2 + M			=	HO_2	+	M		
(2 + 3 + 4)		2 H_2	+	O_2	=	H•	+	OH•	+	H_2O

2.3.5 Ignition by a jet of hot combustion products

According to (J. Warnatz 2006) ignition is defined as: "*the time-dependent process of starting with reactants and evolving in time towards a steadily burning flame*". Ignition processes are always dependent on time.

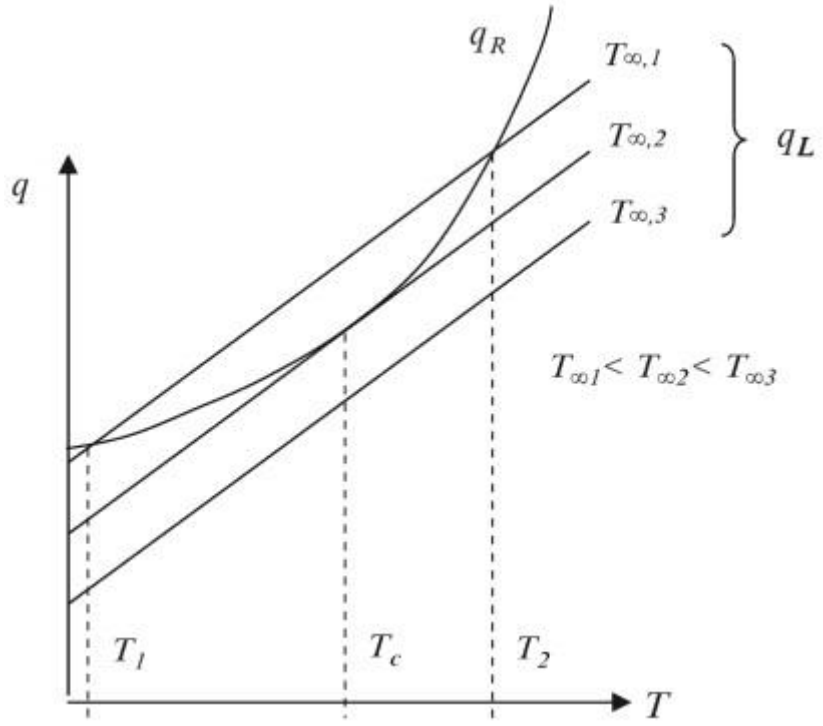

Figure 2.16: *Volumetric heat release rate versus temperature with different surrounding temperatures. Based on (Sara McAllister 2011).*

In 1955 (Frank-Kamenetskii 1955) came up with the thermal explosion theory. This theory states that when the heat generation exceeds the heat loss, it results in ignition. The ignition volume due to the exothermal reaction between air and fuel, determines the heat generation curve, q_R, see Figure 2.16. The heat loss line, q_L, shows a linear relationship with the temperature drop between the ignition volume and the surrounding gas.

Using the energy conservation theory "in equals out", the temperature development is expressed as follows:

$$\rho c_p \frac{\partial T}{\partial t} = \underbrace{\left(-\rho c_p u \frac{\partial T}{\partial x} + k \frac{\partial^2 T}{\partial x^2}\right)}_{heat\ loss} + \underbrace{\hat{\dot{r}}_{fuel} \hat{Q}_c}_{heat\ generation} \qquad \textbf{2.1}$$

Simplifying the equation gives:

$$\rho c_p \frac{\partial T}{\partial t} = -q_L + q_R \qquad \textbf{2.2}$$

where

- $\frac{\partial T}{\partial t}$ is the temperature change with respect to time
- q_L is the heat loss to the surroundings
- q_R is the heat generated

Ignition is reached when the heat generated is equal to the heat loss, $q_L = q_R$. The temperature decreases if the heat generated is less than the heat loss. If the amount of heat generated is greater than the amount of heat lost, the temperature increases.

The ignition curve is a simplified model and is therefore not ideal. It does not depend on the temperature differences that exist throughout the volume, but depends only on the heat transfer in the material itself and to the surroundings.

2.3.6 Flame extinction in gaps

(J. Warnatz 2006) states that there are two main reasons for flame extinctions in gaps. The first reason is heat transfer between the flame and the cool walls, which is illustrated in Figure 2.17. The second reason is removal of reactive intermediates by surface reactions. The walls will adsorb some radicals, causing the combustion to become somewhat limited.

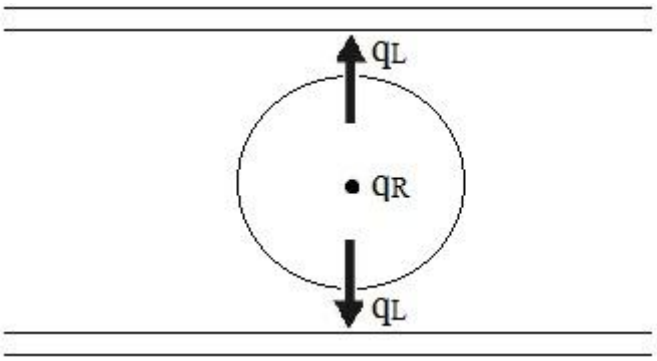

Figure 2.17: *Illustration of heat transfer from flame to gap walls.*

2.3.6.1 Heat transfer from flame to gap walls

The following theory is based on (Warren L. McCabe 2005):

Heat can be transported in two different ways; either by conduction or convection.

Conduction is defined as: "*If a temperature gradient exists in a continuous substance, heat can flow unaccompanied by any observable motion of matter. Heat flow of this kind is called conduction*". The basic relation for heat flow by conduction is that the heat flux is proportional to the temperature gradient, but with opposite sign. This is shown in Fourier's law (for one-dimensional heat flow):

$$\frac{dq}{dA} = -k\frac{dT}{dx} \qquad \textbf{2.3}$$

where

- q is the rate of heat flow in direction normal to surface
- A is surface area
- T is the temperature
- x is the distance normal to surface
- k is the proportionality constant or thermal conductivity

Convection is the transport of energy/heat by movement or flow, and is therefore the most relevant transportation method for this study. There are two types of convection; free convection and forced convection. Free convection is when a fluid is put in motion due to density differences between the fluids. Forced convection occurs when the fluid is set in motion as a result of an external force. Both free and forced convection can be related to the present work as it deals with explosions and thus temperature and density differences. Newton's law of cooling shows that the convective flux is proportional to the temperature differences between the surface and the fluid:

$$\frac{q}{A} = h\left(T_s - T_f\right) \qquad \textbf{2.4}$$

where

- h is the heat transfer coefficient
- T_s is the temperature of the surface
- T_f is the temperature of the bulk of fluid

In the present work, several explosions will be penetrated through a narrow gap consisting of two steel surfaces. Surface layers called "boundary layers" will be formed between the two surfaces in the flame gap opening. (Warren L. McCabe 2005) defines a boundary layer as follows: "*A boundary layer is defined as that part of a moving fluid in which the fluid motion is influenced by the presence of a solid boundary*". Heat transfer will therefore occur when a fluid flows on or between surfaces. This heat transfer will change the temperature of the fluid close to the surface of the plate, and will generate a temperature gradient. The fluid will have a velocity of approximately zero near the wall, and the velocity will increase all the way out to the bulk velocity.

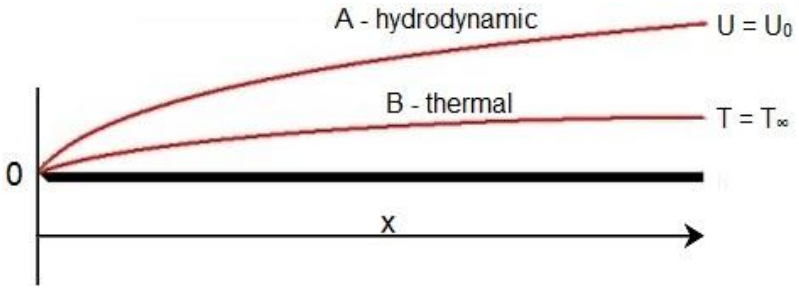

Figure 2.18: *Hydrodynamic and thermal boundary layers on a flat plate.*

Figure 2.18 shows two boundary layers. Boundary layer A describes the hydrodynamic boundary layer while B describes the thermal boundary layer. The relationship between the thicknesses of these two boundary layers depends on the Prandtl number. This is a dimensionless number, which is the ratio of the diffusivity of momentum v or μ/ρ to the thermal diffusivity α or $k/\rho c_P$:

$$Pr \equiv \frac{\upsilon}{\alpha} = \frac{c_p \mu}{k} \qquad \textbf{2.5}$$

For gas, the Prandtl number is usually close to 1.0. This means that the two boundary layers have almost the same thickness. Since the viscosity and thermal conductivity increase with temperature at about the same rate, the Prandtl number is almost independent of temperature.

2.3.6.2 Cooling from mixing with cold unburned gas in the secondary chamber

As the explosions penetrate through the flame gap opening between the primary chamber and the external chamber, see Figure 3.1, a turbulent jet will develop in the external chamber from the hot combustion gases escaping from the gap opening.

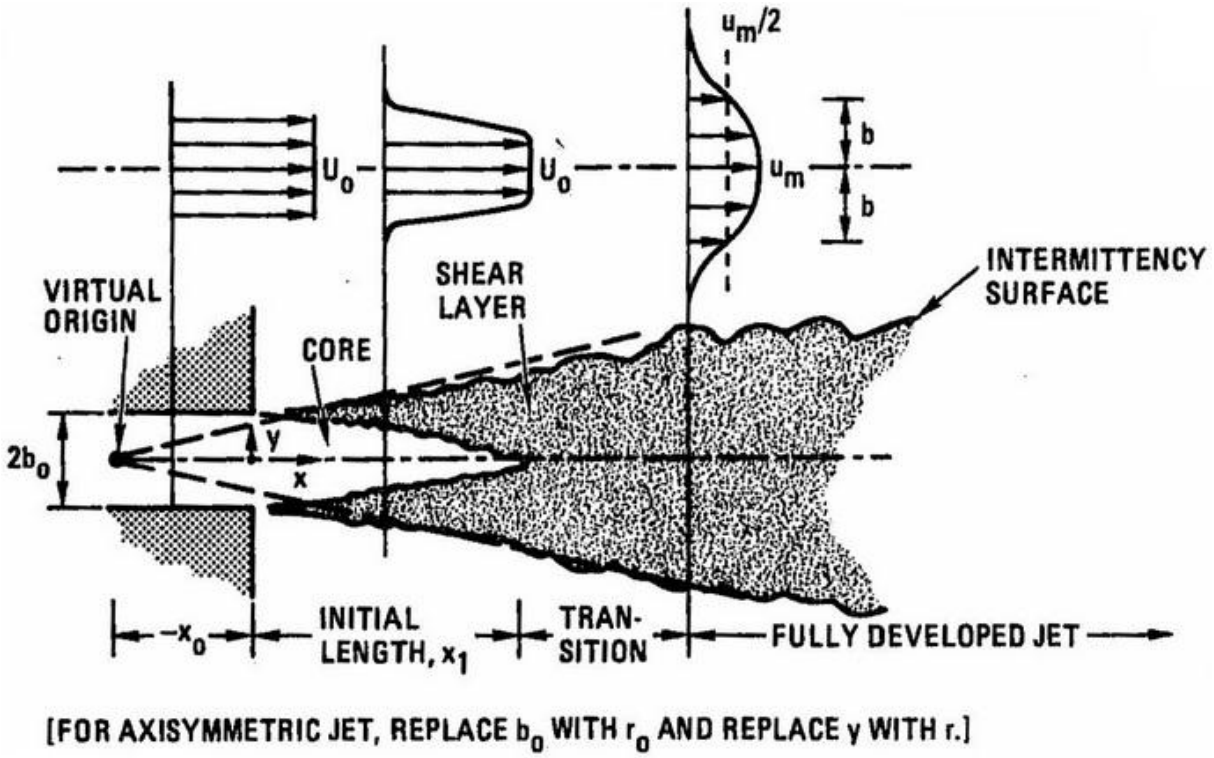

Figure 2.19: *Illustration of a turbulent jet. From (Michael Sandford 2011).*

Turbulence is known as a chaotic regime where the properties change. These properties include low momentum diffusion, high momentum convection, and rapid variation of pressure and velocity in space and time. As shown in Figure 2.19, there are three regions that describe the development of a turbulent jet; core region, transition region, and the fully developed turbulent jet region.

If an explosion is to occur inside a flameproof enclosure, see Section 2.2.2, the pressure inside the chamber will rise rapidly and force the combustible gases to penetrate through the gap opening at a significantly high velocity. This jet develops into a turbulent jet due to the high unstable explosion pressure and the high velocity. Another important factor that plays a role in the turbulence development is the temperature difference between the burnt and the unburned gases. Hot molecules move faster than cold molecules, which will have a mixing effect on the two gases. When the jet has become fully turbulent, the maximum cooling point of the hot combustion gases is reached. This is because the interaction rate between the burnt and the unburned gases are at a maximum.

2.3.7 Effect of wall roughness on fluid flow

When dealing with fluid flow, the Reynolds number gives important information about the flow properties.

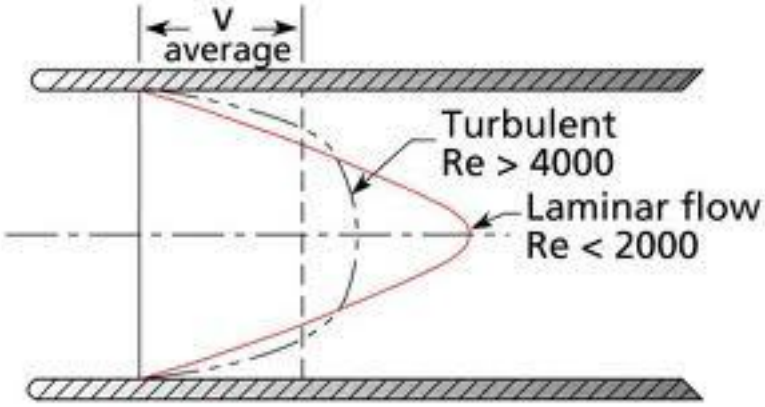

Figure 2.20 : *Illustration of fluid properties at different Reynolds numbers. From (Valve 2007).*

It is a dimensionless number and can be defined by the ratio of the dynamic pressure (ρu^2) and the shearing stress ($\mu u / L$). Reynolds number can then be expressed as:

$$Re = \frac{\rho \bar{V} D}{\mu} \qquad \textbf{2.6}$$

where

- ρ is the density of the fluid
- V is the average velocity
- D is the characteristic length (diameter for pipes)
- μ is the viscosity of liquid

The Reynolds number gives an indication of whether the flow is turbulent or not. As seen in Figure 2.20, the flow is characterized as turbulent if Re > 4000.

In turbulent flow for a given Reynolds number, a rough pipe leads to a larger friction factor than a smooth pipe does.

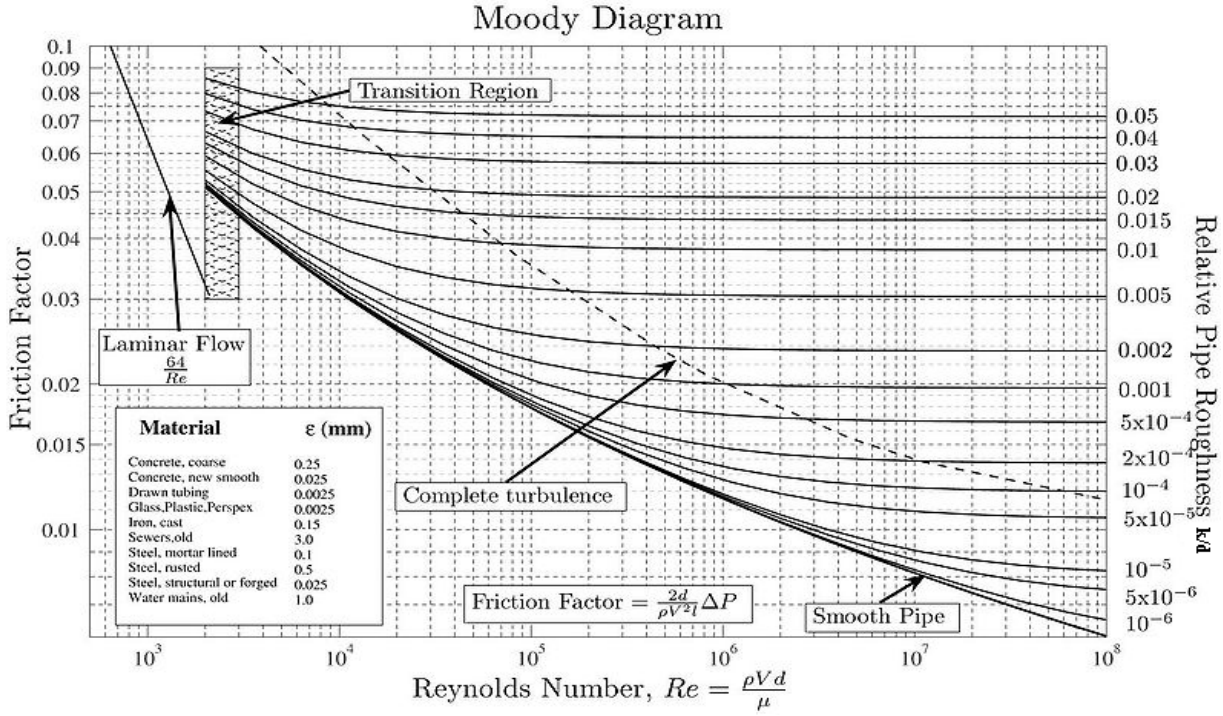

Figure 2.21 : *Friction factor plot for circular pipes (L. W. Moody, "Friction Factors for Pipe Flows"). From (Warren L. McCabe 2005).*

The roughness parameter, k, is the height of a single unit of roughness. The friction factor is a function of both Reynolds number and the relative roughness $\xi = k/D$, where D is the diameter of the pipe.

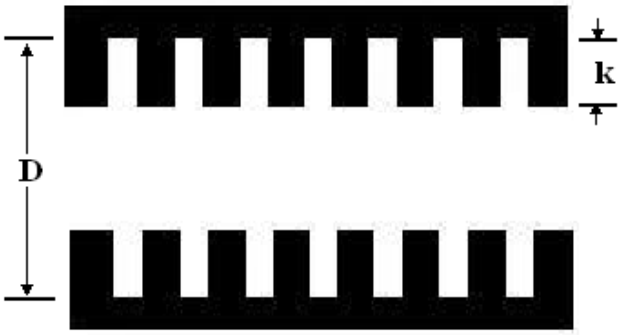

Figure 2.22: *Illustration of roughness. From (Solheim 2010).*

Two equal Reynolds numbers in turbulent flow gives a higher heat-transfer coefficient for rough tubes than for smooth ones.

The friction factor can also be described by the following equation:

$$f = \frac{\Delta p_s D}{2L\rho \bar{V}^2} \qquad \textbf{2.7}$$

where p is the pressure and L is the length. From Equation 2.7 it can be seen that the diameter is inversely proportional with the pressure. This means that the smaller the gap/opening is, the higher the pressure will be.

2.3.8 Effect of turbulence on the heat transfer

The Nusselt number is a dimensionless number that describes the ratio between the convective heat transfer and the conductive heat transfer across the boundary:

$$Nu = \frac{hL}{k_f} = \frac{Convective\ heat\ transfer\ coefficient}{Conductive\ heat\ transfer\ coefficient} \qquad \textbf{2.8}$$

where

- h is the convective heat transfer coefficient
- L is the characteristic length
- K_f is the thermal conductivity of the fluid

The graph in Figure 2.23 illustrates that the Nusselt number increases as the Reynolds number, which is a measure of the turbulence level, increases. Since convection depends on the movement of the fluid, the Reynolds number will influence the amount of heat being transferred as convection instead of as conduction. A large Nusselt number means that convection will be the dominant form of heat transfer.

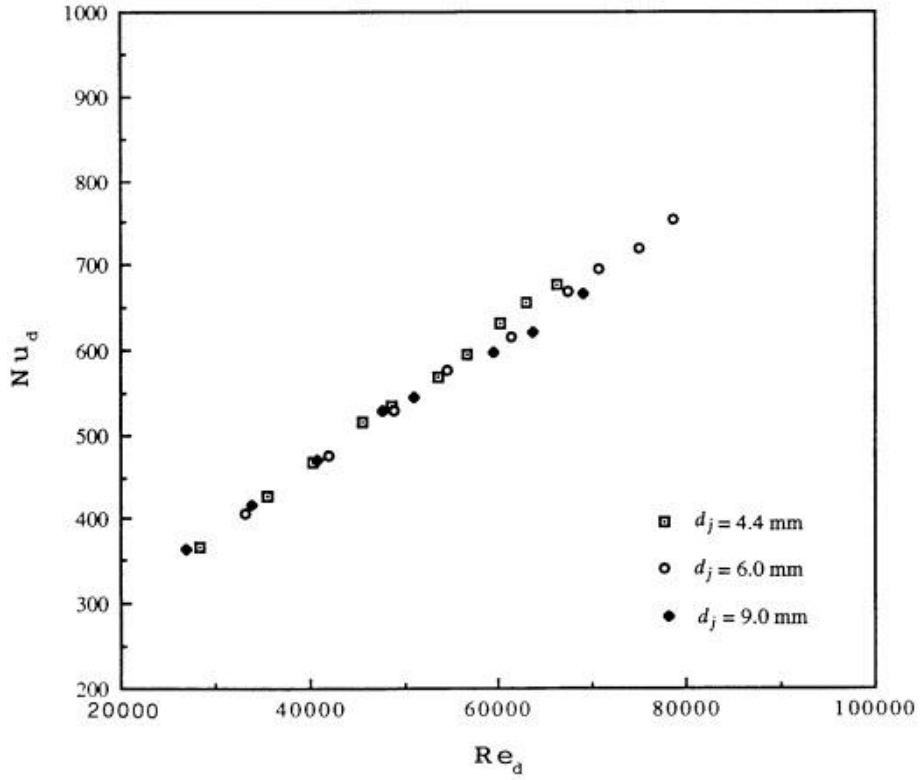

Figure 2.23 : *Nusselt number as a function of Reynolds number for surface roughness 6.3 μm, for three nozzels. From (Gabour 1993).*

Figure 2.23 shows a linear relationship between the Reynolds number and the Nusselt number when the surface has a constant roughness of 6.3 μm. When the Nusselt number increases, the heat loss due to the movement of molecules is of greater matter than the heat loss to the walls.

Roughness on a surface in a pipe, or in a flame gap which is the case in this research, may cause fluctuations and hence form turbulence. (Warren L. McCabe 2005) states that for equal Reynolds numbers the heat transfer coefficient in turbulent flow is somewhat greater for a rough tube than for a smooth one. The effect of roughness on heat transfer is much less than on fluid friction, so the roughness is neglected in practical calculations. McCabe also explains that in high velocity flow of compressible gases in pipes, friction at the wall raises the temperature of the fluid at the wall to above the average fluid temperature.

2.4 Literature review of previous work

2.4.1 Philips' work

(Phillips 1971) investigated the physical mechanisms of flameproof protection and MESG. He developed a theory based on the following stages:

- The spherical shape of the propagating flame front
- How and when the flame front reaches the flange gap when it is centric or off-centric
- Quenching of the flame when the gap width is smaller than the quenching distance
- Heat exchange with the gap wall
- A three dimensional jet of hot combustion products is formed from the gap exit
- Mixing of the jet and the external atmosphere

To gain better knowledge of the re-ignition process, Phillips used the Schlieren system to examine what happened in the external explosion chamber.

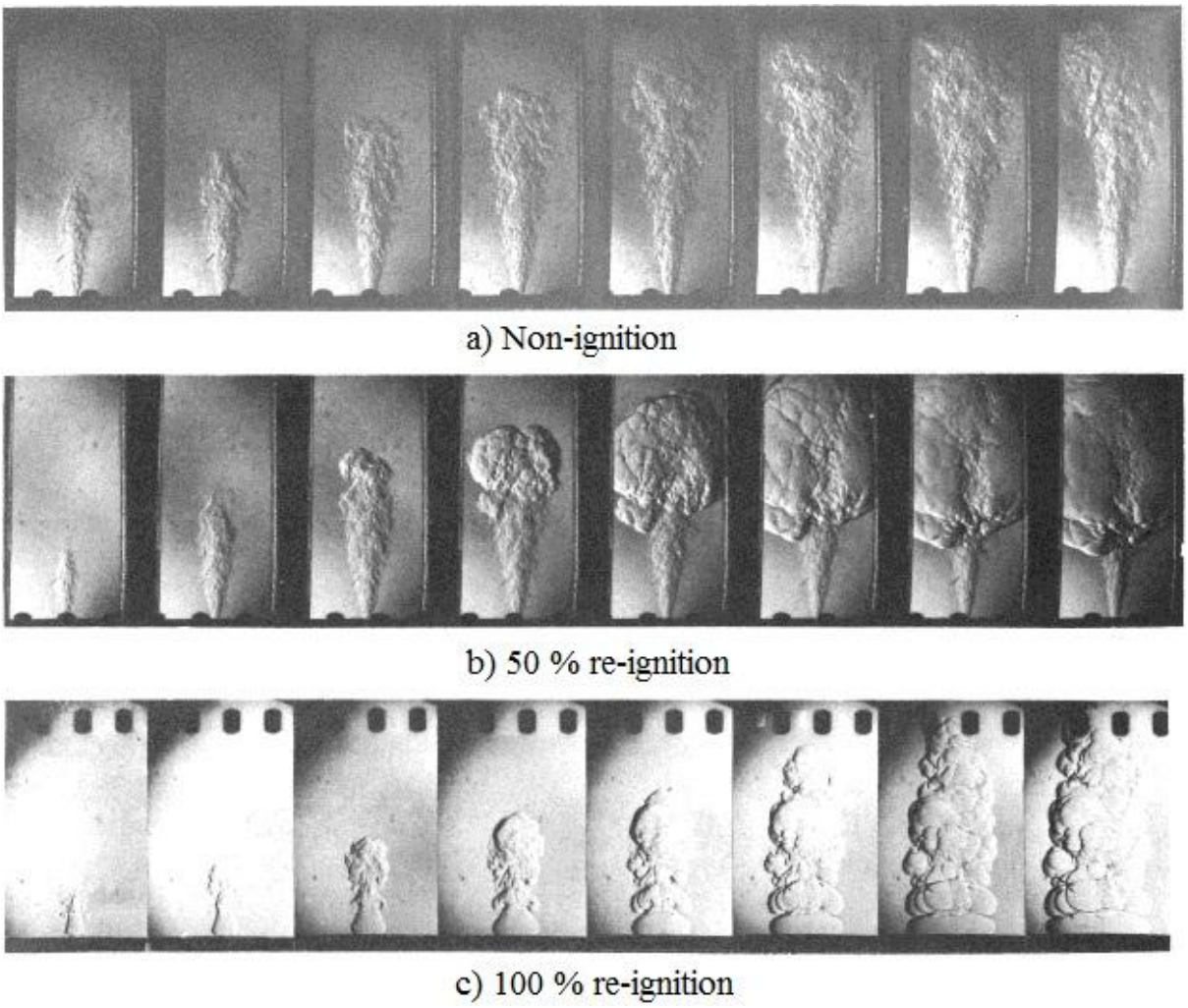

Figure 2.24 : *Schlieren photos of a) non-ignition b) 50 % re-ignition and c) 100 % re-ignition. From (Phillips 1971).*

From the photo series of the non-ignition process, we can only observe the jet. But in the photo series in which we have 50 % re-ignition, the flame front can clearly be seen as a ball-like object. When the gap width was increased it resulted in 100 % re-ignition, and the explosion became more violent. Phillips stated that the reason for explosion transmission through the flange gap was due to the jet of hot combustion products.

Phillips' experiments showed that there was a limiting gap opening that permitted transmission of the explosion, and that distance was about half the quenching distance. His experiments also showed that the optimal ignition location to generate re-ignition was close to the gap opening, with some exceptions for the more reactive gases such as hydrogen.

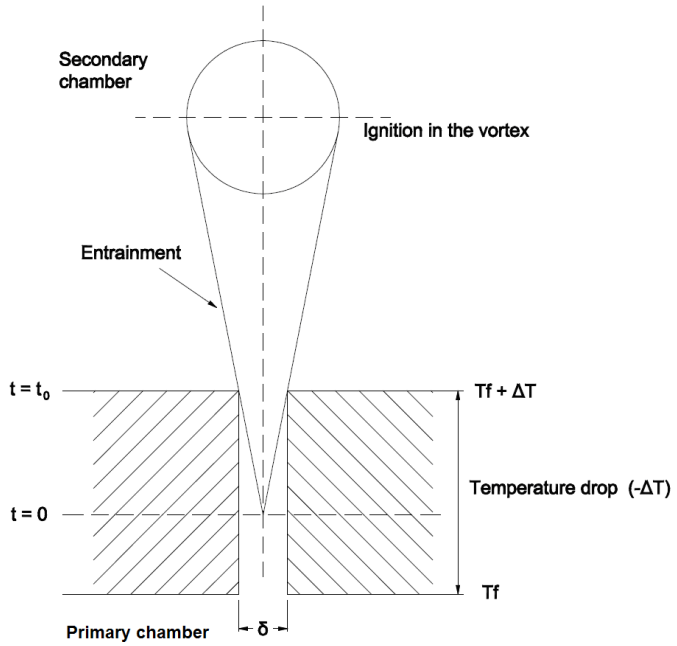

Figure 2.25 : *A two-dimensional model of the jet of hot combustion products. Based on (Phillips 1971).*

Phillips' conclusion was that the heat generation must be greater than the heat loss to the walls and the heat loss due to the mixing with the unburned gases in the secondary chamber. By setting up an energy balance across an element of the jet, he developed the following formula:

$$\psi = \frac{1}{\eta} \cdot \frac{d\eta}{dt} + \frac{1}{m} \cdot \frac{dm}{dt} \qquad \textbf{2.9}$$

where

- ψ is the reaction rate function
- m is the mass of the gas
- t is the time

and where the combustion efficiency, η, is given as:

$$\eta = \frac{(T - T_u)}{(T_f - T_u)} \qquad \textbf{2.10}$$

where

- T is the temperature
- T_u is the ambient temperature
- T_f is the maximum flame temperature

By solving Equation 2.10, (Phillips 1971) created a plot of the change in temperature with time, see Figure 2.26.

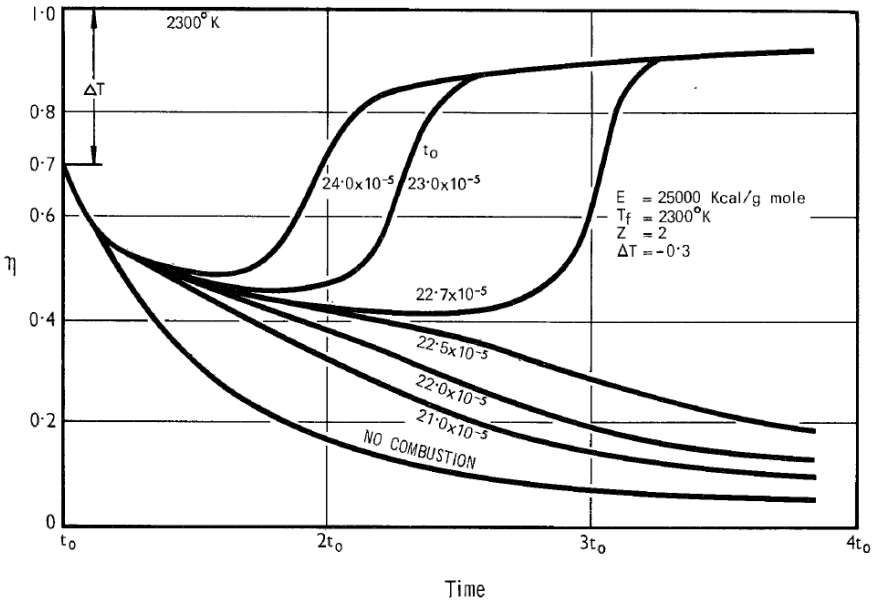

Figure 2.26 : *η denotes a non-dimensional temperature $(T-T_u)/(T_f-T_u)$ and t_0 denotes starting time in seconds from a point source until the vortex fills the orifice. From (Phillips 1971).*

The bottom curve describes the situation of no combustion. The temperature drops rapidly by cooling from the walls and the mixing with the unburned gas (η = 0). The three lines above the "no combustion" line do not ignite the external chamber, but combustion will occur over a short period of time. The three top lines represent ignition; the temperature drops in the beginning, then the heat generated from the combustion exceeds the heat loss and ignition takes place in the external chamber, which causes a temperature rise.

2.4.2 The Influence of Flow Parameters on Minimum Ignition Energy and Quenching Distance (Ballal and Lefebvre 1975)

Ballal and Lefebvre conducted experiments where they studied how the effect of pressure, velocity, mixture strength, turbulence intensity, and turbulence scale influenced the minimum ignition energy and the quenching distance. The test apparatus used was a specially designed closed-circuit tunnel. A fan made it possible to drive air through the tunnel at velocities up to 50 m/sec. As ignition source on the apparatus, two plain electrodes of 1 mm diameter were used.

The conclusion from (Ballal and Lefebvre 1975)'s experiments was that both the quenching distance and the minimum ignition energy increased with the four following parameters:

- Increase in velocity
- Reduction in pressure
- Departures from stoichiometric fuel/air ratio
- Increase in turbulence intensity

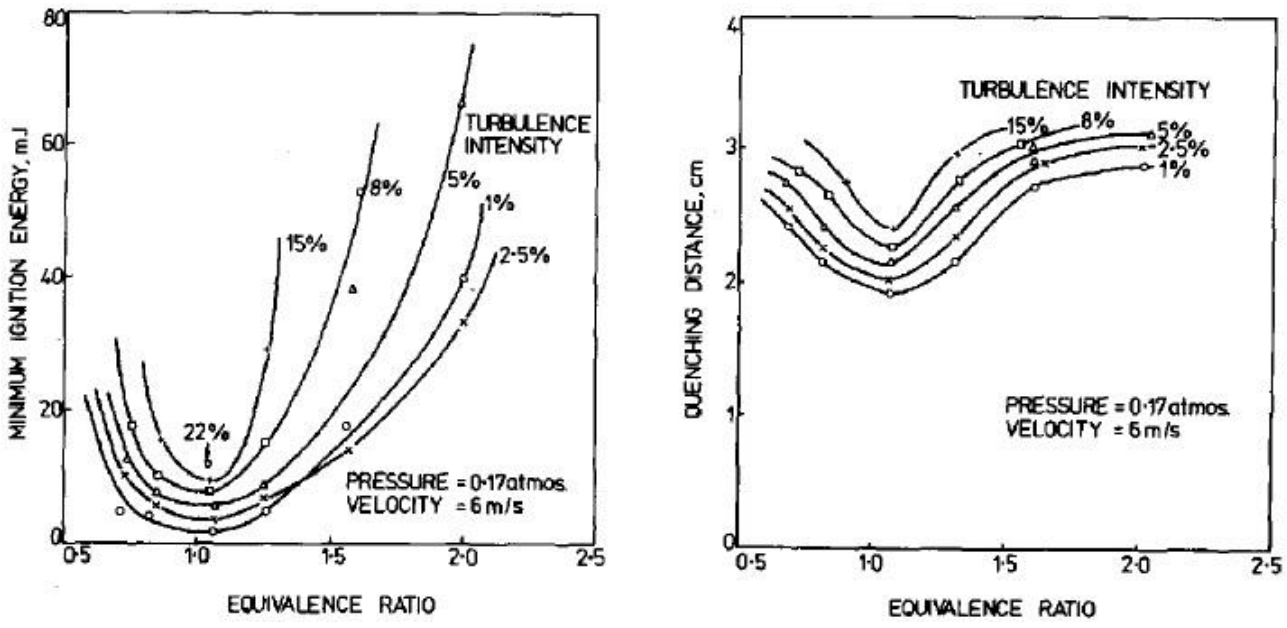

Figure 2.27 : *Effect of turbulence intensity on minimum ignition energy and quenching distance for different equvalence ratios. From (Ballal and Lefebvre 1975).*

The turbulence intensity affects the combustion process in several ways. The combustion process accelerates due to the increased diffusion with oxygen as a result of increased surface area. However, as the turbulence intensity increases, the heat loss to the surroundings also increases. The overall affect from turbulence intensity is shown in Figure 2.27; as the

turbulence intensity increases, both the minimum ignition energy and quenching distance increases.

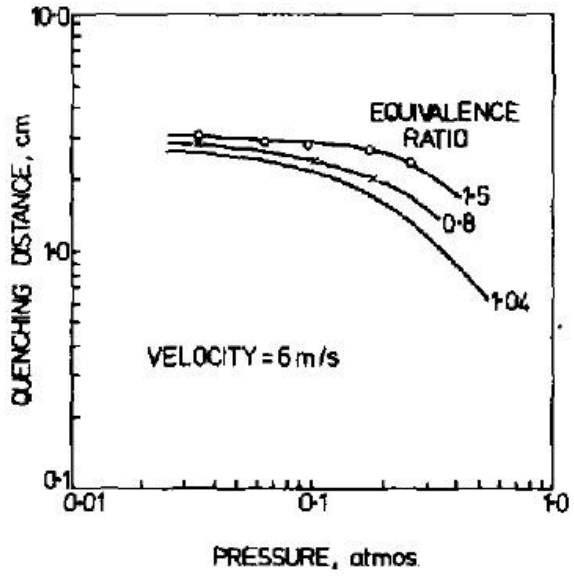

Figure 2.28 : *Influence of pressure and mixture strength on quenching distance. From (Ballal and Lefebvre 1975).*

Figure 2.28 shows that as the pressure decreases the quenching distance increases.

2.4.3 The study of (Redeker 1981)

Redeker studied how different parameters affected the MESG and thus the safety of flameproof enclosures. His study included parameters such as:

- Influence of inner volume of enclosure
- Influence of point of ignition
- Influence of gap length
- Influence of different air to fuel mixture ratios
- Influence of different initial pressures
- Influence of different initial temperatures

I concentrate on the parameters I think have the most impact on my thesis, and go a bit deeper into the theory of them.

2.4.3.1 Influence of inner volume of enclosure

Redker decided to investigate the influence of inner volume by using two different apparatuses with adjustable volume enclosures. Both apparatuses had a spherical inner volume and a closed outer volume. The first apparatus could adjust its volume from 1-8 dm^3, and the second apparatus could be adjusted from 0.5-20 cm^3.

The experiments showed that the safe gap distance decreased as the inner volume of the enclosure increased, but only till it reached 20 cm^3. The safe gap distance was then near constant till 1 dm^3 was reached.

Redeker also implemented the experiments in an apparatus where the outer enclosure could release pressure. The same result applied here from 0.5-20 cm^3, the safe gap distance decreased with increasing inner volume. But when the volume then was increased from 20 cm^3 to 8 dm^3, the safe gap distance kept constant as Figure 2.29 shows.

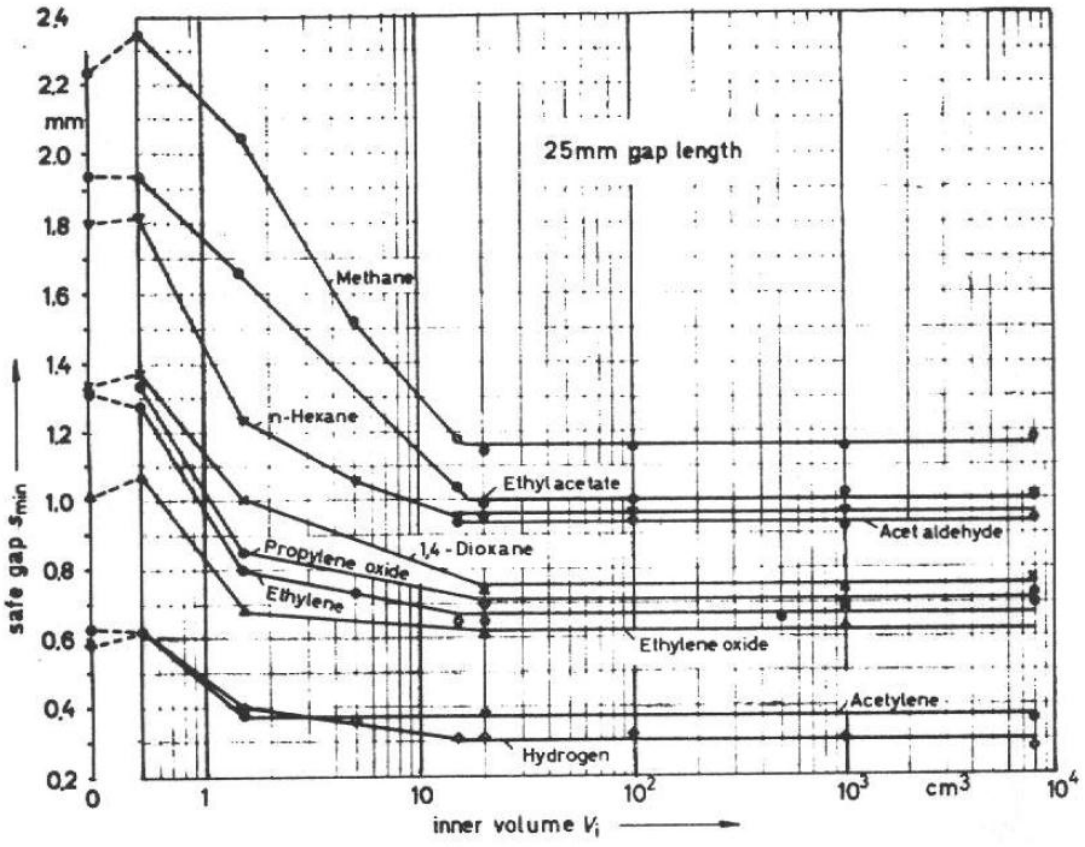

Figure 2.29 : *Safe gap s_{min} for the most incendive mixtures as a function of the inner volume of the PTB test apparatus. In the test apparatus with larger volume (> 1 liter) the inner volume was surrounded by a pressure relieving flexible outer enclosure. From (Redeker 1981).*

2.4.3.2 Influence of point of ignition

By stepwise moving the ignition source further and further away from the opening, results could be recorded. This was the procedure through all Redeker's experiments, and he implemented them in different volumes.

The effect of the location of the ignition source depends on the volume of the inner enclosure. Redeker concluded that for volumes bigger than 20 cm^3, the effect of the point of ignition was of higher importance than for smaller volumes.

2.4.3.3 Influence of gap length

Redeker used the 20 cm^3 apparatus and discovered that as the gap length increases, so did the safe gap distance. The safe gap increased at a high rate until the 25 mm gap length was reached, then it increased at a significantly lower rate. See Figure 2.30.

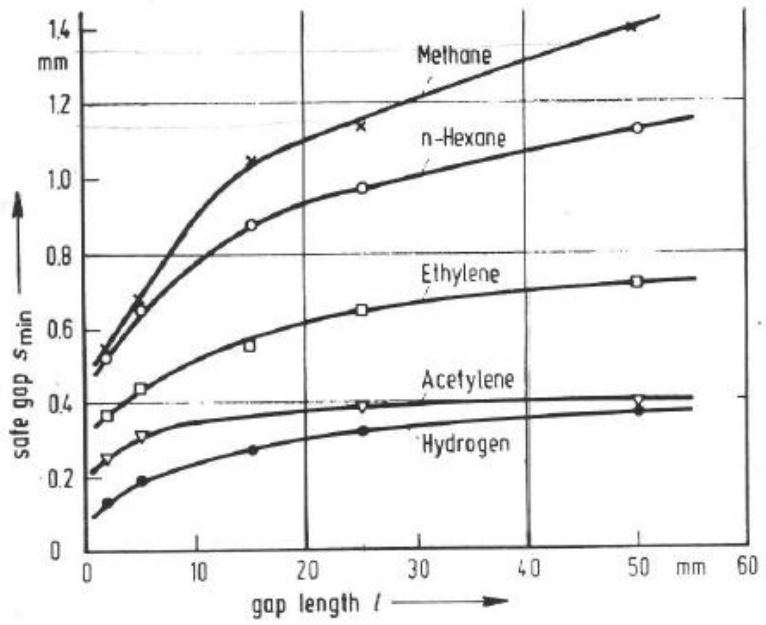

Figure 2.30 : *Safe gap s_{min} for the most incendive gas/air and vapour air mixture as a function of location of gap length l, determined in the test apparatus of 20 cm^3. From (Redeker 1981).*

2.4.3.4 Influence of different initial pressures

Redeker also studied how different initial pressures in the enclosure affected the safe gap. All his results showed an increase in the safe gap due to a reduction in pressure. Figure 2.31 shows the linear relationship between the safe gap and the pressure reduction.

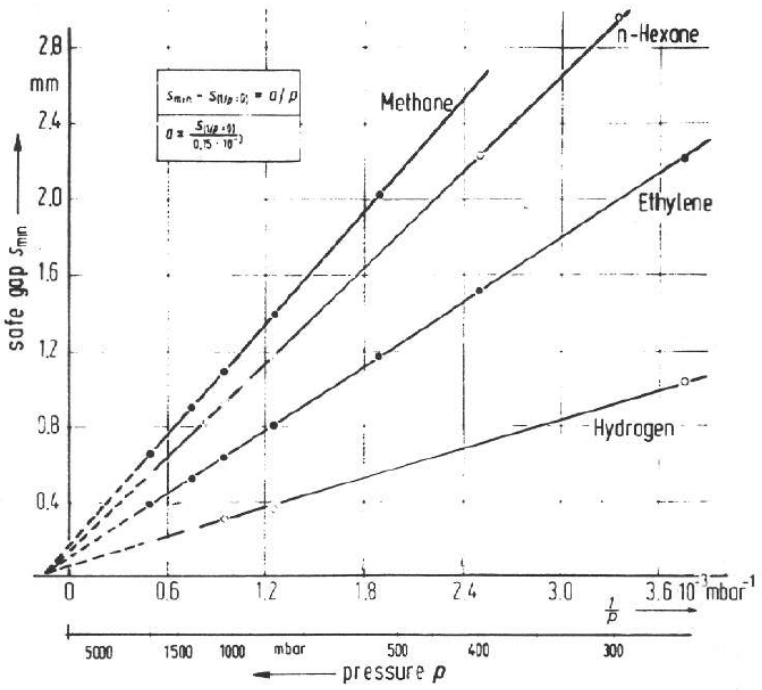

Figure 2.31 : *Safe gap s_{min} as a function of the pressure p for the most incendive gas/air and vapour air mixture prior to ignition, determined in the 20 cm^3 standard safe gap test apparatus. From (Redeker 1981).*

2.4.4 A Study of Critical Dimensions of Holes for Transmission of Gas Explosions and Development & Testing of a Schlieren System for Studying Jets of Hot Combustion Products (Larsen 1998)

Larsen's study showed that the channel hole diameter, gas mixture concentration, and the point of ignition have an influence on the probability of ignition of the external gas. He introduced a new term, MESD (Maximum Experimental Safe Diameter). MESD defined the largest hole diameter that prevented explosion transmission at the most dangerous point of ignition. Most of his experiments were conducted in a 1-liter primary chamber apparatus as shown in Figure 2.32 with 4.2 % propane - air.

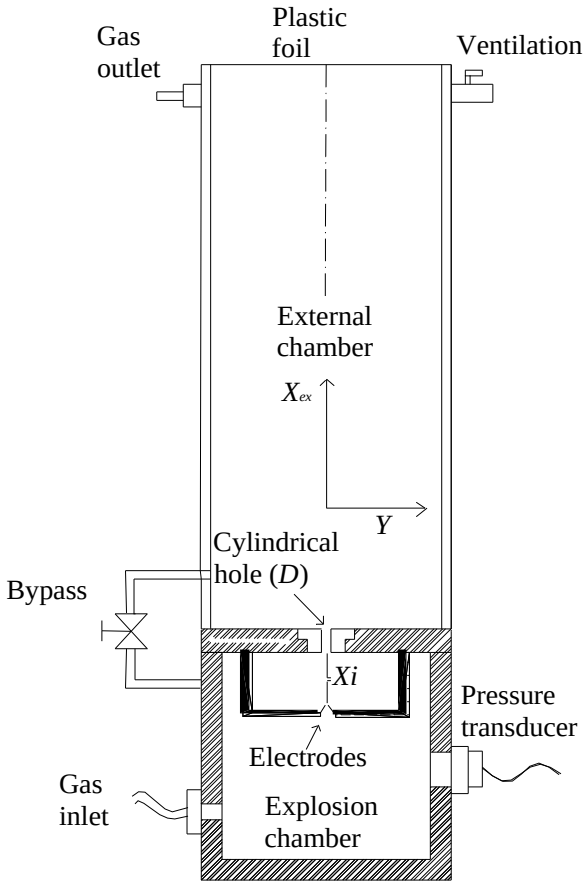

Figure 2.32 : *Experimental apparatus with 1-liter primary explosion chamber. From (Larsen 1998).*

From his experiments he created a plot of the diameters D_s and D_{10} for various ignition distances X_i, see Figure 2.33. (Larsen 1998) defines the diameters:

- D_s as the "*Safe diameter, the largest diameter giving no explosion transmission in 10 trials*"

  and

- D_{10} as "*The smallest diameter giving explosion transmission in 10 subsequent trials*"

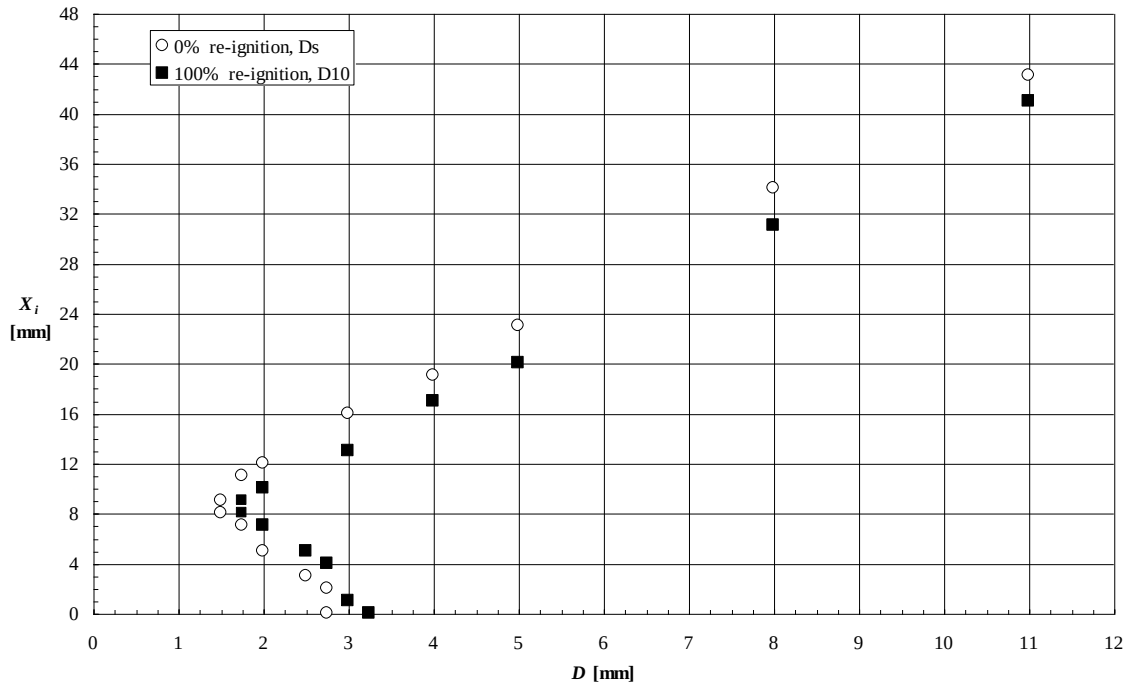

***Figure 2.33**: Safe diameter D_s and D_{10} for various ignition distances X_i. Primary volume V = 1 liter with bottom end removed and 4.2 % propane-air. From (Larsen 1998).*

The plot shows a clearly pattern, and as the ignition distance X_i varies, the safe diameter reaches a minimum of 1.5 mm. Larsen also completed the same experiments in the same 1-liter apparatus, but with the bottom end removed, and in a 21 ml primary explosion chamber. The safe diameter turned out to be almost the same for the three apparatuses of different volumes, but the distance from the hole to the ignition point varied. The 21 ml chamber had its minimum D_s at X_i = 3-4 mm, the 1-liter chamber gave a minimum D_s at X_i = 8-9 mm, and the 1-liter chamber with open bottom had a minimum D_s at X_i = 40mm. From this Larsen could make the conclusion that the point of ignition to yield minimum D_s depends on the volume of the chamber. The reason for this relationship is that the pressure rise in the chamber depends on the volume.

The pressure build-up is also dependent on the point of ignition. As the ignition point is moved from the hole inlet and towards the center of the chamber, the maximum explosion pressure, $p_{max,}$ increases, and the time to reach p_{max} decreases.

Larsen looked into the gas-air concentration and discovered that the maximum explosion pressure p_{max} was at its highest in the stoichiometric region.

2.4.5 Experimental Investigation of the Critical Dimensions, and the Effect of Damages, on Flame Gap on Explosion Safe Equipment (Opsvik 2010)

Opsvik's main intension of his study was to investigate the effect of different damages and wear-outs on Ex'd' safety equipment with propane as the explosive gas. The damages he tested were rusted and sand blasted flanges. The MESG results for all of Opsvik's experiments can be seen in Figure 2.34.

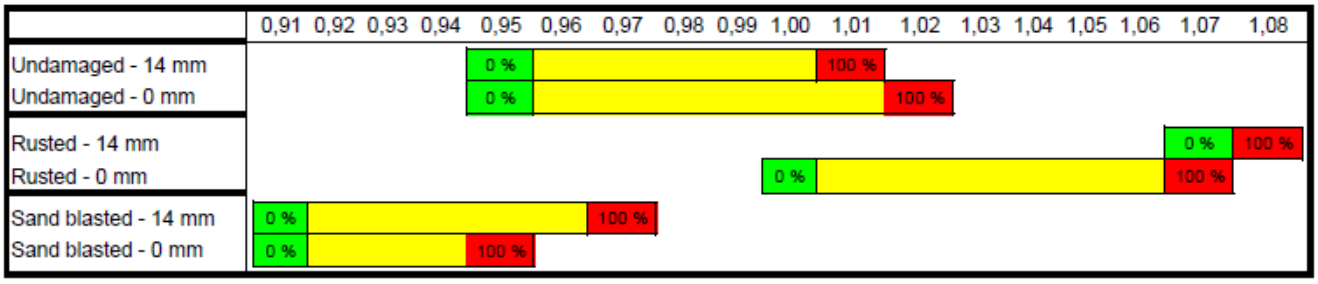

Figure 2.34 : *Explosion experiments with variation in flange openings. No re-ignition is indicated with the green color, while 100 % re-ignition is red. The transition range is the yellow area. From (Opsvik 2010).*

(IEC 2002) standard specifies that the position of the ignition source should be 14 mm from the gap opening. Opsvik therefore uses this position in his experiments. He also implemented experiments where the point of ignition was close to the gap opening, ≈ 0 mm.

To be able to easily change the flanges surfaces, a flexible apparatus had to be developed. A plane-flange apparatus was therefore built especially for Opsvik's purpose. The plane-flange apparatus was made in accordance with the different requirements, such as geometry, widths, and pressure, of IEC 60079.

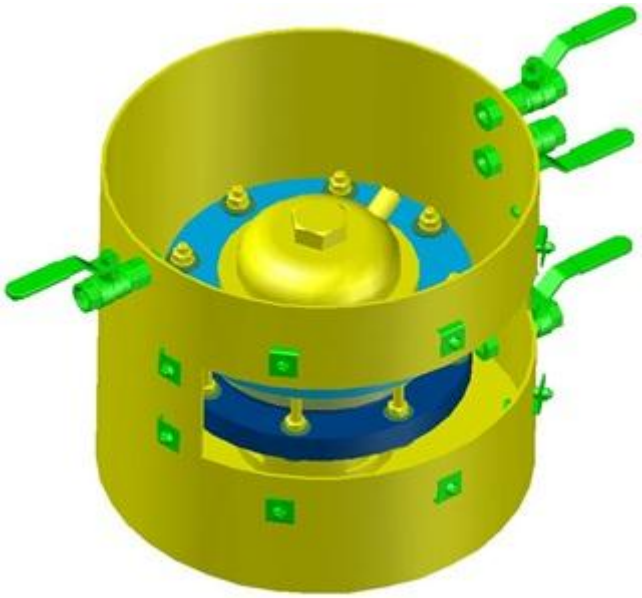

Figure 2.35 : *The plane-flange apparatus used in Opsvik's experiments. From (Opsvik 2010).*

The main conclusion of (Opsvik 2010)'s investigation was that the heavily rusted steel surface did not reveal any significant loss of flame gap efficiency, but the sandblasted surface gave a slight reduction of the efficiency.

2.4.6 An Experimental Study of the Influence of Major Damage of Flame Gaps Surfaces in Flameproof Apparatus on the Ability of the Gaps to Prevent Gas Explosion Transmission (Grov 2010)

In the experiments performed by Grov, premixed 4.2 % propane in air was used as the explosive gas. Both a plane circular flange apparatus (PCFA), which was used by Opsvik, and a plane rectangular slit apparatus (PRSA) were used. The "worst case" point of ignition was used in both apparatuses, namely 14 mm.

The different surfaces Grov investigated had grooves in them, either lengthwise or crosswise, where the lengthwise grooves are the ones in the same direction as the flow of the combustion.

Figure 2.36 : *Lengthwise and crosswise grooves respectively on the PCFA. From (Grov 2010).*

Figure 2.37 : *Lengthwise and crosswise grooves respectively on the PRSA. From (Grov 2010).*

(Grov 2010) gave a special naming system of the slits with grooves. An example of a slit name could be CH-8.2.3. The first letter tells us in which apparatus the experiment was performed in: either the Plane Circular Flange Apparatus or the Plane Rectangular Slit Apparatus. The second letter gives us information about the direction of the grooves: Horizontal (crosswise) or Vertical (lengthwise). The digits tell us the numbers of grooves, width of grooves, and depth of grooves on the gap surface respectively.

The main parameter examined in Grov's results was the differences in MESG values and efficiency of the damaged gaps compared to the undamaged gaps.

Table 2.8 : *Overview of experiments and MESG from different flame gap surface configurations. From (Grov 2010).*

Apparatus	Gap Surface Configurations	MESG (Ignition point 14 mm)	Mean Pressure at MESG [barg]
PCFA	Undamaged	0.95	0.128
PCFA	Sand blasted	0.91	0.144
PCFA	Corroded	1.07	0.100
PCFA	Plexi	N/A	N/A
PCFA	CH-8.2.3	1.14	0.286
PRSA	Undamaged	0.98	3.157
PRSA	PH-7.2.3	1.10	4.209
PRSA	PV-10.1.4	1.12	1.783
PRSA	Plexi plane slit	0.98	3.147
PRSA	Corroded 1	0.83	3.137
PRSA	Corroded 2	0.82	3.217
PRSA	Sand blasted	0.93	3.815

The overall conclusion of Grov's work was that surface damaged slits did not cause a reduction in the gap efficiency. In some cases the opposite reaction was observed, the gap efficiency was actually improved with damages on the surface, particularly for the crosswise grooves.

2.4.7 An Experimental Investigation of the Influence of Mechanical Damage, Rust and Dust on the Ability of Flame Gaps to Prevent Gas Explosion Transmission (Solheim 2010)

Solheim continued the work of Grov, but concentrated the investigation on multiple crosswise grooves and rusted grooves. Premixed 4.2 % propane in air was used as the explosive mixture in the same apparatus as Grov used, namely the Plane Rectangular Slit Apparatus, PRSA. Solheim completed ten explosions on each of the rusted slits and counted the numbers of re-ignitions achieved. For the slits with grooves, the MESG value was found to compare them to an undamaged slit's MESG value.

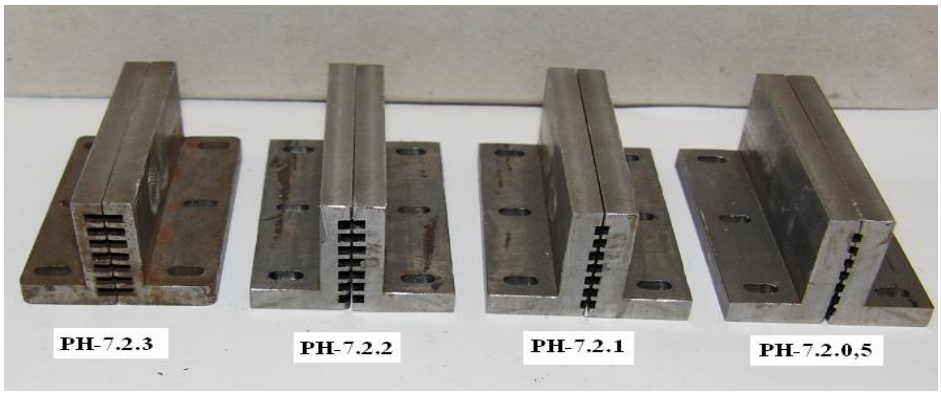

Figure 2.38: *Four different slits sets with multiple crosswise grooves with various depths. From (Solheim 2010).*

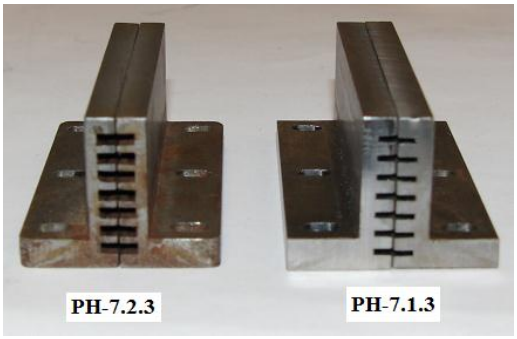

Figure 2.39 : *Two different slit sets with multiple crosswise grooves with various widths. From (Solheim 2010).*

Solheim also investigated how the damaged slits affected dust explosions by mixing aluminum flakes and pollen particles one at a time with air, in the Plane Circular Flange Apparatus, PCFA and the PRSA. Pollen is used by Solheim as a term for a mixture of cornstarch and lycopodium.

The conclusion due to rusted surfaces strengthens the conclusion of (Grov 2010). The gap efficiency was not reduced in any of the experiments performed. The slits with crosswise grooves take up more heat due to the increased surface area than the undamaged slits, which result in no re-ignition in the external chamber. Thus, the slits with grooves also increased the efficiency of the safe gap.

When it came to dust, the experiments performed in the PRSA showed that both aluminum and pollen dust easily fell through the flange to the primary chamber. Aluminum caused re-ignition in the external chamber in more than half of the experiments, but pollen did not cause re-ignition. Dust must therefore be treated as a hazardous element in areas where flameproof enclosures are being used.

2.5 Basic corrosion theory

(Davis 2000) defines corrosion as "*a chemical or electrochemical reaction between a material, usually a metal, and its environmental that produces a deterioration of the material and its properties*". The most common way rust is formed is based on nature of the corrodent: corrosion can be either wet or dry. A wet corrosion means that a liquid or moisture is necessary for the forming of rust, while a dry corrosion usually involves a reaction with gases of high temperature.

The most common material an Ex'd' safety equipment is made of, is carbon steel. Steel is a homogeneous mixture of two or more metal elements. Iron is the major component of steel.

The following theory is based on (Chang 2006):

The formation of rust on iron is probably the most common example there is. There are two criteria for formation of rust, oxygen O_2 and water H_2O. A part of the surface works as an anode, where an oxidation occurs:

$$Fe(s) \rightarrow Fe^{2+}(aq) + 2e^-$$

Another part of the surface will work as the cathode, where the electrons given up by the iron reduce oxygen to water:

$$O_2(g) + 4H^+(aq) + 4e^- \rightarrow 2H_2O$$

Thus, the overall reaction will be:

$$2Fe(s) + O_2(g) + 4H^+(aq) \rightarrow 2Fe^{2+}(aq) + 2H_2O(l)$$

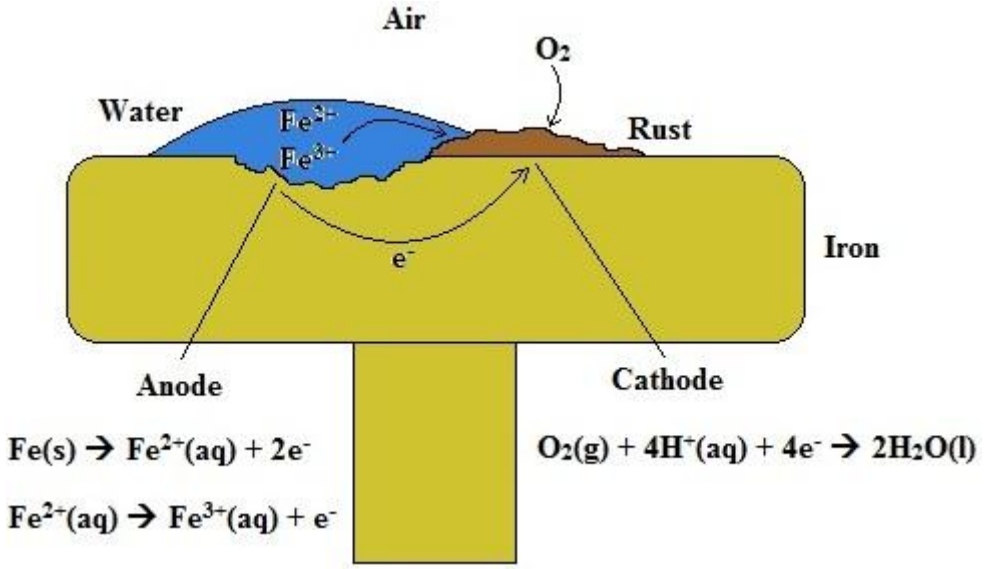

Figure 2.40 : *Illustration of rust formation on an iron surface.*

(Bardal 1994) states that seawater has chlorine content that provides maximum corrosion rate. But the corrosion rate is still not particularly high in relation to, for example, freshwater. This is because seawater contains Ca- and Mg-salt. I will not go specifically into the details, but the various precipitates from these salts form a protective film on the surface of the iron and prevent oxygen diffusion.

Since the corrosion rate depends on the amount of oxygen available, it will be at its highest in what (Bardal 1994) calls the droplet zone. In the droplet zone, thin water films will occur on the surface of the iron, and the supply of oxygen in this area is high.

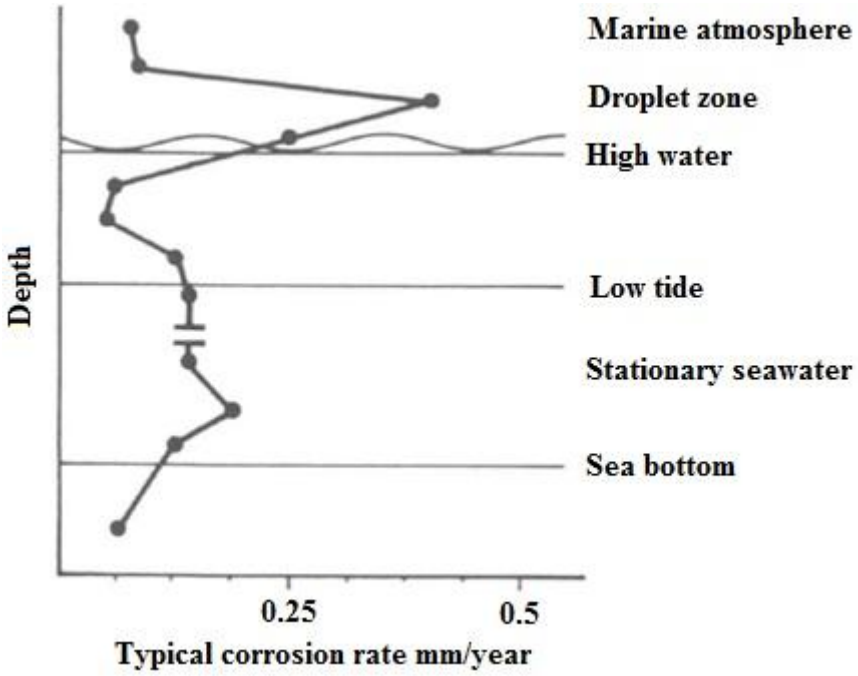

Figure 2.41 : *Corrosion rates (mm/year) on steel in seawater as a function of depth. Based on (Bardal 1994).*

As we can see from Figure 2.40, rust formation increases the roughness of the surface. As discussed in Section 2.2.3.2, this results in repair of the parts where the roughness exceeds what is required (>6.3 μm). In the long run, this leads to high costs.

3 Experimental Apparatuses and Procedures

This chapter contains information about all experimental apparatuses and procedures. The different experiments to be carried out in the present research are introduced in this chapter, as well as the motivations for implementing the experiments.

3.1 General experimental procedure

One apparatus has been used in the present work; the plane rectangular slit apparatus, see Section 3.2. The PRSA was built for (Larsen 1998)'s master thesis in 1998. Later (Einarsen 2001), (Grov 2010) and (Solheim 2010) have all used it. The PRSA is currently being used by (Steiner 2012), (Larsen 2012), and me.

The explosive test gas used in the present work is hydrogen mixed with air. The "worst case" ratio used throughout the work is tested to be 30.5 vol% hydrogen in air, see Section 4.1.

Worst-case scenarios are always used throughout the experiments when it comes to ignition point, gas-air ratio, and gap opening between the primary chamber and secondary chamber (MESG). MESG is used as a parameter describing if the explosion causes a re-ignition in the secondary chamber or not. The term gap efficiency is further on used as an expression for the ability of the flame gap to prevent a re-ignition.

3.2 The plane rectangular slit apparatus

As Figure 3.1 shows, the PRSA has two chambers, the primary chamber and the secondary/external chamber. The ignition source is located in the primary chamber, and a slit is separating the two chambers from each other. The slit has an adjustable gap opening, but in the present work, the MESG dimensions are often desirable to determine. The primary chamber has a volume of 1000 cm^3 and the external chamber has a volume of 3000 cm^3.

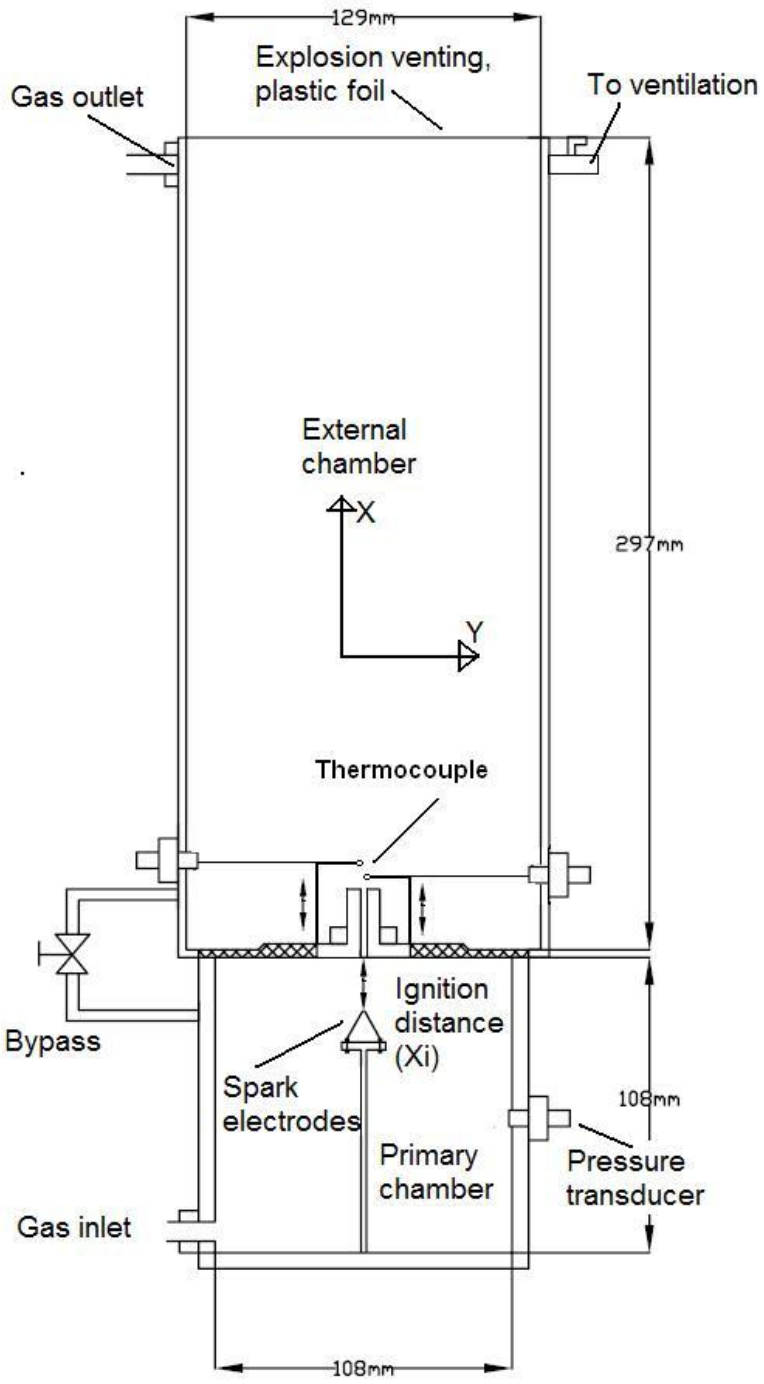

Figure 3.1 : *A cross section of the PRSA with a 1000 cm^3 primary chamber, and a flame gap of 25 mm width, used for determination of MESG for different gap surfaces in hydrogen/air mixture. From (Solheim 2010).*

Eckhoff designed the original version of the apparatus in 1998. The original version is shown in Figure 2.32, and was used by both (Larsen 1998) and (Einarsen 2001). Einarsen was the first to investigate the effect of damages on the slit's surfaces. Especially one problem with the original version of the apparatus had to be improved, and that was the procedure of tightening the slit. When Einarsen was to tighten his slits, the only opportunity was to tighten them at the top and without a value of torque used. By tightening the slits this way, a uniform

gap opening was unlikely to be achieved. In the modified version it is possible to tighten the slits at both the top and the bottom. The distance shims used in the present work are also of a higher accuracy than the ones used by Einarsen. In addition a torque screwdriver is used to make sure that all the slits are tightened with equal amount of strength.

3.2.1 The slits

As explained in Section 3.2, the slit is the part separating the primary chamber from the external chamber. To make sure the gap opening is uniform, a torque screwdriver is used on all the four screws on the bottom, as shown in Figure 3.2, and on the two screws at the top.

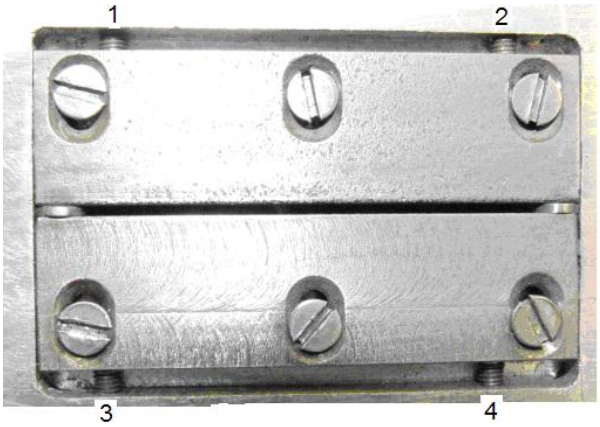

Figure 3.2 : *The flame gap opening that separates the primary chamber from the secondary chamber. The screws 1-4 are tightened with the same torque. From (Grov 2010).*

Table 3.1: *Slit dimensions.*

Slit Dimensions			
Width	**Length**	**Height**	**Gap Opening**
25 mm	56 mm	25 mm	Varying distances

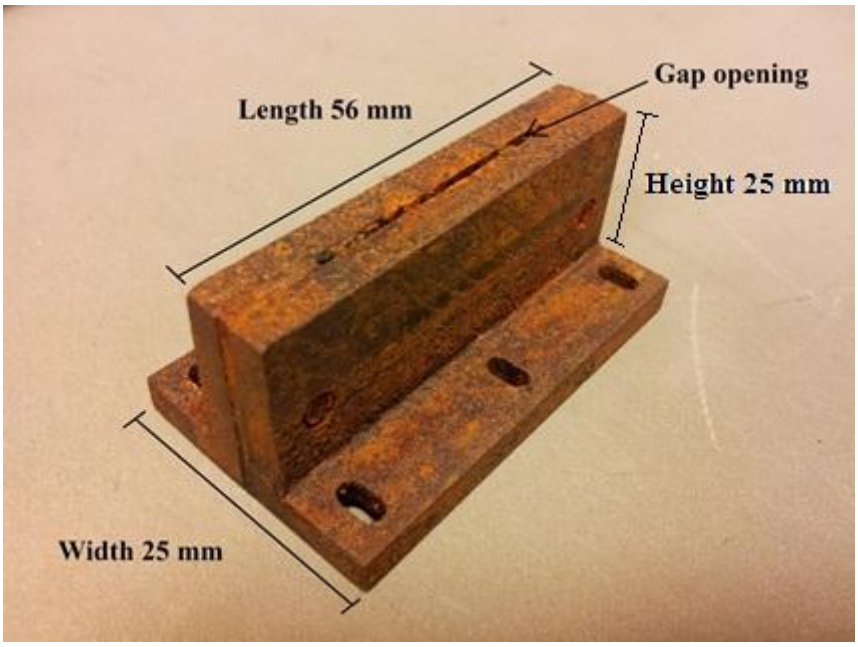

Figure 3.3 : *A rusted slit and its dimensions.*

3.2.1.1 Distance bits

Figure 3.4 a) shows the sheets of various thicknesses that have been used as distance bits in the slits' gap openings. Bits were cut out by hand and added together till the desired thickness was achieved, and thus placed on the two sides of the slits' inside to form the most uniform opening possible, see Figure 3.4 b). Thereafter the slit was tightened with a torque of 20 cNm.

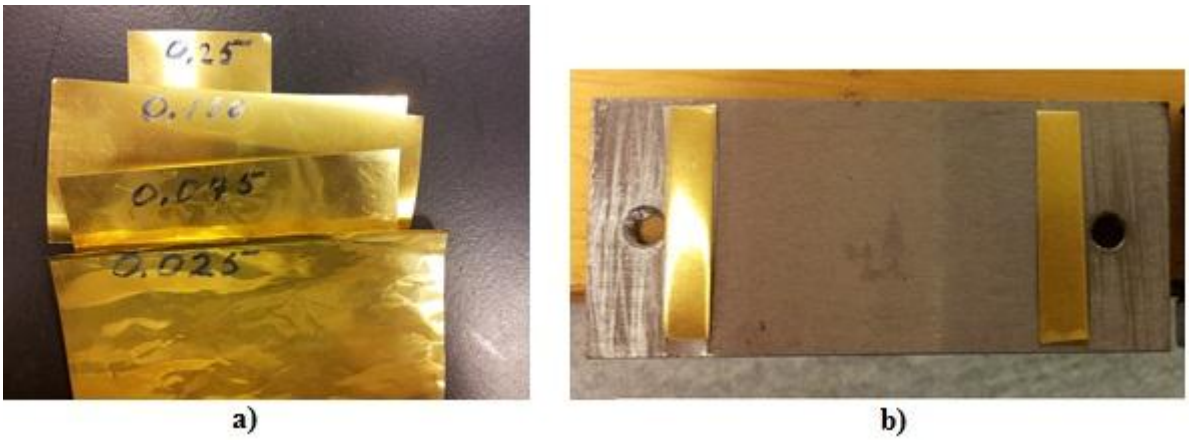

Figure 3.4: *a) Distance sheets.* *b) Distance bits placed in the slit.*

3.2.2 Thermocouples in the Plane Rectangular Slit Apparatus

For temperature measurements, thermocouples are placed in the PRSA. The thermocouples' positions are above the flame gap opening on the plate that separates the primary chamber from the secondary chamber. They can easily be replaced with either longer or shorter ones to adjust the distance from the gap opening.

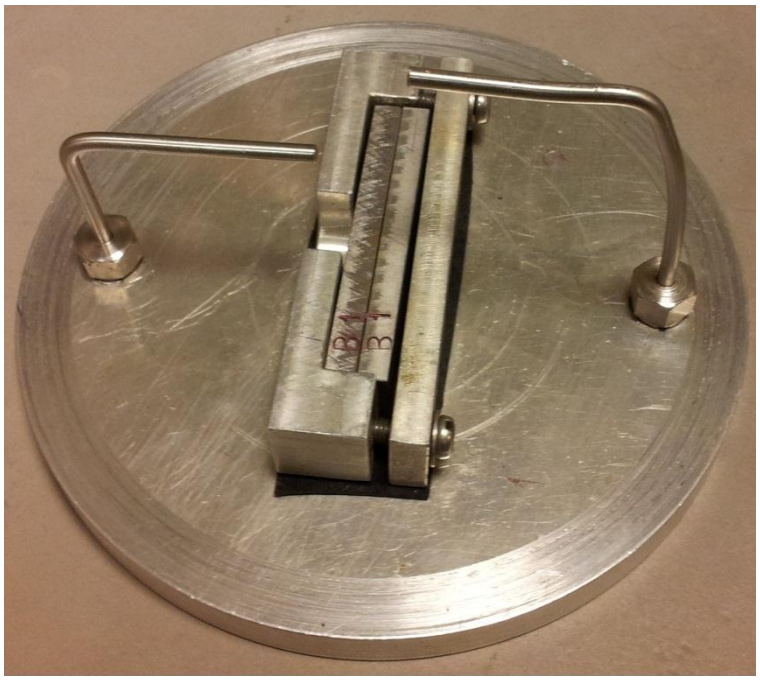

Figure 3.5 : *Thermocouples in the PRSA for temperature measurements.*

3.2.3 Sealing of cracks on side of the flame gap opening

When I carried out my first experiments for MESG determination, much smaller MESG values than the theoretic one were found. It turned out that the slit was a bit too small for the opening in the separation plate between the two chambers, so two cracks were found on both sides of the slit. These small cracks were bigger than hydrogen's MESG value and did therefore cause re-ignitions. The area around the slit was then sealed with a hard rubber material.

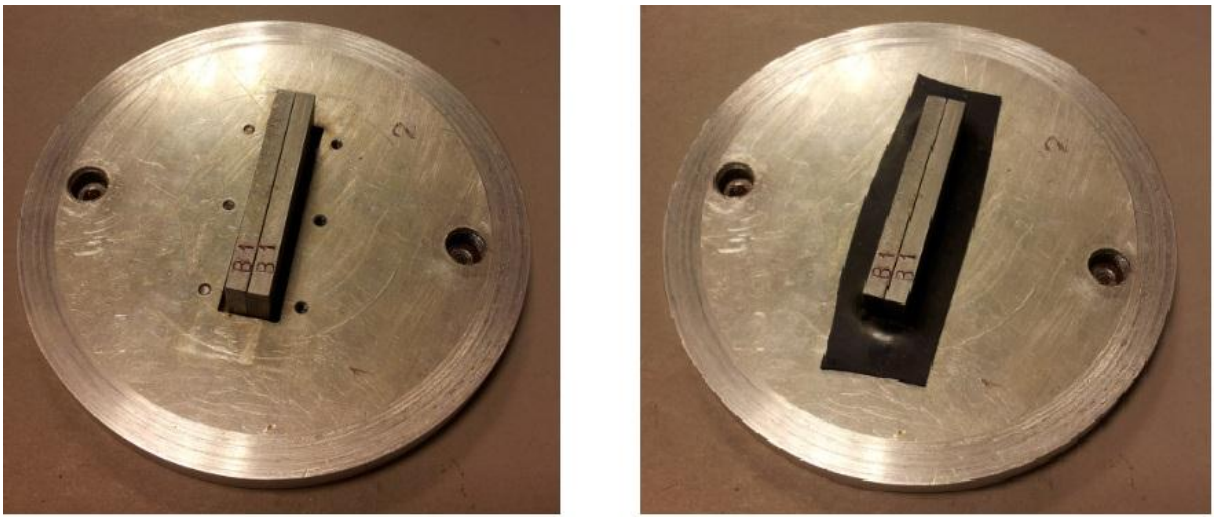

Figure 3.6 : *The first picture shows the original version of the separation plate between the primary and secondary chamber. The second picture shows the improved sealed version.*

After the area around the slit was sealed, MESG values close to the literature MESG value was found. This proves that the sealing was a good enough, and an important improvement to make.

3.2.4 Point of ignition in the plane rectangular slit apparatus

The ignition source in the primary chamber consists of two electrodes that generate a spark, see Figure 3.7. It is adjustable and can be moved vertically from the flame gap opening and towards the bottom of the chamber. (Grov 2010) performed experiments on the most harmful position of the ignition source, and made the conclusion of 14 mm from the gap opening. Experiments for determination of the most favorable point of ignition for re-ignitions will also be performed in the present work. Section 4.2 gives details about the experiments. The distance from the gap opening found to be the "worst case" ignition point, is the one being used throughout the research in the present work.

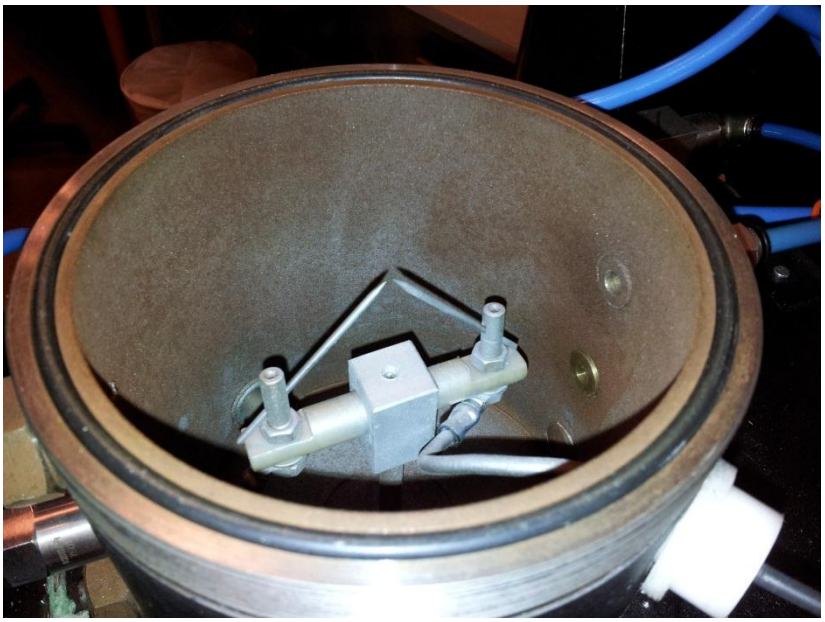

Figure 3.7 : *Ignition source.*

3.2.5 Pressure relief

Pressure relief, also called venting, is a safety device used to achieve a lower maximum pressure inside a container after an explosion has occurred. The pressure relief is designed to be the weakest part of the container, thus the pressure relief's p_{stat} has to be lower than the container's p_{stat}.

As the container registers a pressure rise caused by an explosion, the vent, as the weakest part, will open rapidly and allow hot combustion products to freely flow through and out to the surroundings.

Figure 3.8 : *Plastic foil used as the pressure relief during all experiments on the PRSA.*

The pressure relief used during this work's experiments is plastic foil fastened with a rubber band over the top of the chamber, see Figure 3.8. This is a quick and easy pressure relief to deal with since it does not need an accurate measure. The excess plastic foil will be attached on the outside of the explosion chamber and will have no effect on either the explosion or the pressure relief.

3.2.6 Direction of flow in the plane rectangular slit apparatus

When an explosion occurs, in our case in a container, the flame front expands with a spherical shape. When the flame front then hits the gap opening, hot combustion products will be pushed through the gap opening and into the secondary chamber. This direction of flow will therefore be as shown in Figure 3.9.

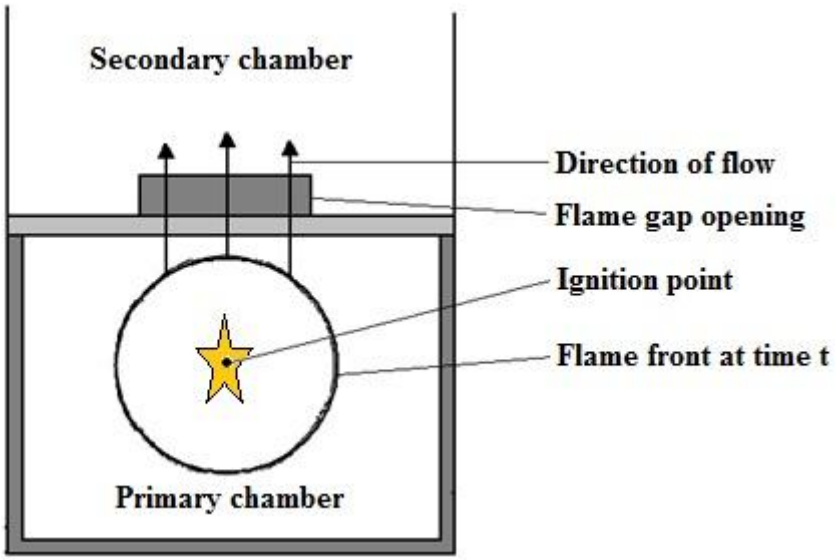

Figure 3.9 : *The direction of flow through the flame gap opening and into the secondary chamber.*

3.2.7 Crosswise and lengthwise grooves

Crosswise and lengthwise grooves refer to the direction of the grooves compared to the direction of flow. Lengthwise grooves are in the same direction as the flow, while crosswise grooves are perpendicular to the direction of flow. Both width and depth of the crosswise grooves will be varied. The number of seven grooves will be kept constant during all experiments on these slits.

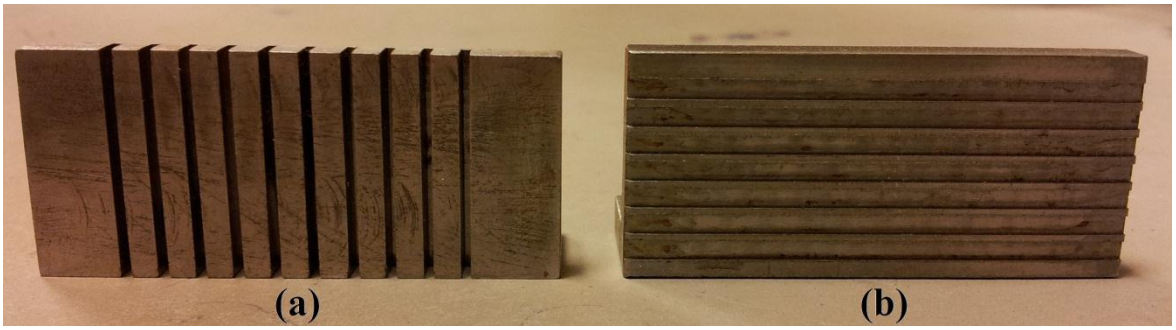

Figure 3.10 : *(a) shows lengthwise grooves and (b) shows crosswise grooves.*

3.2.8 Naming of slits

Both crosswise and lengthwise grooves of different dimensions were used by (Grov 2010). It was therefore important to create a commonly used naming system to separate the slits from each other due to their different dimensions. (Grov 2010) created the naming system used further on. See Section 2.4.6 for more information about the naming principle.

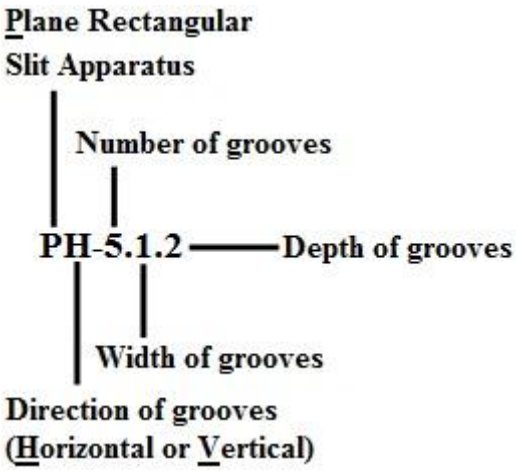

Figure 3.11: *Explanation of the naming principle created by (Grov 2010). Based on (Solheim 2010).*

3.3 Experiments carried out and the motivation for implementing the different experiments

3.3.1 Experiments for finding the most favorable hydrogen concentrations for re-ignitions

The stoichiometric ratio for a hydrogen – air mixture is 29.6 vol% hydrogen, but the maximum burning velocity of hydrogen appears at a concentration of 40.1 vol% hydrogen in air. Because of these two statements, it is interesting to determine at what hydrogen concentration the mixture provides the most re-ignitions in the secondary chamber.

Motivation

Ex'd' safety equipment are located where there is a risk of an explosion atmosphere to occur. Leaks are the one thing that could lead to the formation of an explosive atmosphere. The explosive atmosphere will change with time, as the fuel most likely will be diffused with air. The concentration of fuel, in this case hydrogen, in air, will therefore vary over time in the event of leakage.

3.3.2 Experiments for finding the most favorable ignition point for re-ignitions in the secondary chamber

Experiments for finding the most favorable ignition point for re-ignition were performed, although the (IEC 2002) standard specifies that the ignition distance shall be 14 mm from the gap opening. The Plane Rectangular Slit Apparatus used in the present work does not have the same geometric dimensions as the standard apparatus used for MESG determinations. The most favorable ignition point for re-ignitions may therefore vary. Experiments are conducted for both an undamaged slit and a slit with multiple crosswise grooves, PH-7.2.3. A certain gap opening was used in both cases. A gap opening of 0.30 mm was used for the undamaged gap, and a gap opening of 0.35 mm was used for the damaged gap, PH-7.2.3. The distance that provided most re-ignitions out of ten explosions was further on used as the standard ignition point.

Motivation

Ex'd' safety equipment contains electrical devices, which may cause an ignition, but the point of ignition can vary as the electrical devices are located different from one Ex'd' container to another. It is therefore important to use the worst-case scenario to achieve the best possible results from the experiments.

3.3.3 Undamaged flame gap surfaces

An undamaged and "ideal" surface is needed to be able to compare damaged surfaces to the undamaged ones, and further on draw conclusions on differences between the results due to the efficiencies of the safe gap. Experiments were performed on undamaged slits for MESG determination and temperature measurements.

3.3.4 Rusted flame gap surfaces

Ex'd' equipment are often placed in outdoor environment where rust will form over time. It is therefore of great interest to investigate important parts of this safety equipment, in this case the slits, and see how rust affects the gap efficiency. To make sure the rust was formed as realistic as possible, the whole slit was mounted in advance of the rusting process.

A total of twelve slits were rusted for this experiment. Six of them rusted for one month, and the other six for another month (two months in total). Since rust affects the surface roughness of the slits, these one and two months period of time will most likely result in different surface roughness. Figure 3.12 shows the rust formed in the flame gap opening on one of the six slits that have been exposed to sea water for one month, while Figure 3.13 shows the rust formation after two months in sea water.

Four of the slits added to rusting, for both one month and two months, had a gap opening equivalent to the MESG. This was done because the MESG values were individual for each slit, and it has not previously been examined in diversity what happens when slits with MESG

are rusted. The MESG values have been varying from 0.28 mm to 0.31 mm. For such a reactive gas as hydrogen, it is even more important to examine carefully whether it is possible to achieve a re-ignition at the MESG. The re-ignition will then most likely be caused by glowing rust particles, as the minimum ignition energy of hydrogen is extremely low, 0.02 mJ. Two of the remaining four slits have a lower gap opening than the MESG, and two have a higher gap opening than the MESG.

When experiments for determination of MESG values were conducted on the slits in undamaged conditions, prior to the rusting process, an ignition point of 14 mm and the stoichiometric ratio were used as standard test conditions. Since it was uncertain how time consuming the worst-case ignition point and concentration experiments would be, these test conditions were used as they have been showed to be the worst-case conditions for previous and similar experiments. The experiments on these slits in undamaged states were also prioritized first, as their rust formations were to take place over one and two months periods. The worst-case ignition point and concentration ratio found in the present research were later used as standard test conditions.

The slits were placed in a tidal zone where they were exposed to seawater, rainfall, and air. Rust formed from a tidal zone is carried out as realistic as possible, since these parts located offshore are exposed to all the same factors: seawater, rainfall, and air.

Figure 3.12 : *One of the six slits that have been exposed to sea water for one month.*

Figure 3.13 : *One of the six slits that have been exposed to sea water for two months.*

Table 3.2 : *Specifications of the eight different rusted gap surfaces.*

Specifications	**Undamaged gap surface**	**Rusted gap surface, 1 month**	**Rusted gap surface, 2 months**
Material	Carbon steel	Carbon steel covered with rust	Carbon steel covered with rust
Ra [μm]	0.2	6.5*	9.0*
Rz [μm]	2.0	35*	45*
Heat capacity [J/g·°C]	0.452	0.452*	0.452*
Thermal conductivity [W/m·K]	45	45*	45*
Length of slit [mm]	25	25	25
Width of slit [mm]	56.3	56.3	56.3
Thickness of slit [mm]	5	5	5*

* The values Ra and Rz for the rusted gap openings are estimated based on the measurements (Grov 2010) did in his work. The reason why these values are estimated from his work and not measured is because the measurement equipment is not capable of measuring such great values of roughness as the corrosion forms. Another reason is that the gap opening has been deliberately positioned for rusting while being screwed together to make the situation as realistic as possible. It is therefore not desirable to disassemble the two parts of the slit in order to measure the roughness. The heat capacity and the thermal conductivity also change due to the rusted steel surface, but it is not certain to what extent. But, since Grov put the slit's

parts separately for rusting, the amount of rust cannot be compared to the amount of rust achieved on the slits used in the present work. Grov's flame gap surfaces have been in direct contact with seawater. The direct contact with water may have caused a small amount of rust particles formed on the surface to be flushed off. In contrast to this procedure, the slits used throughout the present experiments were assembled when placed at seawater for rust formation. The gap opening surfaces have thus not been as directly exposed to water flow as if they were to be places at sea side unassembled. Water has streamed through the gap opening, but has not had equal opportunity to flush away rust particles as it had for Grov's unassembled slit parts. The fact that the slits were assembled when put for rusting causes rust particles to form between the two assembled slit walls. Since hydrogen's MESG value is only 0.29 mm, this small gap leads in particular to increased attachment to, and between, the two gap walls. A slightly greater roughness is thus estimated for the present slits.

Motivation

Since Ex'd' safety equipment often is placed outdoor, rust is the most common damage to occur on it. It is therefore important to investigate how rust affects the safety of the equipment.

Investigations of rust on Ex'd' equipment, or flameproof enclosures, have been performed at an earlier stage by (Opsvik 2010), (Grov 2010), and (Solheim 2010). Improvements have been made from each research to the other. Solheim had the slits assembled when put for rust formation, while both Opsvik and Grov had the slits parts for rusting separately. All earlier investigations have been carried out with propane, and gave different results. Opsvik got an increase in the MESG value of 12.6 %, while Grov introduced his results of an MESG value reduction of 15.3 %. These various results motivated Solheim to continue with the same gas (propane) and carry out more experiments. Solheim had five slits of different gap opening for three months to rust. Two of the slits gave 100% re-ignition in undamaged state, one slit got three re-ignitions out of ten explosions, and the last two gave no re-ignition. None of the rusted slits gave re-ignition, even though they had an average roughness much higher than the required value of 6.3 μm from (IEC 2007a).

Others have not yet tested hydrogen, which is the present work's gas.

3.3.5 Flame gap surfaces with various depths on multiple crosswise grooves

Surfaces with grooves of different depths were used in experiments to investigate the effect they had on the MESG. Figure 2.38 shows the four slits used in these experiments. Table 3.3 gives a complete overview of the properties and characteristics of the four slits.

Table 3.3 : *Specifications of the different slit sets with various depths. From (Solheim 2010).*

Specifications	PH-7.2.3	PH-7.2.2	PH-7.2.1	PH-7.2.0,5
Material	Carbon steel	Carbon steel	Carbon steel	Carbon steel
Rz [μm]	2.0	2.0	2.0	2.0
Ra [μm]	0.2	0.2	0.2	0.2
Length of slit [mm]	25	25	25	25
Width of slit [mm]	56.3	56.3	56.3	56.3
Thickness of slit [mm]	5.0	5.0	5.0	5.0
Number of grooves	7	7	7	7
Width of grooves [mm]	2.0	2.0	2.0	2.0
Depth of grooves [mm]	**3.0**	**2.0**	**1.0**	**0.5**
Heat capacity [J/g·°C]	0.452	0.452	0.452	0.452
Thermal conductivity [W/mK]	45	45	45	45

Motivation

(Grov 2010) and (Solheim 2010) have previously conducted similar experiments, but they have both been carried out using propane as the explosive gas. It has not previously been investigated whether the outcome is the same or not with hydrogen as the explosive gas. It is therefore of my interest to perform the same experiments, but with a different gas.

The research of Grov and Solheim resulted in increased gap efficiency and thus an increase in the MESG value. Their MESG value increased from 0.98 mm to 1.10 mm, which is an improvement of the gap.

3.3.6 Flame gap surfaces with various widths on multiple crosswise grooves

Two different slits were used during the experiments with various widths on the multiple crosswise grooves. Specifications on the slits can be seen in Table 3.4.

Table 3.4 : *Specifications of flame gap surfaces with different widths on the multiple crosswise grooves. From (Solheim 2010).*

Specifications	PH-7.1.3	PH-7.2.3
Material	Carbon steel	Carbon steel
Rz [μm]	2.0	2.0
Ra [μm]	0.2	0.2
Length of slit [mm]	25	25
Width of slit [mm]	56.3	56.3
Thickness of slit [mm]	5.0	5.0
Number of grooves	7	7
Width of grooves [mm]	**1.0**	**2.0**
Depth of grooves [mm]	3.0	3.0
Heat capacity [J/g·°C]	0.452	0.452
Thermal conductivity [W/mK]	45	45

Motivation

The motivation for conducting these experiments was to see if the widths of the multiple crosswise grooves lead to a change in the efficiency on the gap. (Solheim 2010) performed the same experiments in his thesis, but with propane as the explosive gas. Solheim discovered that the MESG value increased as the width of the crosswise grooves increased. An undamaged slit gave an MESG value of 0.98 mm, PH-7.1.3 gave MESG 1.00 mm, and PH-7.2.3 gave an MESG value of 1.10 mm. The gap efficiency increased with increasing widths.

These experiments, in common with the other ones, have not previously been tested with hydrogen. It is therefore of interest to investigate the outcomes when hydrogen is used instead of propane.

3.4 Temperature measurements over the flame gap opening

(Solheim 2010) made a temperature measurement system that made it possible to measure the temperature of the penetrating combustion gases right above the gap opening in the explosion chamber. This system consisted of two thermocouples that were mounted on each side of the Plane Rectangular Slit Apparatus; see Figure 3.1, just above the flame gap opening. Solheim attached the two thermocouples to two replaceable rods. These rods could be replaced with other rods, either shorter or longer ones, to perform temperature measurements at different altitudes. Temperature measurements were performed on the penetrating combustion gases just above the flame gap opening of the slits with multiple grooves. The temperatures carried out from these experiments were then compared with the temperatures taken from experiments conducted with undamaged slits. The experiments on the slits with multiple grooves were also carried out with different gap openings to see how this affected the temperature.

Motivation

The motivation for the temperature measurements was to see how the different slit surfaces affected the temperature above the flame gap opening. The values obtained from the experiments will give an indication of an increase or decrease in the probability of re-ignition, due to higher or lower temperature.

3.5 Filling and analysis of gas mixture

To make sure the gas-air ratio is the same throughout all experiments, a gas analyzer was used. The gas analyzer used was a Servomex 4200 Industrial Gas Analyzer, which has its specialty in analyzing oxygen. The 4200 series is intended to form flammable mixtures. Four gas streams may be controlled simultaneously.

The concentration of hydrogen in air used in the present work is 30.5 vol%. This means that the quantity of oxygen at the experimental ratio is 14.6 vol%. Calculations for stoichiometric ratio are shown in Appendix A. Two displays show the gas flows of hydrogen and air. A needle valve can regulate each gas flow separately till the desired concentration is achieved. A mechanical flowmeter was installed to be able to regulate small amounts of fuel. The gas analyzer fills both the primary and secondary chamber to achieve a uniform concentration. The gas returning from the explosion chamber is the one being analyzed.

Hydrogen of quality 5.0, which is high-purity hydrogen, was used in the present work. The quality number is a two-digit numerical code that describes the purity of the gas. The first digit tells us how many numbers of nines we have in total, and the second digit tells us the number that comes after the last nine. A quality of 5.0 does therefore correspond to 99.999 % pure gas. Such a high-purity level contributes to minimize the uncertainty of the chemical composition and reaction of the gas. See Appendix C-1 for a detailed schematic description of the Servomex 4200 Industrial Gas Analyzer.

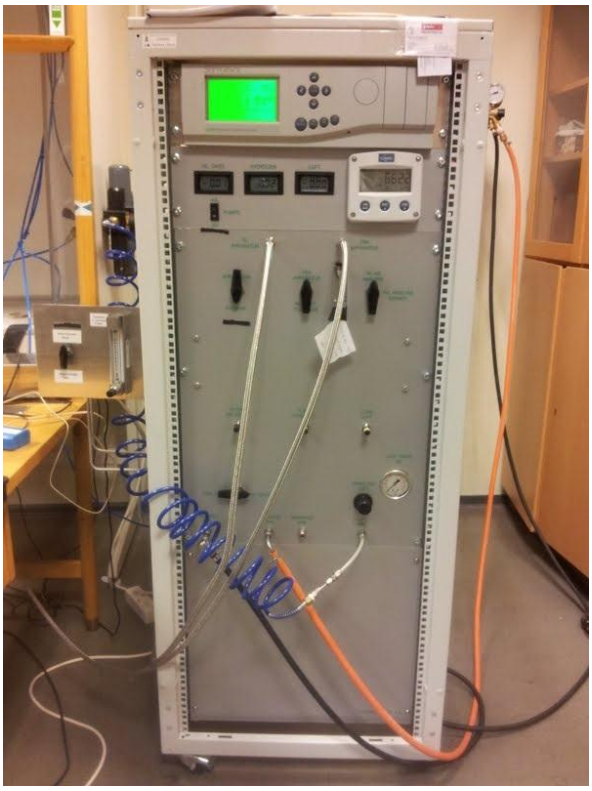

Figure 3.14 : *The Servomex 4200 Industrial Gas Analyzer used for filling and analysis of the gas mixture.*

3.6 Measurement methods and data storage

This chapter is similar to chapter 3.6 in (Opsvik 2010).

3.6.1 Data acquisition system

When a uniform and homogenous hydrogen-air mixture was contained within the explosion apparatus, a spark was generated in the primary chamber and the explosion pressure build up in the primary chamber was measured. Measurements data was stored in a computer so the results could be analyzed and compared at a later stage.

A NI USB 6009 card was connected to the computer and performed both controlling and logging of the experiment. This NI-CAD card is programmed by LabView software, which is documented in Appendix B-2.5. The software enables the user to change all setup parameters, within the limitations of the card and hardware.

3.6.2 Control system

A tailor made data acquisition and control system was made to control the experiments. Digital ports were used to remote triggering of the experiment and to reset and activate the pressure measurement system. Figure 3.15 shows the control and measurements system.

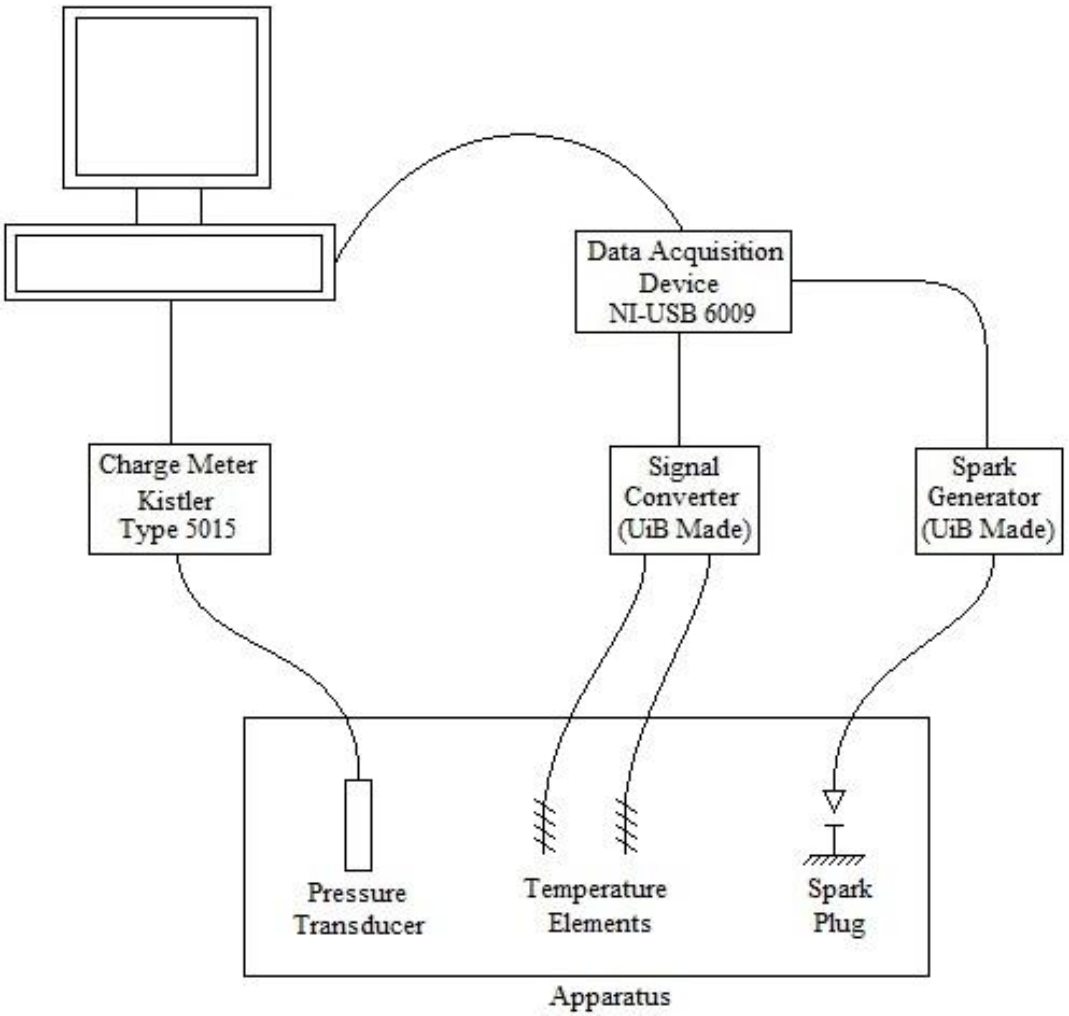

Figure 3.15 : *Control system and data acquisition.*

3.6.3 Pressure measurements

In order to measure the explosion pressure in the primary chamber as a function of time $p_i(t)$, a set of piezo electric transducers with a charge amplifier were mounted in the cylinder wall. Additional information and calibration certificates can be found in Appendix E.

3.6.4 Temperature measurements

Temperature measurements were taken from all experiments. Two thermocouples classified as type *k* were used to measure the temperature of the hot combustion gases penetrating through the gap opening from the slits. Type *k* thermocouples are made out of two different metals, see Appendix C-2 for detailed information. This mix of metals leads to a small voltage that increases with temperature. The signal was amplified through an operational amplifier (AD597) and saved on the computer.

3.7 Sources of error

This chapter is similar to chapter 3.8 in (Opsvik 2010).

3.7.1 Data acquisition system

Amplification of measured signal is important in order to understand the achieved values and to compare them with each other at a later stage. One A/D converter reads all the channels during the experiments. Switches inside the card choose which channel to read. If one channel is not satisfactory amplified, the signal from another channel could influence the signal read next.

3.7.2 Gas concentration measurements

This part is based on (Henden 2011)'s section 3.1.5.

The gas analyzer measures oxygen with a paramagnetic oxygen sensor, and it measures hydrogen using an infrared analyzer. The paramagnetic oxygen analyzer is a high accurate measurement technique for oxygen concentration. Due to the oxygen paramagnetism, the oxygen molecules will be drawn to the strongest part of a magnetic field where two nitrogen-filled glass bulbs are places on a rotatable dumbbell. The nitrogen has opposite polarity and will be displaced by the oxygen so that the dumbbell will start rotating. An opposing current is applied to keep the dumbbell at its original position, and this current is directly proportional to the partial pressure of oxygen and is represented electronically as vol% oxygen. The uncertainty of the oxygen analyzer is 0.1% of the measured range of 0-100 vol%, yielding and inaccuracy for measured concentrations of $\pm$ 0.1.

The infrared gas analyzer absorbs energy in the infrared part of the spectrum. This absorption is selective and is occurring at a special frequency corresponding to the fluctuations in the molecules. Measurements of different wavelengths enable detection of a gas and the degree of absorption gives the concentration of the gas. A calibration with two known gas concentrations has to be implemented in order to measure the range of concentrations in between. The uncertainty of the infrared analyzer is 2 % of the measuring range of 0-10 vol%, yielding an inaccuracy of $\pm$ 0.2 for the measures concentrations.

3.7.3 Atmospheric pressure, temperature, and air content

The normal mode of operation of the gas analyzer is to discharge the gas sample from the measuring cell at atmospheric pressure. The sensitivity of the cell will be proportional to the atmospheric pressure. The effect is that of a span change, so the error introduced is zero at zero concentration and maximum error at full scale. A change of 1% in the atmospheric pressure will thus cause a change of typical 1% of reading.

The manufacturer has stated that the effect of temperature change is less than 0.2% of full-scale display + 0.4 of reading, per degree Celsius.

The air coming from the gas analyzer to the explosion chamber is air taken directly from the area it is placed in. When concentration calculations have been made, a content of 21 % oxygen and 79 % nitrogen in the air has been assumed. This may not completely match the real content of the air where the gas analyzer is placed, and may thus be a source of error in order of the explosion pressure, as the reaction may not be of the desired and calculated proportions.

3.7.4 Air humidity

The hydrogen gas used in the experiments is mixed with pressurized air supplied from local distribution network. No measurements of humidity are done, but the air is filtrated and dried in a unit downstream the air compressor. In any case the quality of the air is not documented, pollution in form of oil, dust particles, or water may exist in the supplied air. This may have an effect on the results.

3.7.5 Pressure

There is uncertainty in the pressure readings due to the resolution of the pressure transducer. Kistler, the manufacturer of the piezoelectric transducer, states that the accuracy of the transducer is $\leq \pm 0.08\%$ of full-scale output when the calibration range is in the area of 0 to 25 bars. This gives an accuracy of ± 0.02 bars at the used measuring range, which is well within acceptable limits.

The pressure transducer is mounted a fixed distance at the vertical chamber wall of the primary chamber. The transducer may not detect local pressure gradients in the chamber.

3.7.6 Temperature

The thermocouples used in this work are not constructed to measure temperatures in explosions. The extremely rapid increase in temperature due to the explosion causes some uncertainty to the measured temperature, but it is assumed that the temperature differences measured between different experiments are valid.

3.7.7 Condensed water

Water will, of a certain amount, condense on the inside of the walls of the primary chamber after an explosion, and this may represent a significant source of error. Water may evaporate from the warm explosion apparatus walls during gas filling and the subsequent period of turbulence settling, altering the gas composition. Water in the gas mixture may affect reaction mechanism and heat capacity, whereas a small portion of the water at the vessel walls may evaporate during the explosion. It is generally assumed that the explosions will be too rapid for significant amounts of water to evaporate.

3.7.8 Experiments

There are uncertainties due to construction tolerances in size of volumes, ignition positions, and flange diameters and distances. In addition there is accuracy related to the experimental work, although good experimental procedures would counteract this, with reference to Appendix B-2.2.

The dimension of the distance shims is observed to have a variation of approximately ± 1 hundredths of a millimeter.

3.7.9 Distance bits

Since the distance bits were cut out by hand, some curvature or bends may have been formed on their edges. Bended distance bits would result in a slightly larger flame gap opening than desired, which may explain the different MESG values achieved for the undamaged slits prior their delivery for rust formation.

3.7.10 Experimental apparatus, PRSA

The plane rectangular slit apparatus has several hoses that supply the gas mixture from the gas analyzer to the primary and secondary chamber, but the secondary chamber also has a hose that leads directly to the exhaust. When the primary and secondary chambers are filled with the right gas mixture, all valves on the hoses from the gas analyzer to the experimental apparatus are closed. But such a shut-off valve is not available for the hose leading to the exhaust, which may cause leakage to the exhaust of a certain amount of the gas mixture before an ignition of the explosion takes place. This is a source of error that will have a greater impact on the current work compared to previous work, since hydrogen is the most volatile gas in relation to propane and ethylene, which have been used in the work of others.

4 Experimental Results and Discussion

This chapter contains results and discussion of the various experiments conducted during this research. The primary sections of the chapter are the results from the re-ignition experiments with rusted gap openings and the determination of MESG values for slits with multiple crosswise grooves. The aim is to compare the MESG values of the rusted slits and the slits with grooves, to the undamaged slits' MESG values. The MESG value provides an indication of whether the efficiency has increased or decreased.

The chapter also contains other essential results as the worst-case hydrogen concentration, worst-case ignition positions for both undamaged- and damaged slits, and temperature measurements above slits with multiple crosswise grooves.

4.1 Finding the most favorable hydrogen concentration for re-ignition

In this part of the experimental work, a total of 50 explosions have been carried out; ten explosions at each of the five different concentration ratios. Since the gas analyzer only analyses the amount of oxygen present, the hydrogen concentration is calculated from the analyzed amount of oxygen. Appendix A shows the calculations procedures of hydrogen and oxygen concentrations.

4.1.1 Results

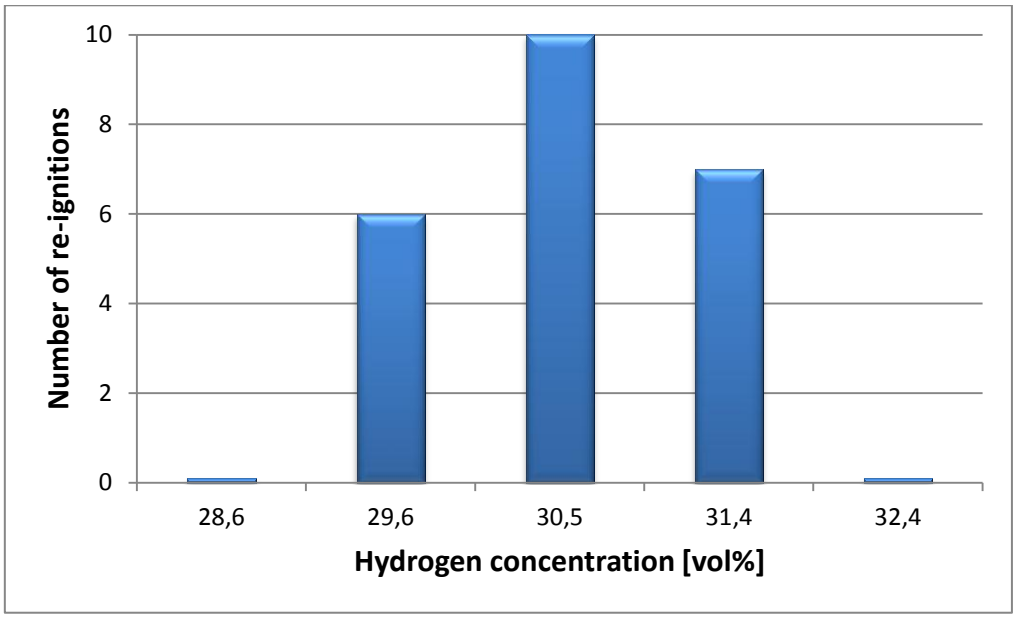

Figure 4.1 : *Plot of the number of re-ignitions out of ten attempts per different hydrogen concentration, with a gap opening of 0.31 mm for an undamaged gap.*

Figure 4.1shows that the hydrogen concentration that achieves the most re-ignitions in the outer chamber is at 30.5 vol% hydrogen. This is slightly above the stoichiometric mixture. The second concentration measure bar in the graph illustrates the number of re-ignitions at stoichiometric ratio, which is only at a concentration of 0.9 vol% lower than the concentration that provides the highest number of re-ignitions.

Table 4.1 : *Mean maximum explosion pressure for different hydrogen concentrations. Ten explosions were performed for each concentration. A gap opening of 0.31 mm was used on an undamaged slit.*

Concentration of H_2 [vol%]	Mean maximum pressure [barg]
28.6	2.529
29.6	2.485
30.5	2.440
31.4	2.438
32.4	2.441

Figure 4.2 shows the pressure development from experiments performed with the five different concentrations between 28.6 vol% H_2 and 32.4 vol% H_2. The gap opening is 0.31 mm for all experiments. The graph shows that all curves have a similar slope.

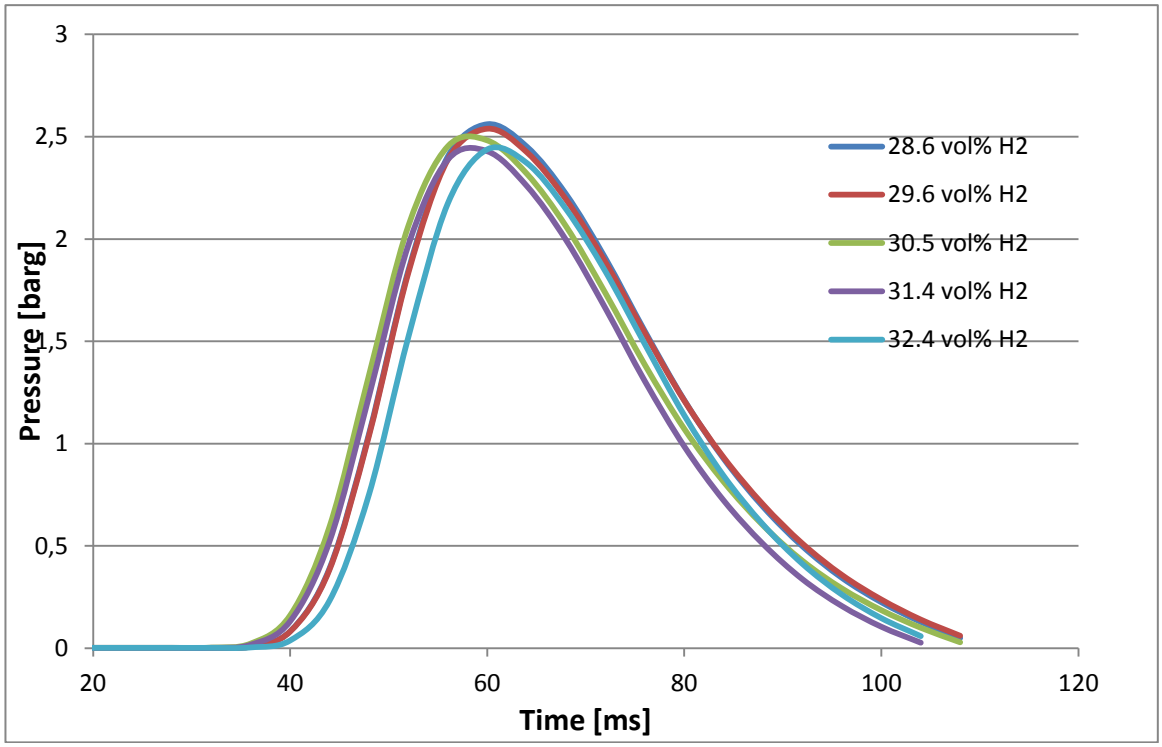

Figure 4.2 : *Pressure development in the primary chamber for explosions of mixtures with various concentrations between 28.6 vol% H_2 and 32.4 vol% H_2.*

Since the ignition is initiated manually, it is difficult to know exactly when the pressure begins to rise. To make the graphs easier to compare, they are positioned so that they reach their maximum pressure at about the same time.

4.1.2 Discussion

A certain concentration range was tested for generation of re ignitions in the secondary chamber during this section of the experimental work. The basis for the determination of the concentration range was the stoichiometric ratio. From there, it was tested both richer and leaner mixtures until no re-ignition was achieved. This resulted in a concentration range of 28.6 – 32.4 vol% hydrogen in air.

Section 2.1.1 and (M. Kröner 2003) explains how the burning velocity varies with respect to the concentration of hydrogen in air. Kröner states that hydrogen reaches its maximum burning velocity of 3.2 m/s at a concentration of 40.1 vol% hydrogen in air. One may think that the concentration where the burning velocity is at its maximum is the worst-case concentration, but the result from the present work shows that the most favorable hydrogen concentration for re-ignition is at 30.5 vol% hydrogen in air. (IEC 2010) has tested for the most incendive mixture in the IEC standard apparatus showed in Figure 2.13, which gave the result 27 vol% hydrogen. The reason why the result obtained in this section does not coincide entirely with the IEC's result, may be due to the dimension differences in the two apparatuses used, as the most incendive mixture depends on the dimensions of the test apparatus.

The reason why the most favorable concentration for re-ignitions was found to be 30.5 vol%, and not 40 vol% where the burning velocity is at its maximum, may be explained by the graph shown in Figure 2.4. The graph is a plot of the temperature and burning velocity as a function of hydrogen concentration in air. The temperature reaches its maximum value at a concentration just above 30 vol% hydrogen in air, which is in accordance to the most favorable concentration achieved in this section. Where the jet of hot combustion products has the highest temperature, the probability of generating a re-ignition is also at its highest.

It can be observed from Table 4.1 that the mean maximum pressure decreases as the concentration increases, but since only a small range of the concentration was tested, it is difficult to draw any conclusions on why it is so based on the pressure measurements.

4.2 Finding the most favorable ignition point for re-ignition through undamaged slits

A total of 50 explosions were carried out during this section of the research. Ten explosions were conducted for each different point of ignition. The five different ignition positions tested were 5 mm, 10 mm, 15 mm, 20 mm, and 25 mm. The undamaged slit used during these experiments had a gap opening of 0.30, which is just above the undamaged slit's MESG of 0.29 mm.

4.2.1 Results

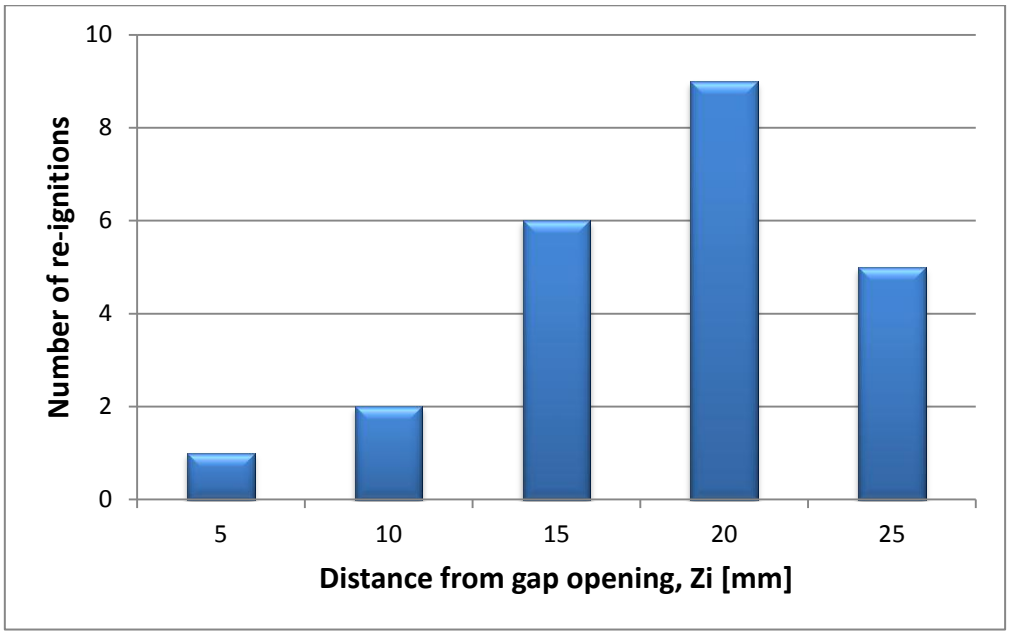

Figure 4.3 : *Plot of the number of re-ignitions out of ten attempts per distance, with a gap opening of 0.30 mm for an undamaged slit.*

Figure 4.3 shows that ignition at 20 mm from the flame gap opening gave most re-ignitions in the secondary chamber, a total of nine re-ignitions. This point of ignition is therefore considered as the most favorable point of ignition for re-ignitions, and is thus the worst-case area for ignition.

4.2.1.1 Mean maximum explosion pressures for different ignition distances

Table 4.2 : *Mean maximum explosion pressure for different ignition points. Ten explosions were performed for each distance. A gap opening of 0.30 mm was used on an undamaged slit.*

Surface configuration:	Undamaged
Gap opening, Y_i [mm]	0.30
Ignition distance, Z_i [mm]	**Mean pressure [barg]**
5	2,465
10	2.469
15	2.432
20	2.508
25	2.575

Table 4.2 shows a systematic increase in pressure, apart from the ignition distance at 15 mm. As the distance from the flame gap opening increases, the pressure also increases.

Figure 4.4 shows the pressure development from experiments performed with the five different distances 5 mm, 10 mm, 15 mm, 20 mm, and 25 mm from the flame gap opening. The gap opening is 0.30 mm for all experiments. The graph shows that all curves have a similar slope.

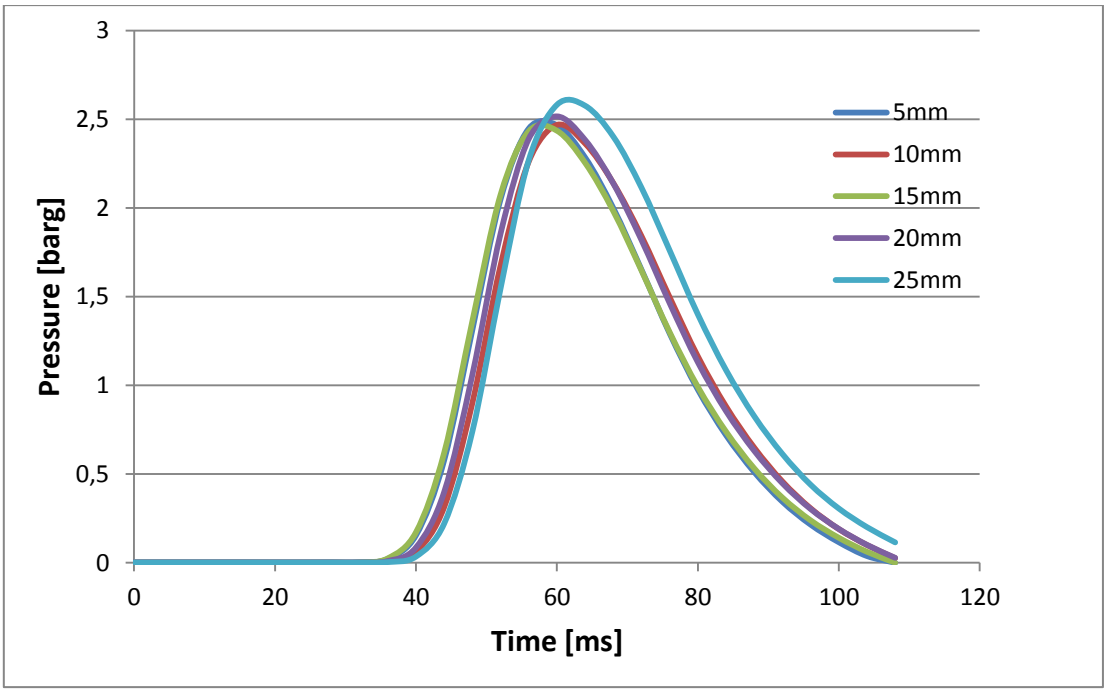

Figure 4.4 : *Pressure development in the primary chamber for explosions with ignition distances 5 mm, 10 mm, 15 mm, 20 mm, and 25 mm from the gap opening.*

4.2.2 Discussion

(Larsen 1998)'s chapter 2 explains how the pressure increases when the ignition source is moved towards the center of the primary chamber, which has a total height of 10 cm. As the ignition source is moved away from the flame gap opening, the combustion process may develop over a longer time period before the flame front reaches the flame gap opening. This increased amount of time leads to an increase in pressure. The flame front will also be affected by the change of ignition position, as it will reach the walls of the primary chamber at different times. This may lead to changes in the pressure and temperature of the combustion gases, as the walls most likely will cool the combustion products before the combustion is completed. The walls will also adsorb some radicals, which affect the combustion in a small degree, as the combustion becomes slightly limited. Section 2.3.4 explains the terms radicals and radical chain reaction.

As the results showed, there occurred most re-ignitions at a distance of 20 mm from the flame gap opening. This is a different outcome than previous research completed by (Grov 2010) and (Solheim 2010) for propane, which gave a favorable ignition point of 14 mm. Possible reasons for this difference between the outcomes of experiments performed with hydrogen and propane may be the maximum burning velocity and the chemical reactivity of the gases. Hydrogen has a maximum burning velocity of 3.25 m/s, while propane has a maximum burning velocity of 0.46 m/s. When the explosive mixture is ignited, the flame front expands as a spherical front, explained in Section 3.2.6. The longer out the flame front is able to spread, the more the pressure and the flux through the flame gap opening will increase. When the burnt gases penetrate through the flame gap opening and into the secondary chamber, they will have a greater flux and thus be more turbulent when ignited at 20 mm, compared to what they would have been if ignited at a distance of 14 mm from the gap opening. Propane has its favorable ignition point for re-ignitions at 14 mm, but propane has a slower chemical reaction time than hydrogen, see Section 2.1.1. Hydrogen can have a more turbulent flow through the flame gap than propane, and yet achieve a re-ignition, since the chemical reaction time is faster than the cooling of the combustion products due to mixing with cold unburned gases. See Section 2.3.6.2 for more detailed information about cooling from mixing with cold unburned gases in the secondary chamber.

Phillips introduced the term critical velocity; see Section 2.4.1, which described the velocity that gave the smallest safe gap opening. When the ignition position was moved away from the gap opening in the present work, the number of re-ignitions increased until the distance reached 20 mm. After moving the ignition position further away than 20 mm, the number of re-ignitions decreased. This demonstrates that there is a critical pressure and flux through the flame gap that leads to an increase in numbers of re-ignitions in the secondary chamber. This can be explained by the fact that an increased velocity through the flame gap reduces the contact time with the gap walls, and thus reduce the amount of cooling of the combustion gases. When the velocity is then further increased, the cooling due to mixing with unburned gases is a greater factor than the less contact time and less cooling from the gap walls. The number of re-ignitions will then decrease.

Phillips also stated that experiments performed by him showed that the favorable ignition position for re-ignitions was close to the gap opening, with exceptions for more reactive gases as hydrogen, which is the gas used in the present work.

The theory discussed is in agreement with chapter 2's theory, except for the theory of increased initial pressure by Redeker. Redeker's experiments resulted in a smaller safe gap opening with a higher initial pressure. The present work shows that the pressure increases as the ignition position is moved further away from the gap opening, but the number of re-ignitions reaches its maximum at 20 mm, although the pressure continues to increase.

The pressure development graph, Figure 4.4, shows that all curves have approximately the same slope and pressure development, but a slightly increase in maximum pressure is observed as the ignition distance from the gap opening increases. Increased pressure due to increased distance from the gap opening corresponds to the theory stated by (Larsen 1998).

4.3 Rusted flame gap surfaces

A total of twelve bolted slits with various gap openings from 0.25 mm to 0.35 mm were put at seaside for rusting; six of them for one month and the other six for two months. Approximately 300 explosions were performed on these twelve slits in total. About 180 explosions prior rust formation and ten explosions were conducted on each finished rusted slit, thus another 120 explosions.

The first explosion in the series of ten explosions is the most important one in order to recreate the danger in the industry. If an accidental explosion was to occur in the industry, the Ex'd' apparatus would be in the same state as the slit in the present work will be during the first explosion, and must therefore be investigated closely.

4.3.1 Results

4.3.1.1 One month of rusting

Table 4.3 : *Ten explosions have been applied to six various slits at both undamaged and corroded state.*

Gap opening, Y_i [mm]	Ignition distance, Z_i [mm]	Number of re-ignitions		Mean pressure [barg]		Pressure of the first explosion [barg]
		Undamaged	Rusted	Undamaged	Rusted	
0.25	20	0	0	2.639	2.370	2.760
0.28	20	0	0	2.627	2.389	2.486
0.29	20	0	0	2.522	2.434	2.725
0.29	20	0	0	2.525	2.491	2.581
0.30	20	0	0	2.560	2.574	2.615
0.35	20	10	4	2.605	2.334	2.660

No re-ignitions were achieved for slits with gap openings between 0.25 mm and 0.30 mm, but when the slit with a gap opening of 0.35 mm was used, four explosions occurred. The undamaged slit with 0.35 mm gap opening provided ten re-ignitions. The efficiency of the safe gap has increased due to the one month rust formation on the flame gap's surface.

After the slits had been exposed to corrosion, they were totally blocked by rust, but after ten explosions were conducted it could clearly be observed that the rust was blown out of the slit as a result of the explosion pressure from the primary chamber. The pressure measurements plotted in Figure 4.5 indicate that most of the rust is blown off the surface on the first explosion. The safe gap then increases due to less rust on the surface, which leads to a higher venting rate through the gap and hence a lower pressure in the primary chamber. Table 4.3 shows that the pressures from the undamaged slits are lower than the first pressure

measurement from the rusted slits, but higher than the mean pressure from ten explosions performed on rusted slits. This will be discussed further in Section 4.3.2.

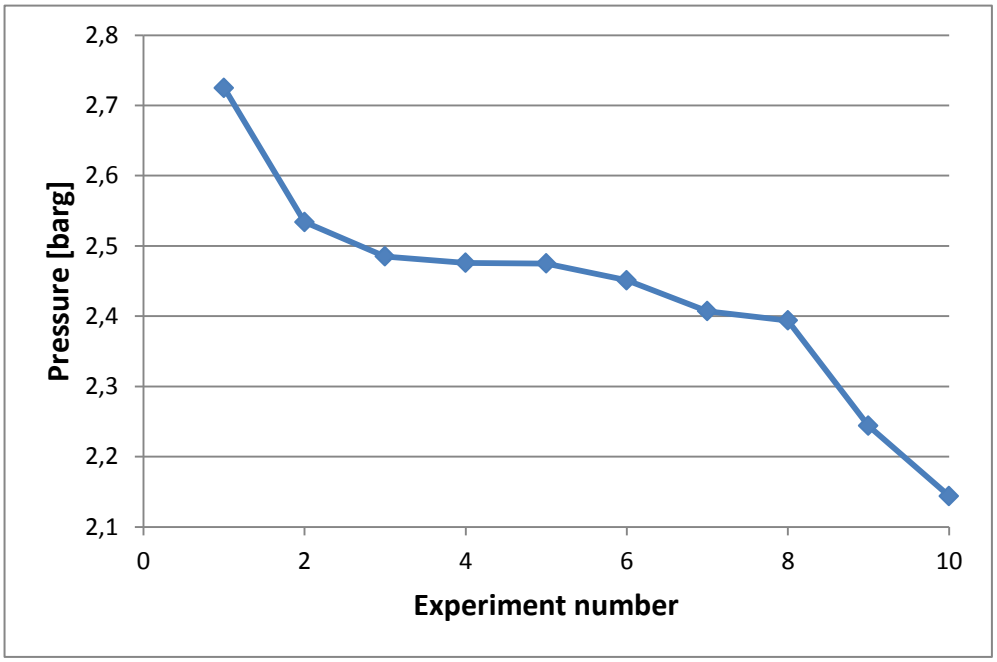

Figure 4.5 : *Pressure data from ten explosions with a one-month rusted slit with gap opening 0.29mm.*

4.3.1.2 Two months of rusting

Table 4.4 : *Ten explosions have been applied to six various slits at both undamaged and corroded state.*

Gap opening, Y_i [mm]	Ignition distance, Z_i [mm]	Number of re-ignitions		Mean pressure [barg]		Pressure of the first explosion [barg]
		Undamaged	Rusted	Undamaged	Rusted	
0.25	20	0	0	2.613	2.926	2.956
0.29	20	0	0	2.621	2.683	2.872
0.29	20	0	0	2.556	2.749	2.794
0.30	20	0	0	2.575	2.905	2.921
0.31	20	0	0	2.559	2.865	2.947
0.35	20	10	0	2.592	2.773	2.828

No re-ignitions were observed for any of the six slits with gap openings between 0.25 mm and 0.35 mm. The undamaged slit with 0.35 mm gap opening provided ten re-ignitions. The

efficiency of the safe gap has increased significantly due to the two months rust formation on the flame gap's surface.

After the slits had been exposed to corrosion, they were totally blocked by rust, and after ten explosions were conducted, a totally blocked safe gap was still observed. The explosion pressure from the primary chamber did not blow out any observable amount of rust particles from the gap opening. The safe gap does therefore not increase, which keep the pressure measurements almost constant. The pressure measurements are plotted in Figure 4.6 and support the statement that a negligible amount of rust was blown off the surface. Table 4.4 shows that the pressures from the undamaged slits are lower than all pressure data from the rusted slits. This will be discussed further in Section 4.3.2.

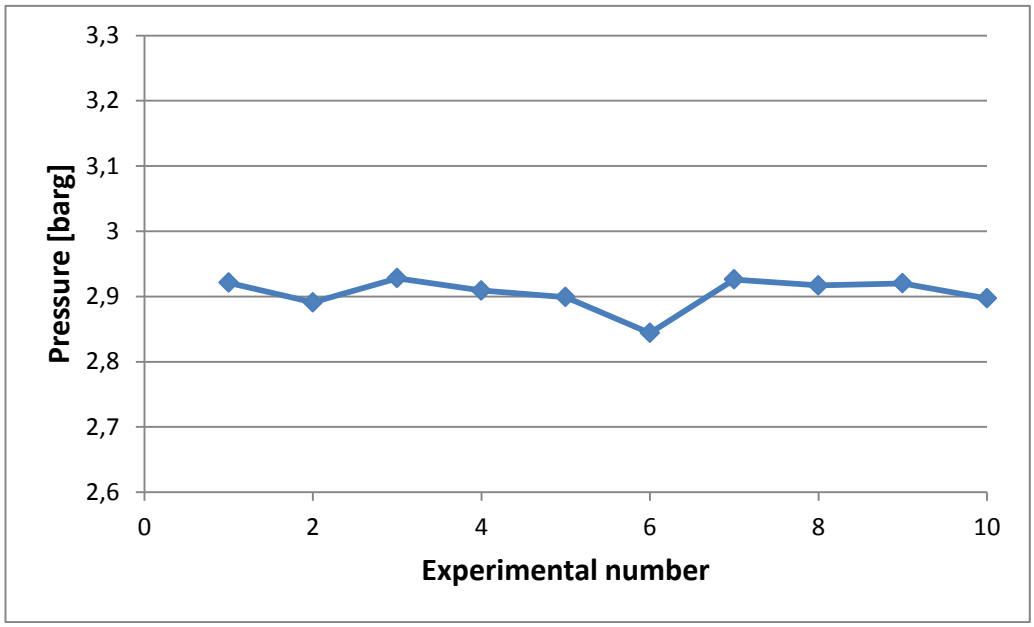

Figure 4.6 : *Pressure data from ten explosions with a two-months rusted slit with gap opening 0.29mm.*

Figure 4.6 has a y-axis of the same scale as the graph in Figure 4.5 so the difference will be shown more clearly.

Pressure development comparison

Figure 4.7 shows the pressure development from experiments performed with a one month rusted slit and a two months rusted slit. The gap openings were 0.25 mm for both experiments, and both pressure developments illustrate the first explosion preformed on each slit. The graph shows that the curves have a similar pressure rise, but decreases with different rates. Since the one month rusted slit had more rust blown out from the gap opening, a more rapid pressure decrease can be observed for this slit than for the two months rusted slit.

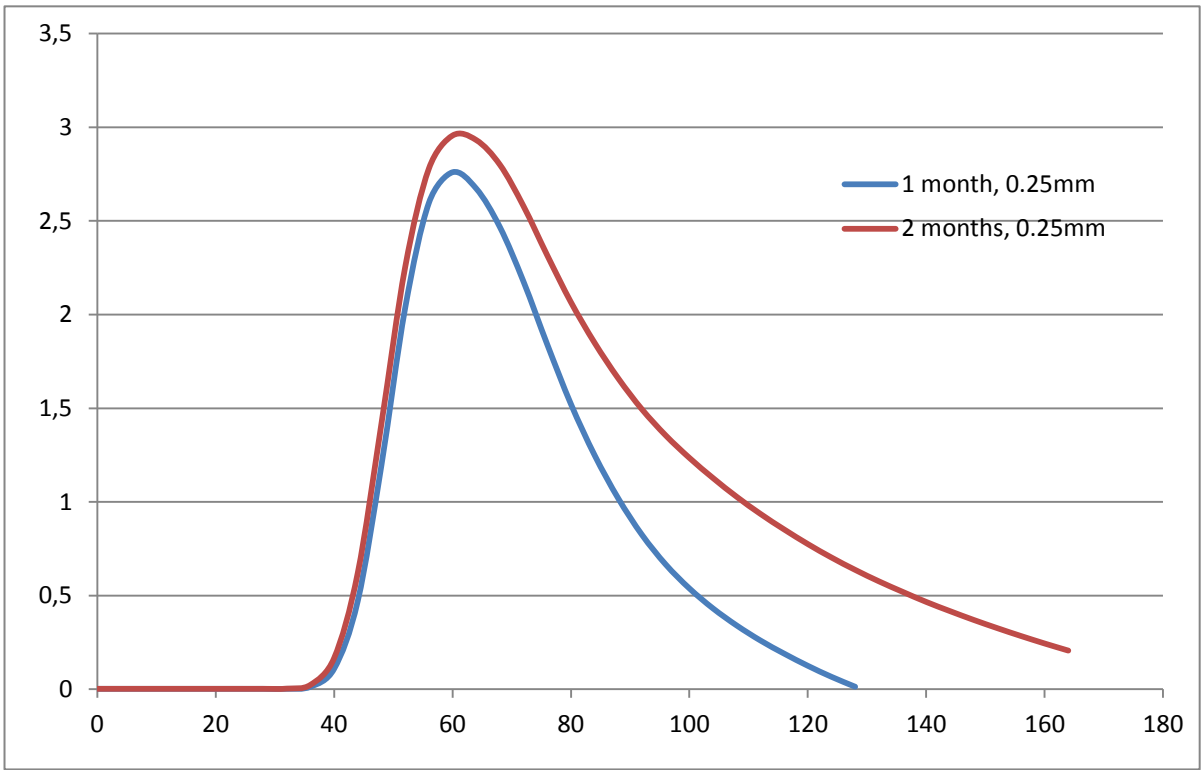

Figure 4.7 : *Pressure development in the primary chamber for an explosion through a one month rusted and a two months rusted slit, both with gap openings of 0.25 mm.*

4.3.2 Discussion

All slits have been exposed to rust formation at sea side, which is the optimal zone for maximum rust formation, illustrated in Figure 2.41 as the droplet zone. At sea side, the slits are exposed to low and high tide, corresponding to the droplet zone where the corrosion rate is approximately 0.4 mm/year. Normal offshore installations are placed in an environment where the corrosion rate is 0.1 to 0.15 mm/year (Bardal 1994). The theory in Section 2.5 describes how rust "eats" in to the steel surface. The given corrosion rate of approximately 0.4 mm/year corresponds to 0.03 mm/year for the slits rusted for one month, and 0.07 mm/year for the two months rusted slits. An undamaged slit with an initial gap opening of 0.29 mm should have a new gap opening after being exposed to one month and two months of rust of respectively 0.32 mm and 0.36 mm. Figure 3.12 and Figure 3.13 show that this is not valid, but rather the opposite is valid in this case. The slits were almost completely blocked by rust.

From Table 4.3 it is observed a higher pressure on the first explosion of the rusted slit than on the undamaged slit. But the striking result is that the mean pressures of the rusted slits are lower than the mean pressures of the undamaged slits. The high pressures from the first explosions on the rusted slits are probably due to the blocked rust opening. The blocked gap openings prevent burned gases to leave the primary chamber, which results in a high pressure. After the first of the ten explosions is completed, the pressure decreases. This is most likely because the rust particles blocking the flame gap opening is torn away from the slit's surface and blasted out to the secondary chamber. However, some rust particles are probably left on the surface, and these can form increased turbulence for the next explosions. This may explain

why the undamaged slits have a higher mean pressure than the rusted ones, as more burned gases penetrate through the gap opening with increased turbulence.

Table 4.4, which gives the results from the two months rusted slits, shows a different pressure trend than for the one month rusted openings. Both the pressure of the first explosions and the mean pressure of the rusted are higher than the mean pressure of the undamaged slits. A possible reason is that a smaller amount of rust is being blasted off the slit's surface. The extra one month of rust formation these six slits have been exposed to, has had a great influence on the amount of rust formed on the surface, and also how well bonded the rust particles are to the slit's surface. Figure 4.8 shows the difference of how large amounts of rust that have been blasted out from the one month rusted and two months rusted gap openings after ten explosions. A significant difference can be observed. The one month rusted slit has approximately the same gap opening as before it was sent to rust formation, while the two months rusted slit still has an almost totally blocked gap opening.

Figure 4.8 : *The left slit is a one-month rusted slit after ten explosions, and the right slit is a two-months rusted slit after ten explosions. Both slits have a gap opening of 0.29 mm.*

Figure 4.5 and Figure 4.6, which show the plot of the given pressures from each of the ten explosions, show the difference in pressure developments between a one month rusted slit and a two months rusted slit. It is clear that the two pressure development graphs are consistent with the results shown in Figure 4.8. For the one month rusted gap, the pressure decreases as the number of explosions increases due to the amount of rust being blasted out from the gap opening. The first explosion obviously blows out rust particles that sit fairly loose on the surface. The next seven explosions show little variation in pressure, which indicates that small amounts of rust are being pressed out from the gap opening. The last two explosions indicate that it may again disappear rust from the slit's surfaces. This has possibly been rust flakes or large rust particles that have been better attached to the walls, and thus required some explosions to be loosened up enough to be released from the wall. For the two months rusted slit, the pressure remains approximately constant as a negligible amount of rust is removed from the gap opening. It can also be observed from Figure 4.7 that the pressure rises of the slits with various rust formation periods are similar, but decreases with different rates. This agrees with the discussion made in this section. The rust formed in the two months rusted slit blocks the flame gap in a greater extent than the rust on the one month rusted slit. This implies that it takes longer for the built up pressure from the primary chamber to vent out to the secondary chamber through a two months rusted slit, hence the slower pressure decrease. But

if the gap opening is totally blocked by rust, as it seems to be just by studying it, the cooling of the gases from the walls explains the pressure fall.

From Table 4.3, it can be seen that four explosions were achieved from the slit with a gap opening of 0.35 mm. There may be two reasons for the re-ignition. The first reason is that glowing rust particles may have been blasted out form the gap opening causing a re-ignition. But a re-ignition caused by glowing particles is unlikely, as the four re-ignitions occurred on the last four explosions. Most of the rust particles will be blown out during the first explosions, as Figure 4.5 shows, where no re-ignitions were achieved. The second and most likely reason for re-ignition is that, since most of the rust now is blown out, the gap opening again becomes greater than the MESG, leading to the re-ignition.

The efficiencies of the safe gaps have increased significantly. The new MESG value for one month rusted slits has increased by approximately 17%, and for a two months rusted slit it has increased by at least 21%. It was not tested for higher MESG values than 0.35 mm, and can therefore only conclude that the MESG value has increased at least by 21%. But as both the pressure development graph, Figure 4.6, and Figure 4.8 of the two months rusted slit after ten explosions indicate, the efficiency of the safe gap could be increased considerably more.

The results achieved in this section support the results (Solheim 2010) got for his propane explosions performed on his rusted slits. Solheim's rust formation on the slits also provided increased efficiencies of the safe gaps.

4.3.2.1 Comparison of the one and two months rusted flame gap openings

It has on several occasions in the rust discussion been stated that the two months rusted flame gap openings have appeared to be completely blocked by rust. To investigate this further there were carried out experiments where it was observed how large amounts of water that managed to penetrate through the gap opening. A waterproof tube was designed to fit the top of the slit, see Figure 4.9, so that the flame gap opening was the only option for water to flow through the slit.

Figure 4.9 : *The waterproof tube designed for testing the water flow ability through the flame gap opening.*

The theory concerning that the two months rusted opening was blocked by rust was strengthened by these experiments. Only one drop of water during the first ten seconds, managed to penetrate through the gap opening, and this drop came out on one of the sides of the slit where the distance bits were placed, see Figure 4.10 b). But for the one month rusted slit, several drops of water ran constantly through the opening, see Figure 4.10 a).

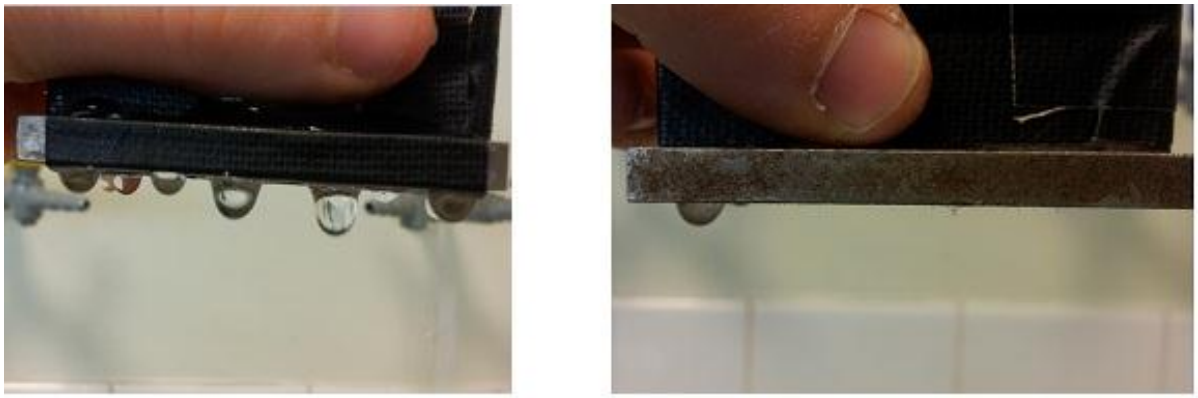

Figure 4.10 : *Water penetration experiments through: a) one month rusted slit , and b) two months rusted slit.*

4.4 Temperature measurements above flame gap surfaces with multiple crosswise grooves

4.4.1 Results

Table 4.5 : *Voltage taken from different slit configurations at MESG and at a constant gap opening of 0.35 mm.*

Slit configuration	Voltage at MESG [V]	Voltage at constant gap opening, 0.35 mm [V]
PH-7.2.3	0.348	3.545
PH-7.2.2	0.322	3.086
PH-7.2.1	0.307	3.060
PH-7.2.0,5	0.307	2.872
Undamaged	0.628	3.647

Voltage and temperature have an approximate linear relationship. Temperature conclusions can thus be drawn by comparison of the voltage conditions. It can clearly be seen from Table 4.5 that the temperature of the combustion gases are highest after they have penetrated through an undamaged slit rather than through a slit with multiple grooves.

4.4.2 Discussion

The thermocouples used in the experiments are thermocouple type *k*, and are able to measure a temperature range of -200 °C to +1200 °C (Picotech 2002). The temperature was measured at a distance of 4 cm above the gap opening. In an explosion there is a rapid temperature rise, which makes it necessary to have a large number of measurements over a short period of time. 1000 measurements were taken per second during these experiments in order to obtain an accurate voltage value.

From Table 4.5 it can be seen that the voltage, and thus the temperature, decreases as the depths of the grooves decrease, and that the highest temperature is achieved for the undamaged slit. Section 2.3.6.1 describes how heat is transferred from the flame and to the gap walls. The heat loss due to the slit's walls is thus greater to a surface with grooves, as a result of the increased surface area, rather than to a surface with no grooves. A striking result is that the temperature above the slits with grooves decreases as the depths of the grooves are reduced. Since the total surface area of the slit's inner walls increases with larger depths of the grooves, one would believe that the heat loss due to the walls would increase. Newton's law, see Equation 2.4 in Section 2.3.6.1, shows that the heat loss is proportional to the surface area. An increased heat loss to the slit's walls should lead to a decrease in temperature in the secondary chamber, but the results according to Table 4.5 do not correspond with this theory. But, according to (Warren L. McCabe 2005), in the high velocity flow of compressible gases in pipes, friction at the wall raises the temperature of the fluid at the wall to above the average fluid temperature. McCabe also states that for equal Reynolds numbers, the heat transfer

coefficient in turbulent flow is somewhat greater for rough tubes than for smooth ones. The effect of roughness on heat transfer is much less than on fluid friction, which may explain why increased temperatures are achieved when the depths of the grooves are increased. Increased friction leads to increased temperature. McCabe also writes that the effect of roughness is neglected in practical calculations.

4.5 Finding the most favorable ignition point for re-ignition through slits with multiple crosswise grooves

A total of 50 explosions were carried out during this part of the investigation, 10 on each different ignition position. The ignition positions investigated were 5 mm, 10 mm, 15 mm, 20 mm, and 25 mm. The slit used was PH.7.2.3. The MESG value for PH-7.2.3 was found; see Section 4.6.1, to be 0.33 mm. A slightly larger gap opening than that, 0.35 mm, was therefore used to achieve some re-ignitions to the outer chamber.

4.5.1 Results

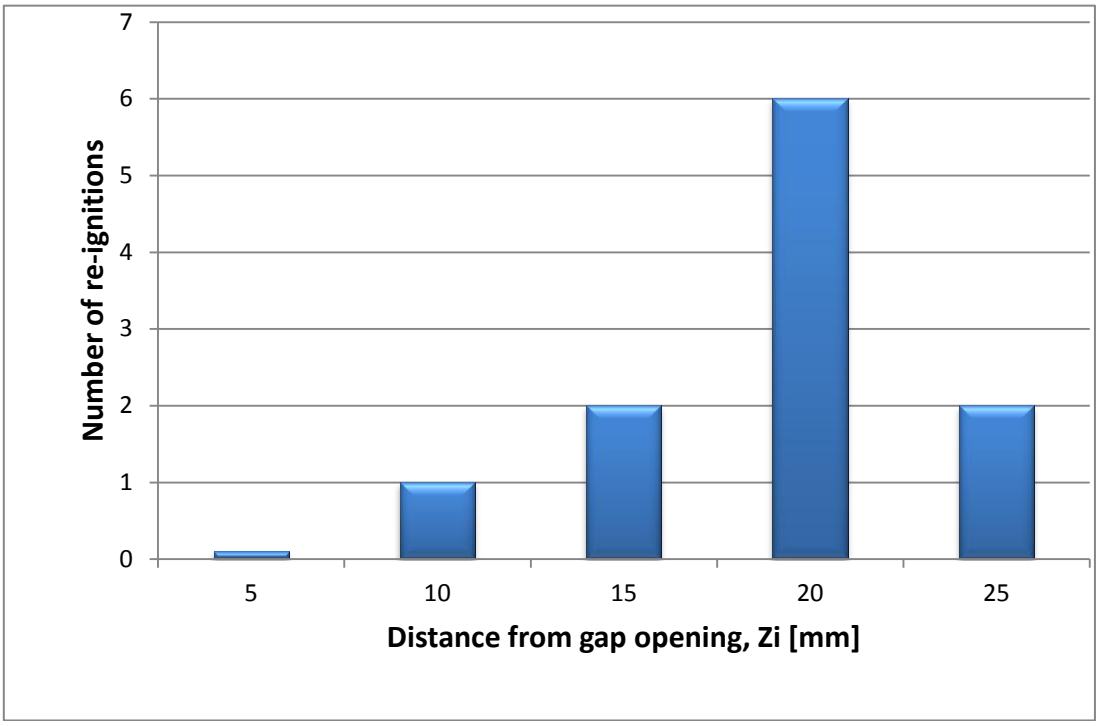

Figure 4.11 : *Plot of the number of re-ignitions out of ten attempts per distance, with a gap opening of 0.35 mm for the slit PH-7.2.3.*

The graph shows that ignition at 5 mm from the gap opening gave 0 % re-ignition, and ignition at 20 mm distance gave seven re-ignitions. It is a clearly peak at 20 mm, which means that this is the most favorable ignition point, and the worst-case area for ignition.

4.5.1.1 Mean maximum explosion pressures for different ignition distances

Table 4.6 : *Mean maximum explosion pressure for different ignition points. Ten explosions were performed for each distance. A gap opening of 0.35 mm was used on the slit PH-7.2.3.*

Surface configuration:	PH-7.2.3
Gap opening, Y_i [mm]	0.35
Ignition distance, Z_i [mm]	**Maximum pressure [barg]**
5	2,944*
10	2.678
15	2.795
20	2.866
25	2.924

* The value is for an explosion in the primary chamber that gave no re-ignition in the secondary chamber, and is therefore not comparable to the other pressure measurements that resulted in re-ignitions

Table 4.6 shows a specific pattern between ignition distance and the mean maximum explosion pressure. As the point of ignition increases, the mean explosion pressure increases systematically.

Figure 4.12 shows the pressure development from experiments performed with the five different distances 5 mm, 10 mm, 15 mm, 20 mm, and 25 mm from the flame gap opening. The gap opening is 0.35 mm for all experiments. The graph shows that all curves have fairly similar slopes.

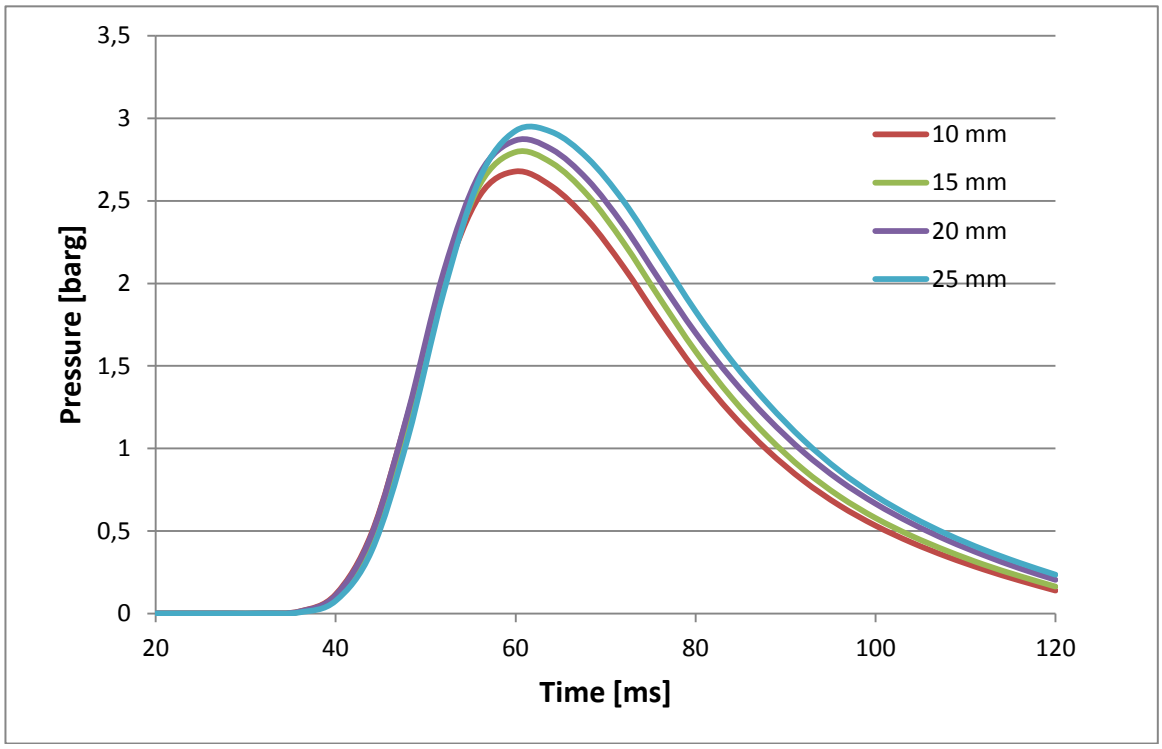

Figure 4.12 : *Pressure development in the primary chamber for explosions with ignition distances 10 mm, 15 mm, 20 mm, and 25 mm from the gap opening.*

4.5.2 Discussion

The experiments conducted for finding the most favorable ignition point for re-ignitions are based on previous research performed by (Larsen 1998), (Grov 2010), and (Solheim 2010). But, the explosive gases used in their researches are propane, while the explosive gas used in the present work is hydrogen. All previous research conducted with propane, resulted in a worst-case ignition point of 14 mm from the flame gap opening. Larsen stated that the maximum pressure increased when the ignition source was moves from the flame gap opening and towards the center of the primary explosion chamber. This is in correlation to the pressures given in Table 4.6. The pressure clearly increases as the distance from the gap opening increases.

The results show a worst-case ignition point of 20 mm from the gap opening. This is in consistent with the results from Section 4.2.1, where it was also found a worst-case ignition point of 20 mm from the flame gap opening. A reason why this distance is greater than the distances found in previous investigations of propane, may be the fact that hydrogen is much more reactive than propane. Hydrogen can therefore tolerate a more turbulent flow through the gap opening than propane can, and still achieve a re-ignition. The flow of the combustion gases penetrating through the gap opening will increase as the ignition point is moved away from the gap and towards the center of the primary explosion chamber. At a lower flow rate than the one achieved at 20 mm, the gap walls will cool down and quench the explosion. At a higher flow rate than the one at 20 mm, the turbulence formed by the penetration through the flame gap opening will be so high that cooling from mixing with the unburned gases in the

secondary chamber will be dominant and prevent re-ignition. A more detailed explanation can be read in Section 4.2.2.

In Figure 4.12, it can be observed that all curves have the same slope, or pressure developments, until they reach their maximum pressures. (Grov 2010) showed in his work that the maximum pressure from explosions vented through slits with grooves were significantly higher than the maximum pressure from explosions vented through undamaged slits. This corresponds to the results in this work; see Section 4.2.1.1 and Section 4.5.1.1. The highly rough surface of the slit PH-7.2.3 causes a higher resistance and hence the increase in pressure. The Moody Diagram, see Figure 2.21, illustrates the correlation between the roughness and the friction factor. The diagram is designed for pipes, but since the dimension of the height of the slit is 70 times larger than the flame gap opening, the diagram can apply to the slit as well. The Moody Diagram tells us that rough pipes lead to a larger friction factor than smooth pipes do. An increase in the friction factor leads to increased resistance, which results in a decreased flux through the gap opening.

From maximum pressure values presented in Table 4.6, it can be seen that the pressure increases as the ignition source is moved towards the center of the primary explosion chamber. This agrees with the results (Larsen 1998) got during his work. When the ignition source is moved away from the gap opening and towards the center of the camber, the flame front will reach the walls and the gap opening at a later stage than if the ignitions source was to be close to the flame gap opening. This means that the pressure can build up over a longer time period, causing a higher pressure, before being vented out through the gap opening. See Section 2.3.3 for more information on ignition point's influence on burning velocity. The pressure would most likely be at its maximum in the center of the chamber. The flame front would then develop as a spherical ball and hit the walls and the gap opening at the same time.

Another possible reason for why an increase in the maximum pressure is observed when the ignition source is moved away from the opening, may be that more unburned gases must be forced through the opening before the flame front reaches it. The densities of the gases change over time due to temperature, making them more volatile. The cold unburned gases therefore require more force than the hot burned gases do, for being pushed through the flame gap opening.

4.6 Experiments performed on slits with various depths on the multiple crosswise grooves

Several experiments were carried out on each slit configuration to determine the MESG value. All slits have seven grooves with a width of 2 mm, but various depths of 3 mm, 2 mm, 1 mm, and 0.5 mm. Detailed measurements about the different experiments can be found in Appendix D-5. Ten explosions in a row without the secondary chamber being re-ignited gave the MESG value. The mean pressure is then calculated from the ten explosions that did not result in a re-ignition. The most favorable ignition position for re-ignitions, see Section 4.5, is used throughout all the experiments. The results from the experiments are shown in Table 4.7.

4.6.1 Results

Table 4.7 : *MESG values and mean pressure from experiments performed of slits with various depths on the seven crosswise grooves.*

Surface configuration	Z_i [mm]	MESG [mm]	Mean pressure at MESG [barg]
PH-7.2.3	20	0.33	2.492
PH-7.2.2	20	0.32	2.546
PH-7.2.1	20	0.33	2.234*
PH-7.2.0,5	20	0.34	2.622
Undamaged	20	0.29	2.524

*The value seems to be divergent from the other values with respect to the increasing pattern that can be observed from Table 4.7. (Solheim 2010) also had an abnormal pressure measurement on exactly the same slit configuration, which may indicate that there might be some inaccuracies due to the dimensions on this certain slit.

Table 4.7 shows that all MESG values for the slits with grooves are higher than the MESG value of the undamaged slit. The highest MESG of 0.34 mm is achieved for the surface configuration PH-7.2.0,5, which is the slit with the smallest depth. But in addition, no clear pattern is observed when it comes to the MESG values. We do not have a decreasing or increasing pattern of the values, but they vary unsystematically.

To look further at how the pressure varies with the different surface configurations, experiments were conducted with the same gap opening. The results are shown in Table 4.8.

Table 4.8 : *Pressure measurements from experiments carried out with a gap opening of 0.35 mm on slits with various depths on the seven crosswise grooves, and on an undamaged slit.*

Surface configuration	Z_i [mm]	Y_i [mm]	Mean pressure [barg]
PH-7.2.3	0.20	35	2.694
PH-7.2.2	0.20	35	2.563
PH-7.2.1	0.20	35	2.527
PH-7.2.0,5	0.20	35	2.422
Undamaged	0.20	35	2.567

Table 4.8 shows a clear pattern between the pressure and the depths of the grooves in the flame gap surface. The pressure decreases as the depth of the grooves decreases.

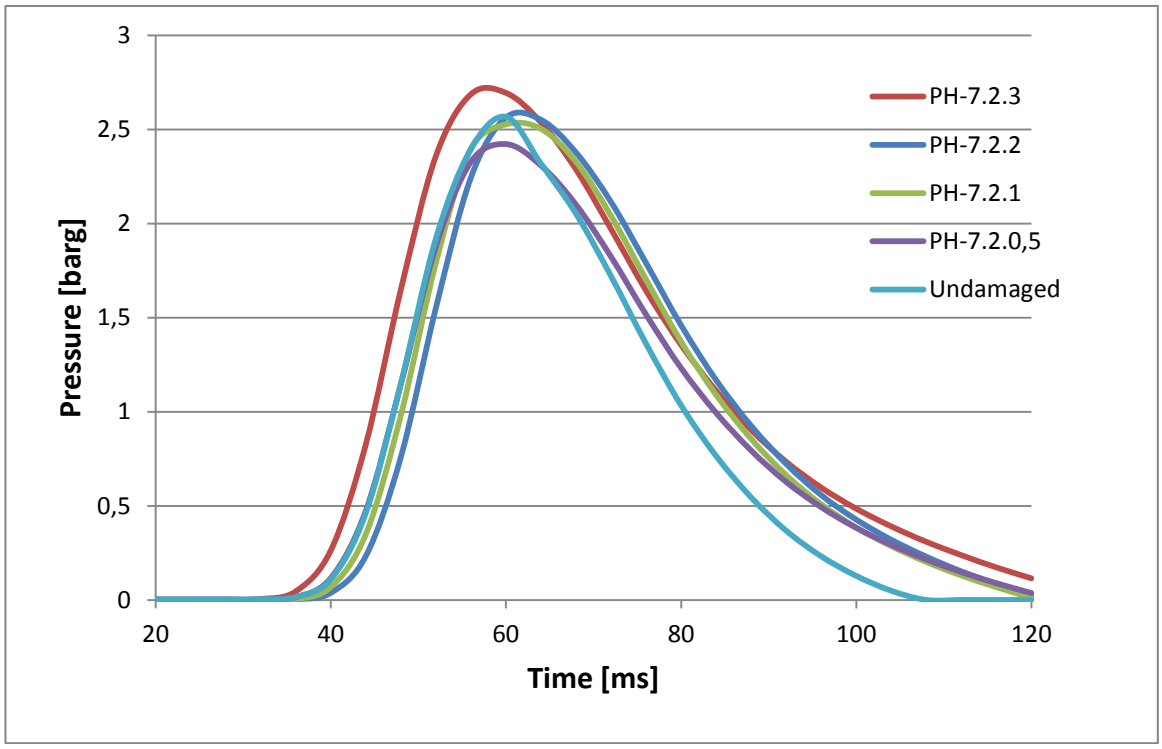

Figure 4.13 : *Pressure development in the primary chamber for slits with seven crosswise grooves with different depths.*

4.6.2 Discussion

Two different experimental series were carried out during this section. The first was to estimate the MESG values of the different surface configuration, and the second was performed with the same gap opening of 0.35 mm to only show how the pressure developed due to the different roughness on the slit's surface.

The first measurement series was of the MESG values. The results in Table 4.7, shows us that the MESG values for slits with crosswise grooves are larger than the MESG value of an undamaged slit. The MESG values have increased from 0.29 mm, which is the MESG of an undamaged slit, to MESG values of 0.32 mm – 0.34 mm. This is an increase of 10 % - 14 % of the MESG value of the undamaged slit. It is thus an improvement of the gap efficiency when crosswise grooves are added to the gap surface. One of the reasons why the efficiency of the safe gap gets improved may be due to the increased turbulence, which is formed in the flow through the opening due to the grooves. The second reason may be as a result of the increased cooling effect due to increased surface area on the slit's walls. The heat transfer between the gases and the walls will increase as the surface area is increased. The increased level of turbulence will also force a larger portion of the hot burned gases to get in contact with the cold walls.

The second series of measurements was performed with the same gap opening of 0.35 mm for all surface configurations. The reason for keeping the gap constant was to make it easier to observe how the pressure varies with respect to the depth of the various grooves in the slit's surface. Table 4.8 shows an increase in pressure as the depth increases, which agrees with the Moody Diagram reviewed in Section 2.3.7, where an increase in the relative roughness leads to a greater friction factor. An increased friction factor results in higher resistance, which again leads to a decrease of the flow through the gap opening. The larger amount of time, due to the reduced gas flow through the gap opening, increases the pressure build up in the primary chamber. It can also be seen from the pressure development graph, see Figure 4.13, that PH-7.2.3, which was the slit with the deepest grooves, had the most rapid pressure development and highest pressure of them all. The other slit configurations all have approximately the same pressure development, but with different maximum pressures.

The most striking result is that the pressure decreases as the depth of the grooves decreases, but for the undamaged slit, the pressure rises again. The reason for this pressure increase may be that a laminar flow is formed between the flame gap surfaces of the undamaged slit, while a turbulent flow will be formed when grooves are added to the slit's surfaces. More gas will escape through the slit when a turbulent flow is present. Hence the pressure increases when a laminar flow is formed in the undamaged slit's gap opening. But**,** the pressures in this section vary with significantly small amounts, which make it difficult to draw any conclusions from the measurements. The differences in pressure might be arbitrary.

The MESG values turned out to be fairly similar for the different surface configurations, which make it difficult to draw any conclusions based only on that measurement. It was therefore more logic to look at the pressure measurements and judge based on those. The pressure measurements indicate that it is harder to achieve a re-ignition with deeper grooves, since the pressure increases with increased depths of the grooves. More turbulence is formed through the flame gap opening at higher pressures, and as long as the turbulence formed gets above the critical level, increased turbulence will result in no re-ignition.

From Table 4.7 and Table 4.8 it can be seen that the pressures increase when the gap opening is extended from the MESG to a gap of 0.35 mm. This may seem unlikely, as it is conceivable that at a larger gap opening, more burnt gases could be released and it will lead to a lower pressure in the primary chamber. But a possible explanation may be that as more burned gases discharge through the larger opening, more turbulence will be formed in the primary chamber, which then will lead to increased burning velocity and a higher pressure.

4.7 Experiments performed on slits with various widths on the multiple crosswise grooves

This section is carried out with the same procedure as described in Section 4.6. The two slits used have both seven grooves with a depth of 3 mm, but with various widths of 2 mm and 1 mm. The results from the experiments are shown in Table 4.9.

4.7.1 Results

Table 4.9 : *MESG values and mean pressure from experiments performed of slits with various widths on the seven crosswise grooves.*

Surface configuration	Z_i [mm]	MESG [mm]	Mean pressure at MESG [barg]
PH-7.2.3	20	0.33	2.492
PH-7.1.3	20	0.50*	2.516
Undamaged	20	0.29	2.524

* This value is unusually high and the possible sources of error are discussed further in the discussion part, see Section 4.7.2.

From Table 4.9 it can be seen that the MESG values have increased as grooves were added to the slit's surfaces.

To look further at how the pressure varies with the different surface configurations, experiments were conducted with the same gap opening. The results are shown in Table 4.10.

Table 4.10 : *Pressure measurements from experiments carried out with a gap opening of 0.35 mm on slits with various widths on the seven crosswise grooves, and on an undamaged slit.*

Surface configuration	Z_i [mm]	Y_i [mm]	Mean pressure at MESG [barg]
PH-7.2.3	20	0.50	2.584
PH-7.1.3	20	0.50	2.382
Undamaged	20	0.50	2.459

4.7.2 Discussion

This section has a similar procedure as the previous Section 4.6 had. Two measurement series were implemented. The first series of experiments was for determination of the MESG values, and the second series was carried out with constant gap opening for pressure comparison between the different slit configurations.

Table 4.9 shows the improved MESG values. The slit configuration PH-7.2.3 has increased the MESG value by 14 %, while the slit configuration PH-7.1.3 has increased the MESG by 72%, which is an unusually high improvement of the MESG value. The PH-7.3.1 differs from all other measurements made on slits with grooves, and is therefore an unlikely trustable result. The grooves of the PH-7.1.3 have been observed not to be symmetrical, which may possibly be the greatest source of error. Since this one value obviously differs, it is difficult to conclude how the width of the grooves affects the MESG value. But it can certainly be said that the efficiencies of the safe gaps are improved.

The second series of experiments are shown in Table 4.10, where a constant gap opening was used to compare the maximum explosion pressures. It can be seen that increased width on the grooves provides an increase in pressure. Less resistance on the slit surface leads to a lower pressure. But the undamaged gap has a higher pressure than the slit PH-7.1.3, which may be caused by the decreased turbulence through the gap. The undamaged slit provides lower resistance through the gap opening than the PH-7.1.3 provides. This would normally result in a lower pressure, but the fact that the turbulence decreases significantly from the slit with grooves compared to the undamaged slit, may be the dominant factor that leads to an increase in pressure. The pressure is then observed to increase when the slit configuration PH-7.2.3 is tested. This may be due to the increased resistance through the gap opening.

It is difficult to draw any conclusions based only on the MESG measurements since the MESG value measured for PH-7.1.3 was not reliable, but based on the pressure measurements, some indications can be stated. The pressure measurements indicates that it is harder to achieve a re-ignition with wider grooves, since the pressure increases with increased widths of the grooves. More turbulence is formed through the flame gap opening at higher pressures, and as long as the turbulence formed gets above the critical level, increased turbulence will result in no re-ignition.

4.8 Comparison of pressure measurements from undamaged slits and slits with multiple crosswise grooves

In this section, pressure measurements from experiments with multiple crosswise grooves on the flame gap surface will be compared with pressure measurements from slits with undamaged gap surface. All experiments are carried out with the most favorable hydrogen concentration and are ignited at the most favorable ignition position for re-ignitions.

4.8.1 Results

Table 4.11 : *Mean pressure from experiments performed with an undamaged slit and the slit with surface configuration PH-7.2.3 at gap openings 0.29 mm and 0.33 mm.*

Surface configuration	Gap opening, Y_i [mm]	Ignition distance, Z_i [mm]	Mean maximum pressure [barg]
Undamaged	0.29 (MESG)	20	2.524
PH-7.2.3	0.29	20	2.879
Undamaged	0.33	20	2.515
PH-7.2.3	0.33 (MESG)	20	2.694

Table 4.11 shows that the flame gap surfaces with crosswise grooves have significant higher pressures than the undamaged flame gap surfaces. The pressure at PH-7.2.3's MESG 0.33 mm, which is 0.04 mm larger than the undamaged slit's MESG, is 0.17 barg higher than the pressure measured from the undamaged slit. The pressure difference between the two slits at 0.29 mm is 0.355 barg, and at 0.33 mm the difference is 0.179 barg.

A pressure development plot is created for the two slit configurations with the same gap opening to better observe possible differences. Figure 4.14 shows that the pressure developments are virtually identical. The only observable difference is that the maximum pressure is higher for the slit with multiple crosswise grooves.

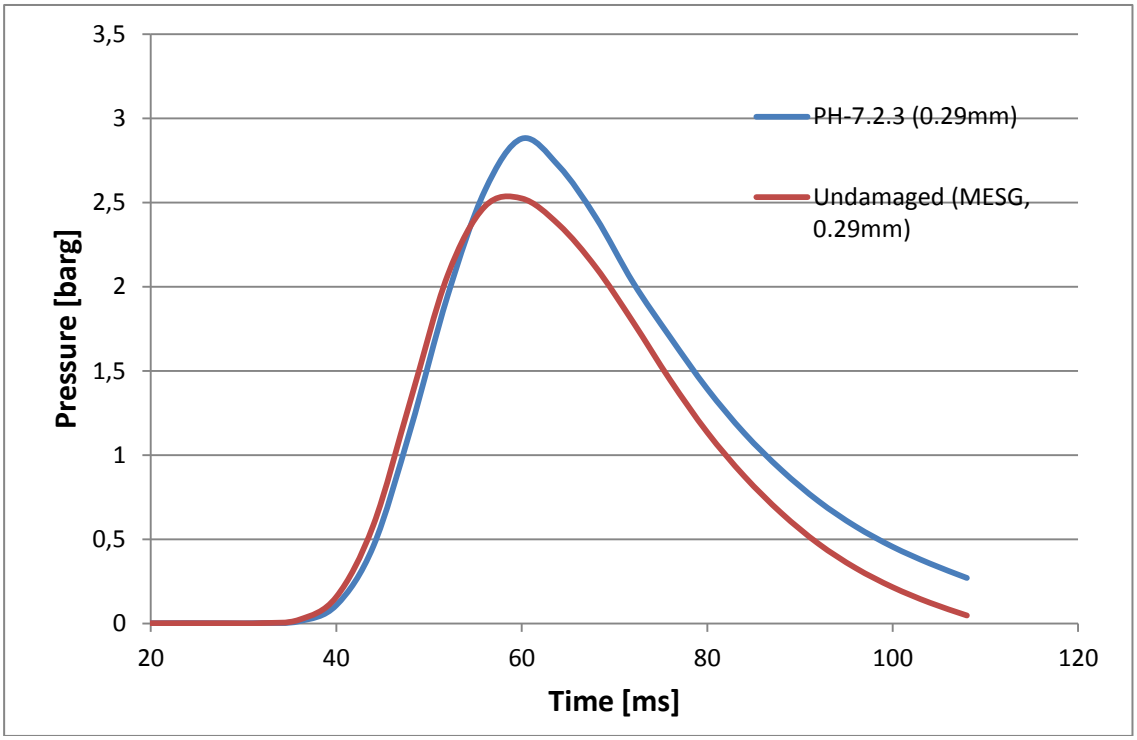

Figure 4.14 : *Pressure development for PH-7.2.3 and an undamaged slit at a gap opening of 0.29 mm.*

4.8.2 Discussion

(Grov 2010) and (Solheim 2010) have previously conducted similar experiments in which both showed that a slit surface with multiple crosswise grooves reduced the probability for re-ignition in the secondary chamber. They also proved that the maximum explosion pressure in the primary chamber increased when slits with multiple crosswise grooves were used compared to undamaged slits. Results given in this work agrees with their statements.

(Grov 2010) concluded that an increased pressure in the primary chamber led to a greater flux of the hot combustion gases through the flame gap when the flame gap surface contained grooves. This result was contradictory to (Solheim 2010)'s results and the results achieved in this present work. The theory in Section 2.3.7 is the basis of the correlations drawn and discussed in this section. The friction factor, *f*, which is a dimensionless number, is a function of the relative roughness, *k/D*. An illustration of the dimensions of a slit with grooves can be seen in Figure 2.22. It shows that the grooves are extremely large compared to the diameter of the gap, which results in an abnormally high relative roughness. As the roughness increases, the flux through the gap decreases. A decrease in flux through the slit opening means it takes longer for the burned gases to penetrate through, which again leads to an increased pressure as the escape of gases occur over a longer time period. The maximum pressure is therefore greater for slits with grooves rather than undamaged slits. Figure 4.14 shows the difference in maximum pressure of the two slits with the same gap opening.

Another factor that is also influenced by the reduced flux of the burnt gases through the flame gap opening, is the cooling effect due to the heat transfer between the hot combustion gases and the cold walls of the slit. Not only have the hot combustion gases more contact time with the walls due to the lower velocity, but the gases also have a larger surface area where heat transfer can occur due to the several grooves on the slit surface.

5 Conclusions

The current international standards, IEC, require that the mean flame gap surface roughness of Ex'd' enclosures is less than 6.3 μm. The slits tested in this work that are categorized as "damaged" are the rusted ones, and the ones with multiple grooves. The reason why they go under the term "damaged" is because these slits' roughness are larger than the required roughness of 6.3 μm. The standards also require that if a flame gap is damaged, it must be renovated back to its original condition, but there is no definition of how damaged a flame gap can be without affecting the efficiency of it. The conclusions in this section provide a more detailed insight to this definition issue.

Preliminary work

To make sure that the results are as accurate as possible, all factors that have an influence on the final result must be examined. The factors that have an influence on the results in this work, and thus have been investigated, are the concentration of hydrogen in air, and the ignition positions.

- The most favorable concentration for re-ignitions was found to be 30.5% hydrogen in air
- The most favorable ignition position for undamaged flame gaps was found to be 20 mm from the flame gap opening
- The most favorable ignition position for damaged slits, or slits with multiple crosswise grooves, was also at a distance of 20 mm from the flame gap opening

Rusted flame gaps

The results found during the preliminary experiments were applied to the experimental work performed in this section with rusted slits. Ten explosions were conducted on each rusted slit, with an explosive gas mixture of concentration 30.5% hydrogen in air. All explosions were ignited at a distance of 20 mm from the flame gap opening.

In total, twelve slits with various gap openings from 0.25 mm to 0.35 mm were placed at sea side for rust formation. Six of the slits were brought back from the rust formation process after one month, and the last six slits were brought back up after two months at sea side. After the rust formation, all slits had a mean surface roughness significantly higher than the required value of less than 6.3 μm.

One month rusted slits:

- No re-ignitions were achieved on the slits with gap openings between 0.25 mm and 0.31 mm.
- Four re-ignitions were observed on explosion number 7, 8, 9, and 10 on the slit with gap opening 0.35 mm.

Two months rusted slits:

- No re-ignitions were achieved for any of the slits with gap openings between 0.25 mm and 0.35 mm.

Final and common conclusion for rusted slits:

- The efficiencies of the maximum experimental safe gaps, MESG, have increase by approximately 17% for the one month rusted slits, and by at least 21% for the two months rusted slits.

Flame gaps with multiple crosswise grooves

The results found during the preliminary experiments were also applied to the experimental work performed in this section with slits with multiple crosswise grooves. The explosive gas mixture had a concentration of 30.5% hydrogen in air and all explosions were ignited at a distance of 20 mm from the flame gap opening.

A total of five slits were investigated. Four of the slits had grooves with various depths and two of the slits had various widths, whereas one of the slits was common and used for both experiments.

- Temperature measurements performed in this research showed that the temperature of the hot combustion gases penetrated through a slit with multiple crosswise grooves are lower than the temperature of the hot combustion gases penetrating through an undamaged slit, despite identical explosion conditions.

- Although the surface of the flame gaps are damaged, which in this case was in the form of added grooves, the efficiency of the safe gap has not been reduced, but rather increased. The MESG value was found to be grater for all flame gaps with grooves than the MESG value of an undamaged slit.

General conclusions

There are some specific trends throughout the work in my thesis that have varied from previous and other ongoing work.

- The pressure developments have generally through all experiments performed in this work been exceptionally similar. Previous work completed by (Solheim 2010), with propane as the explosive gas, has shown various pressure developments throughout his work. This difference is most likely caused by the fact that hydrogen is extremely reactive, and that the burning velocity and pressure development is more rapid and developed over a shorter time period than for propane.

- It was also observed that the flame gaps of the two months rusted slits were almost completely blocked by rust, due to the small MESG value for hydrogen. It is therefore likely that the flame gap opening would be totally blocked by rust after being exposed

for rust over a longer time period, which in itself will not be a problem, unless a detailed inspection should be performed on the equipment.

- A large part of the pressures measured during this research have been lower than the pressures measured by both (Solheim 2010) and (Grov 2010), who previously performed the same experiments with propane, and (Steiner 2012), who is currently writing her thesis with ethylene as the explosive gas. The reason for this pressure difference is probably that hydrogen is a more volatile gas, due to its small molecular size, and a gas with a higher diffusivity than other gases. This causes the hydrogen to flow through the flame gap opening more easily than other gases with larger molecular size and less volatility. Hydrogen would form a negative relative pressure if the combustion took place in a closed container as the number of molecules are reduced from reactants to products, which may also be a factor contributing to lower pressures.

6 Recommendations for Further Work

Preliminary research

- A more accurate procedure, as the one used by (Grov 2010) and (Solheim 2010), should be used to investigate the "worst case" ignition point for undamaged slits and slits with grooves. In this thesis, due to time constraints, there were conducted ten explosions at each different ignition point, where the distance that provided most re-ignitions was defined as the "worst case" ignition point. But for each ignition point it should be determined the flame gap opening that gave 100% re-ignitions and 0% re-ignitions, which is a more accurate procedure.

- Experiments should be performed for high concentrations of hydrogen. The maximum burning velocity of hydrogen is at 40.1% hydrogen in air, which is well above the stoichiometric mixture and the mixture of 30.5% used in the present research.

Rusted flame gaps

- Slits with larger gap openings than 0.35 mm must be placed for rusting, as the slit with 0.35 mm gap opening in this thesis did not achieve any re-ignitions after being exposed to two months of rust formation. It was therefore not possible in this thesis to conclude on how much the efficiency of the safe gaps had increased.

- If possible, some slits should be exposed to rust formation over a longer time period to see if the gap openings at some point will go from being blocked by rust to "eaten up" by rust as he theory claims.

Mechanical damaged flame gaps (slits with grooves)

- More data must be taken on slits with multiple widths on the crosswise grooves to be able to compare the results and draw probably conclusions. In order to accomplish this, new and higher slits will have to be designed, or less than seven grooves must be present on one slit. As of today, there is no room for wider grooves when seven grooves are the number being used.

- Since it was observed asymmetrical grooves on the PH-7.1.3, and PH-7.1.3's MESG value increased by 72%, this is a factor that can be further investigated.

Other recommendations

- (Solheim 2010) performed experiments with dust inside the primary chamber and propane as the explosive gas. In the industry, dust can penetrate through the flame

gaps and accumulate inside the Ex'd' equipment. Experiments with dust inside the primary chamber may be further examined with hydrogen as the explosive gas.

- During the experiments in the present work, a pressure measuring frequency of 250 Hz was used. A greater frequency should be tested to see if the pressure measurements provide different results. A possible outcome may be a pressure development graph containing two pressure peaks. In this case, the first peak will illustrate the pressure when the combustion products begin to flow out through the flame gap opening. The second peak will illustrate the maximum pressure achieved in the primary chamber.

- Simulations of the experiments can be performed

Improvements on the experimental equipment

- All hoses leading to and from the experimental apparatus should contain a closing mechanism so that no gas leaks through the hoses in the time period from when the gas analyzer is being closed to the ignition takes place.

- The plate that separates the primary chamber from the secondary chamber should be improved. The opening of where the slits are being placed is worn and expanded. Leaks on the sides of the slit may occur, which is important to prevent when dealing with such reactive and volatile gases as hydrogen. Even the smallest cracks may result in large errors. If the plate cannot be renewed or improved, a better sealing of the area around the slit should be designed.

References

Air-Liquide. (2009). "Gas Encyclopaedia." from http://encyclopedia.airliquide.com/encyclopedia.asp?CountryID=19&LanguageID=11.

Alcock, J. L. (2001). Compilation of Existing Safety Data on Hydrogen and Comparative Fuels.

Ballal, D. R. and A. H. Lefebvre (1975). "The influence of flow parameters on minimum ignition energy and quenching distance." Symposium (International) on Combustion **15**(1): 1473-1481.

Bardal, E. (1994). Korrosjon og korrosjonsvern, Tapir.

Bellenoue, M., T. Kageyama, et al. (2003). "Direct measurement of laminar flame quenching distance in a closed vessel." Experimental Thermal and Fluid Science **27**(3): 323-331.

Cashdollar, K. L. (2000). "Flammability of Methane, Propane, and Hydrogen Gases." Journal of Loss Prevention in the Process Industries **Volume 13**(Issue 3-5).

Chang, R. (2006). General Chemistry. New York, McGraw-Hill.

Cussler, E. L. (1997). Diffusion, Mass Transfer in Fluid Systems, Cambridge University Press.

Dandy, D. S. (2012, May 24, 2012). "Chemical Equilibrium Calculation." from http://navier.engr.colostate.edu/tools/equil.html.

Davis, J. R. (2000). Corrosion: Understanding the Basics. United States of America, ASM International.

Eckhoff, R. K. (2003). Dust Explosions in the Process Industries, Guld Professional Publishing, Elsevier.

Eckhoff, R. K. (2005). Explosion Hazards in the Process Industries. Houston, TX, Gulf Publishing Company.

Einarsen, R. I. (2001). Experimental determination of critical dimensions of holes and slits in flameproof enclosures, for prevention of explosion transmission to external explosive gas cloud. Master, University of Bergen.

Energy, U. S. D. o. (2009). "A Comparison of Hydrogen and Propane Fuels." from http://www1.eere.energy.gov/hydrogenandfuelcells/pdfs/45408.pdf.

Engineering, S. P. (2011). "MESG Values and NEC Groups."

Frank-Kamenetskii, D. A. (1955). "Diffusion and Heat Exchange in Chemical Kinetics."

Gabour, L. A. (1993). The Effects of Surface Roughness on Stagnation-Point Heat Transfer During Impingement of Turbulent Liquid Jets. Master of Science.

Geoffrey Bottrill, D. C., G. Vijayaraghavan (2005). Practical Electrical Equipment and Installations in Hazardous Areas. Oxford, IDC Technologies, Elsevier.

Grov, A. (2010). An Experimental Study of the Influence of Major Damage of Flame Gap Surface in Flameproof Apparatus on the Ability of the Gaps to Prevent Gas Explosion Transmission. Master of Science, University of Bergen.

Henden, M. J. H. (2011). Minimum Ignition Energy of Propane and Ethylene in Atmospheres of various O2/N2 Ratios. Master of Science, University og Bergen.

IEC (2002). "IEC 2002: 60079-1-1: Electrical apparatus for explosive gas atmospheres Part 1-1: Flameproof enclosures 'd'. Method of test for ascertainment of maximum experimental sade gap."

IEC (2007). "IEC 2007: 60079-17: Part 17: Electrical installations inspection and maintenance."

IEC (2007a). "IEC 2007a: Explosive Atmosphere." Equipment protection by flame proof enclosures.

IEC (2007b). "IEC 2007b: 60079-19: Explosive atmospheres - Part 19: Equipment repair, overhaul and reclamation."

IEC (2010). "IEC 2010: 60079-20-1: Part 20-1: Material characteristics for gas and vapour classification - Test methods and data."

IEC (2011). "IEC 60079-1: Explosive atmospheres - Part 1: Equipment protection by flameproof enclosures 'd'."

J. Warnatz, U. M., R. W. Dibble (2006). Combustion. Berlin, Germany, Springer-Verlag Berlin Heidelberg.

Kalvatn, I. (2009). Experimental Investigation of the Optical Measurement Method for Detecting Dust and Gas Flames in a Flame Acceleration Tube. Master of Science, University of Bergen.

Larsen, E. B. (2012). An Experimental Investigation of the Influence of Heat Transfer on the Ability of Flame Gaps to Prevent Gas Explosion Transmission. Master of Science, University of Bergen.

Larsen, Ø. (1998). A Study of Critical Dimensions of Holes for Transmission of Gas Explosion and Development & Testing of a Schlieren System for Studying Jets of Hot Combustion Products. Master of Science, University of Bergen.

M. Kröner, J. F., T. Sattelmayer (2003). "Flashback Limits for Combustion Induces Vortex Breakdown in a Swirl Burner." Journal of Engineering for Gas Turbines and Power **Volume 125**(Issue 3).

Michael Sandford, W. S., Sanjay Joshi. (2011). "Experimental Comparison of Measured Flow Output of Aquarium Propeller Pumps."

Opsvik, H. E. Z. (2010). Experimental inverstigation of the dritical dimensions, and the effect of damages, on flame gap on explosion safe equipment. Master of Science, University of Bergen.

Petroleum Safety Authority Norway, P. (2010). "Trends in Risk Level in the Petroleum Activity." 18.

Phillips, H. (1971). "The Mechanism of Flameproof Protection." SMRE Research Report 275.

Picotech. (2002). "Thermocouples - A Quick Guide." from http://www.azom.com/article.aspx?ArticleID=1208.

R.Stahl. (2007). "The basis of explosion protection." from http://www.stahl.de/fileadmin/Dateien/explosionsschutz/pdf/grundlagen_en.pdf.

Redeker, T. (1981). Classification of flammable gases and vapours by the flameproof safe gap and the incendivity of electrical sparks.

Safety-Instruction. (2010). "Combustible Dust." from http://safetyinstruction.blogspot.com/2010/08/combustible-dust.html.

Sara McAllister, J.-Y. C., A. Carlos Fernandez-Pello (2011). Fundamentals of Combustion Processes. New York, Springer.

Solheim, F. (2010). An Experimental Investigation of the Influence of Mechanical Damage, Rust and Dust on the Ability of Flame Gaps to Prevent Gas Explosion Transmission. Master of Science, University of Bergen.

Steiner, M. W. (2012). An Experimental Investigation of the Effect of Rust and Mechanical Damage on the Ability of Maximum Experimental Safe Gap to Prevent Gas Explosion Transmission. Master of Science, University of Bergen.

Valve, V.-M. (2007). "Surge Control in Pumping Station." Pump and Pump System Glossary, from http://www.lightmypump.com/pump_glossary.htm.

Vinnem, J.-E. (2006). "On the Analysis of Operational Barriers on Offshore Petroleum Installations."

Warren L. McCabe, J. C. S., Peter Harriott (2005). Unit Operations of Chemical Engineering. New York, McGraw Hill.

Appendix

Appendix A – Calculation of stoichiometric ratio

Calculations based on formulas from (J. Warnatz 2006).

Stoichiometric:

$$2\ H_2 + 0.5\ (O_2 + 79/21\ N_2) \rightarrow 2\ H_2O + 0.5 \cdot 79/21\ N_2$$

2 mol H_2 reacts with 0.5 mol air (O_2 + 79/21 N_2) to form 2 mol H_2O and 3.762 mol N_2.

The mole fraction of the fuel in a stoichiometric mixture with air can then be calculated from the formula:

$$X_{fuel,\ stoichiometric} = 1/(1+v \cdot 4.762)$$

The mole fraction of H_2 can then be calculated:

$$X_{H2,\ stoich} = 1/(1+0.5 \cdot 4.762) = 0.296$$

The stoichiometric ratio of hydrogen in air is 29.6 %.

The percentage of air at stoichiometric ratio is then 100 % - 29.6 % = 70.4 %

If the percentage of oxygen in air is assumed to be 21, there will be 70.4 % · 0.21 = 14.78

The assumed amount of oxygen at stoichiometric ratio is therefore ≈ 14.8 %

Appendix B – Experimental apparatus and procedure

B-1 Equipment data

Table I : *Equipment list.*

Equipment	Type
Gas analyzer	Servomex 4200 Industrial Gas Analyzer
Test gas	Hydrogen quality 5.0 (99.999%)
Computer	Dell Latitude D630
DAQ	NI USB 6009
Pressure transducer	Kistler 701A
Charge amplifier	5015A0000
Spark generator	Tailor made
Thermocouples	Tailor made (see Appendix C-2)
Experimental apparatus	Plane Rectangular Slit Apparatus

B-2 Experimental procedure – The Plane Rectangular Slit Apparatus

B-2.1 Adjusting procedure for the flame gap opening in the PRSA

This part based on (Grov 2010)'s section A 2.4.

1. Remove the external chamber, by turning the whole chamber counter clockwise.

2. Remove the top of the primary chamber where the flame gap opening is located.

3. **Option 1**, if shims are available:

   Locate the distance shims in both sides through the gap, see Figure I, and make sure that the distance shims penetrate all the way through the gap to ensure a uniform opening.

   Option 2, if distance bits have to be cut out by hand:

   Open all screws and remove the flame gap opening. Disassemble the flame gap opening, place the distance bits all the way from the top to the bottom to achieve a uniform opening, and mount the flame gap opening back together.

4. Fasten the two screws in the top of the gap, shown in Figure II, with a torque of 20 cNm.

5. Fasten the four screws on the side of the gap, see Figure III and Figure IV, with a torque of 20 cNm.

6. Fasten the six screws on the bottom of the gap with a torque of 1 Nm, see Figure III.

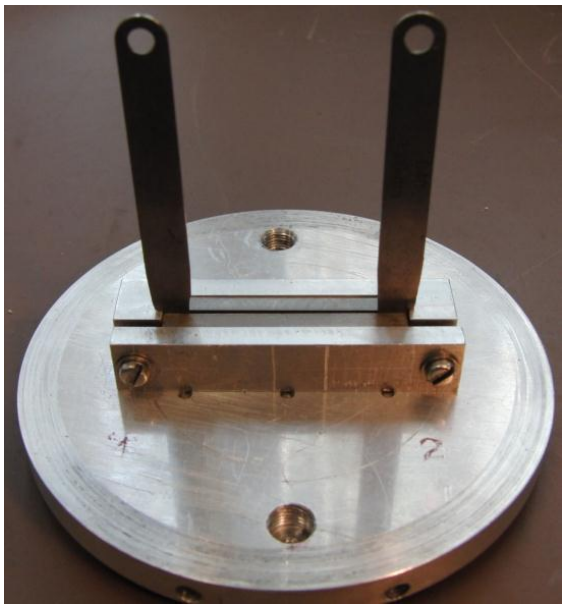

Figure I : *The picture shows the upper part of the flame gap in the PRSA. Distance bits are placed in the flame gap, and the two screws seen in the picture are fastened with a torque of 20 cNm.*

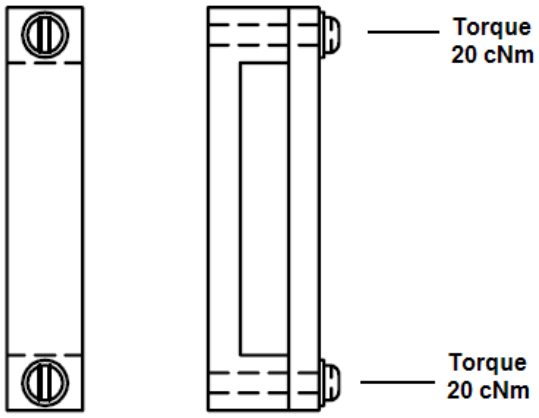

Figure II : *A drawing of the clamp around the upper part of the flame gap. The clamp is installed to achieve a uniform flame gap opening. The two screws are fastened with a torque of 20 cNm.*

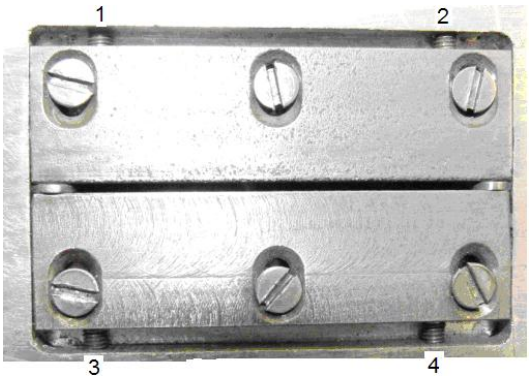

Figure III : *A picture of the bottom part of the flame gap in the PRSA. This part is placed inside the primary chamber. The numbers 1-4 illustrates screws that are tightened with a torque of 20 cNm, which is the same torque as the upper part of the flame gap is tightened with. The distance bits can be seen on each side of tha gap opening.*

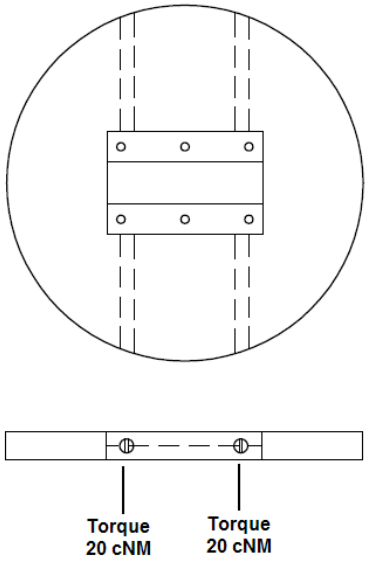

Figure IV : *A drawing of the bottom of the flame gap. This side is facing down towards the primary chamber. It can be seen where the screws that clamp the gap together are located.*

B-2.2 Experimental procedure on the Plane Rectangular Slit Apparatus (PRSA)

Based on (Grov 2010)'s section A 2.5.

The reference values in the procedure, with respect to flow, are based on experiences with a gas concentration of 29.6 % hydrogen.

With reference to the schematic in Figure V, the following steps have to be accomplished:

1. Attach the plastic foil on top of the apparatus.
2. Turn on the spark generator.
3. Open valves 1, 2, 4, and 5 on the plane rectangular slit apparatus
4. Open the valve for air supply. Air pressure set to 1 barg.
5. Start the gas analyzer pump.
6. Turn the valve on the gas analyzer to "til apparatur".
7. Adjust the air and gas flow to 1.50 nl/min and 0.80 nl/min respectively.
8. Wait till the gas concentration reaches the stoichiometric ratio, which means when the gas analyzer shows 14.78 % O_2. Adjust the air flow if the right concentration is not achieved.
9. Turn off the gas analyzer pump.
10. Close valves 1, 2, 4, and 5 on the plane rectangular slit apparatus.
11. Turn the valve on the gas analyzer to "til avtrekk" and turn the hydrogen flow to zero to avoid waste of gas.
12. Turn on the fan in the exhaust cupboard and secure the area.
13. Wear ear protection.
14. Activate the Labview program.
15. Save the given measurements from Labview.
16. Flush with air from valve 3 prior to new experiments.

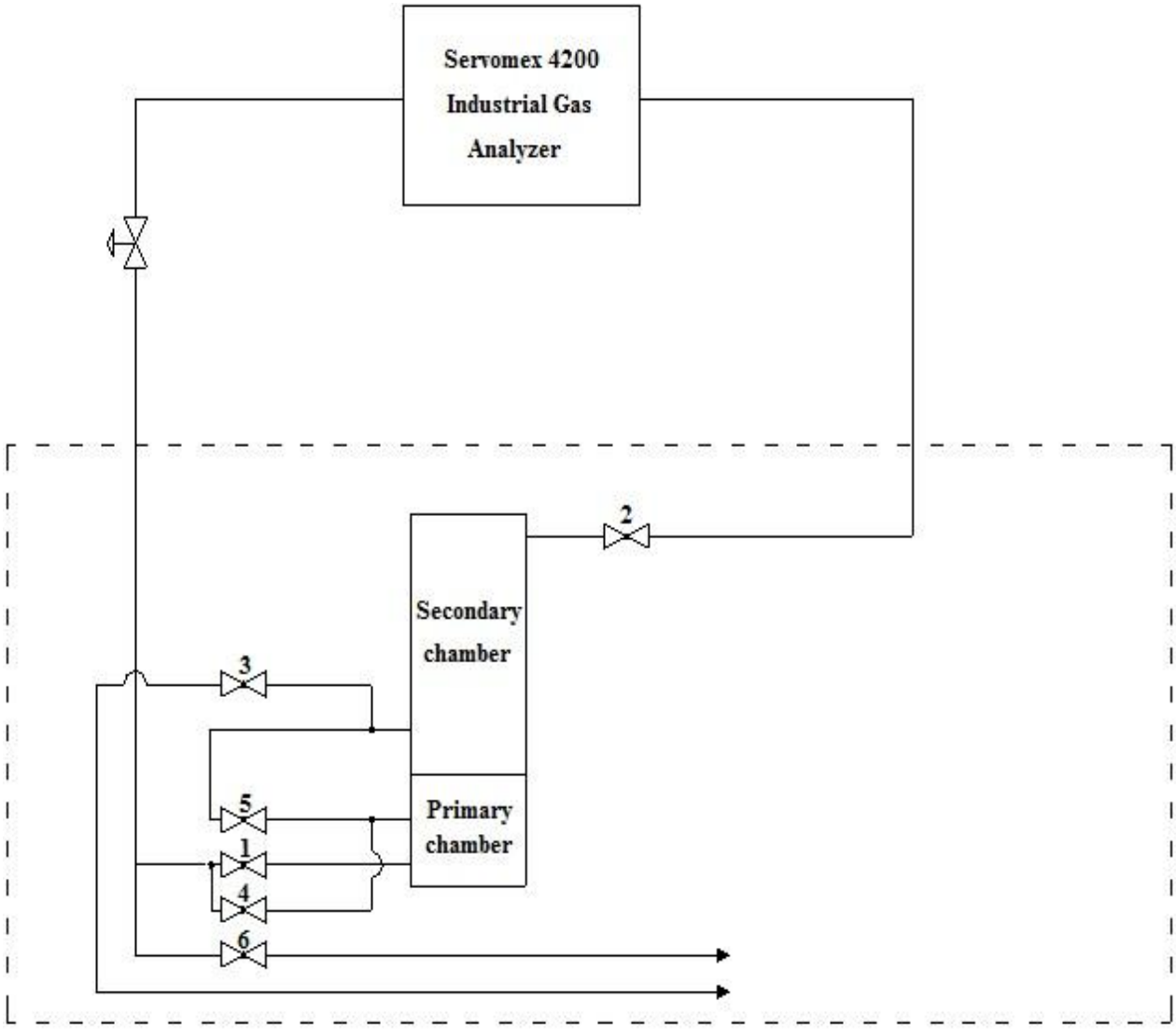

Figure V : *Schematic illustration of the Plane Rectangular Slit Apparatus.*

B-2.3 Checklist

From (Opsvik 2010).

Table II shows a checklist for the experiments performed in the PRSA. This checklist is created as a helping tool for remembering the most important steps in terms of safety and measurements when performing the experiments.

Table II : *Checklist of the procedure for experiments in the experimental apparatus PRSA.*

What to check	√
Spark generator on	
Data acquisition system is turned on	
Valves in correct position	
Secure area	
Ear protection	
Activate experiment	
Measurement data saved with a proper filename and location	
Check test area after secondary explosions	

B-2.4 Calibration procedure

Based on (Henden 2011)'s Appendix A.

Before the gas analyzer could be used, it had to be calibrated for oxygen. A certain procedure had to be followed before the analyzer was ready to be calibrated. The display mode must be "measure", and you have to press the following buttons quickly: "enter", "quit", "right arrow", "measure", "arrow up", "menu". Then the password 1812 has to be entered, and the gas analyzer is ready to be calibrated. It is important to remember to turn the pump on before calibrating. Turn the first arrow to "to exhaust fan", the second arrow to "mixed test gas", and the third arrow to "to HC analysis". The inlets for air and HC gases have to be closed, and the bottom left arrow has to be turned to "calibrations gas in".

To calibrate for 0 percent oxygen, 99.999% hydrogen is added through the opening marked "calibration gas inlet". The percentage number of oxygen is chosen in the calibration gas, and the value chosen is shown in the display next to the value found by the gas analyzer. When the analyzed value is stabilized, we have the difference between the analyzed value and the value used in own calculations. The enter button is then pressed, and the analyzer calibrates itself. It will now show 0 percent oxygen when no oxygen is present.

To calibrate for high level of oxygen, air was being used. The gas analyzer vendor approved this and stated that air would provide an accurate enough value for calibration. The percentage of oxygen in air was assumed to be 20.95%, and the gas analyzer was calibrated to this value.

B-2.5 Data acquisition system

Based on Opsvik.

Two programs were made in Labview, one for pressure and another for temperature, in order to store the measurements data taken from all the experiments. Figure VI shows the front panel of LabView, where you choose which program to use. Figure VII and Figure VIII show, respectively, measurement controllers of pressure and temperature measurements. In the block diagram, input/output-channel settings can be chosen by the use of the data acquisition (DAQ) assistants. To activate the experiments, press the arrow buttons that are marked with a red circle around them in the figures. After every experiment it is important that the measurements are being stored and that they have a valid file name, for example .txt.

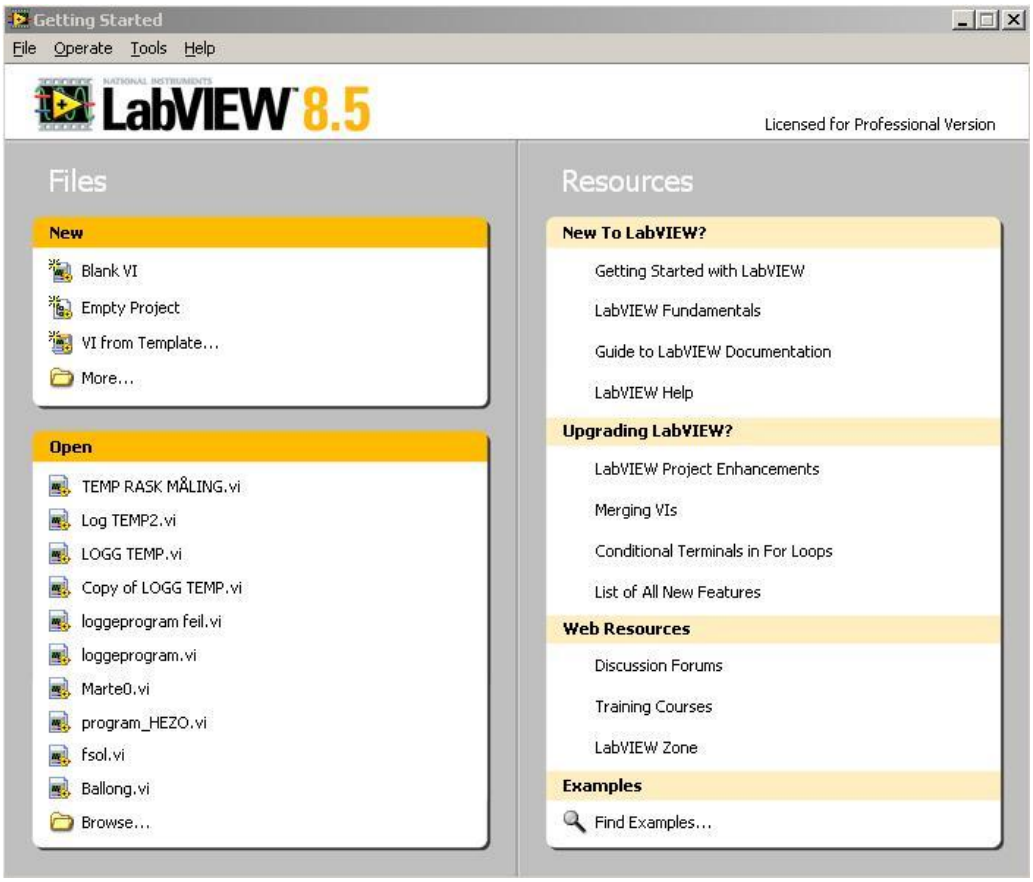

Figure VI : *LabView front panel.*

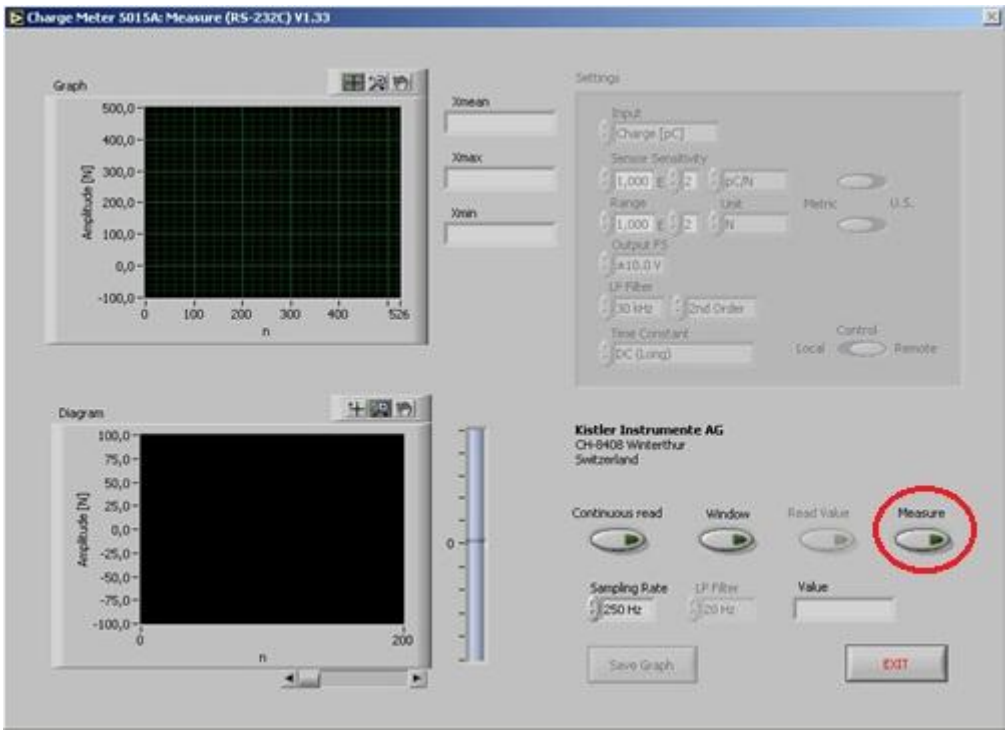

Figure VII : *Control panel for pressure measurements.*

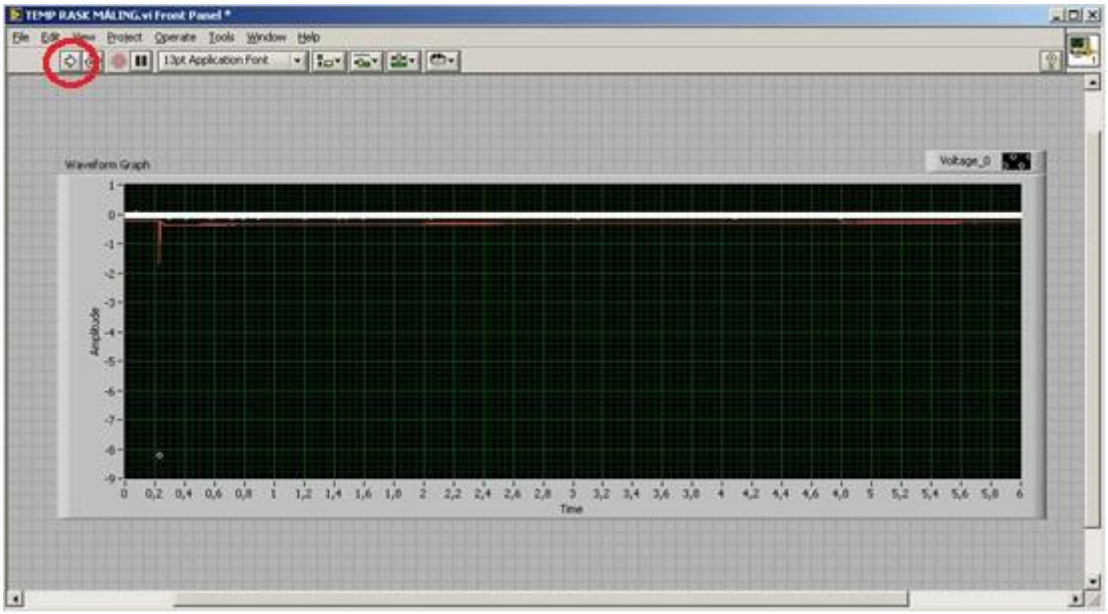

Figure VIII : *Control panel for temperature measurements.*

Appendix C – Experimental equipment

C-1 Gas analyzer

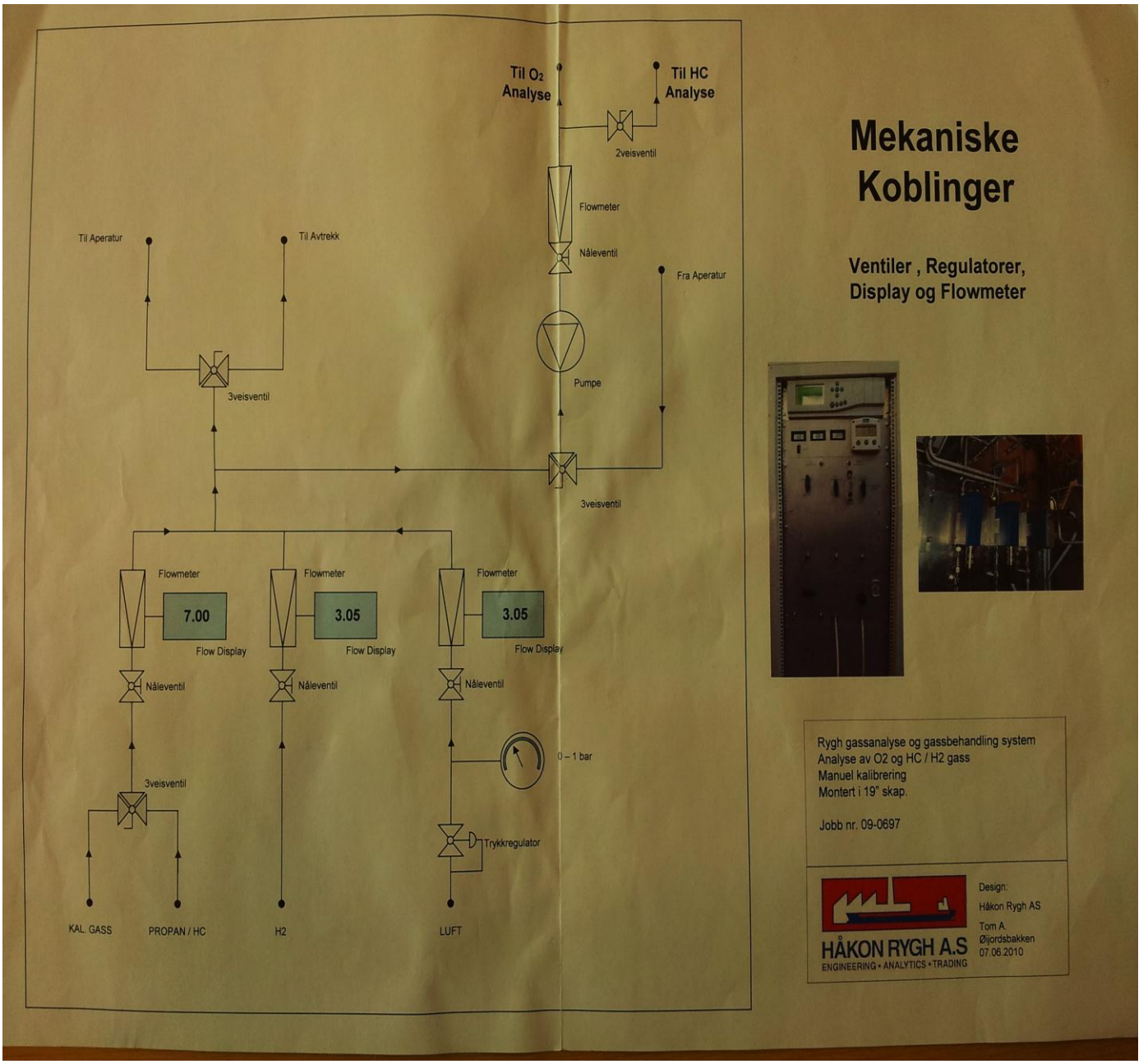

C-2 Thermocouples

Based on (Kalvatn 2009).

A thermocouple consists of a junction of two different metals. The junction creates a small voltage that increases with temperature. There is a variety of different thermocouples and they are classified by which materials the junction is made of. The most common type of thermocouples are type *k*, which is used in this project. The two materials used are Nickel-Chromium and Nickel-Aluminum. (Picotech 2002) states that ts temperature range is from -200 °C to +1200 °C, and its sensitivity is approximately 41 μV/°C with an accuracy of about ± 2.5 °C. The thicknesses of the metal wires are 0.3 mm. As shown in Figure IX, the use of thermocouples can be easy using only a voltmeter.

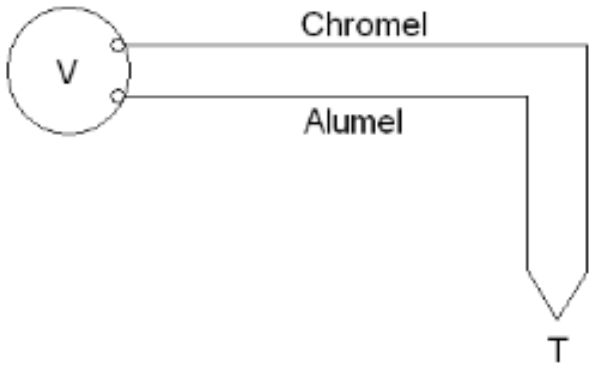

Figure IX : *Schematic of temperature measurement using a voltmeter and a thermocouple. From (Kalvatn 2009).*

Appendix D – Measurements data from experiments

D-1 Data from finding the most favorable hydrogen concentration

Concentration O2:	15,0
Concentration H2:	28,6
Gap opening, Y_i [mm]:	0.31
Mean pressure [barg]:	2,529
P_{max} [barg]	**Re-ignition**
2,549	no
2,529	no
2,527	no
2,496	no
2,561	no
2,515	no
2,522	no
2,519	no
2,536	no
2,537	no

Concentration O2 [%]:	14,8
Concentration H2[%]:	29,6
Gap opening, Y_i [mm]:	0.31
Mean pressure [barg]:	2,485
P_{max} [barg]	**Re-ignition**
2,524	yes
2,539	no
2,500	no
2,479	yes
2,491	yes
2,455	no
2,471	yes
2,478	yes
2,457	no
2,459	yes

Concentration O2:	14,6
Concentration H2:	30,5
Gap opening, Y_i [mm]:	0.31
Mean pressure [barg]:	2,440
P_{max} [barg]	**Re-ignition**
2,434	yes

2,416	yes
2,465	yes
2,434	yes
2,437	yes
2,430	yes
2,444	yes
2,437	yes
2,445	yes
2,458	yes

Concentration O2:	14,4
Concentration H2:	31,4
Gap opening, Y_i [mm]:	0.31
Mean pressure [barg]:	2,438
P_{max} [barg]	**Re-ignition**
2,429	yes
2,431	yes
2,439	yes
2,456	no
2,434	yes
2,428	yes
2,451	no
2,435	yes
2,447	no
2,427	yes

Concentration O2:	14,2
Concentration H2:	32,4
Gap opening, Y_i [mm]:	0.31
Mean pressure [barg]:	2,441
P_{max} [barg]	**Re-ignition**
2,438	no
2,426	no
2,439	no
2,465	no
2,448	no
2,437	no
2,397	no
2,488	no
2,435	no
2,433	no

D-2 Data from finding the most favorable ignition point for re-ignition through undamaged slit

Surface configuration:	undamaged		
Mean pressure [barg]:	2,465		
Gap opening, Y_i [mm]	**Z_i [mm]**	**P_{max} [barg]**	**Re-ignition**
0.30	5	2,428	no
0.30	5	2,573	yes
0.30	5	2,477	no
0.30	5	2,479	no
0.30	5	2,447	no
0.30	5	2,495	no
0.30	5	2,463	no
0.30	5	2,417	no
0.30	5	2,431	no
0.30	5	2,441	no

Surface configuration:	undamaged		
Mean pressure [barg]:	2,469		
Gap opening, Y_i [mm]	**Z_i [mm]**	**P_{max} [barg]**	**Re-ignition**
0.30	10	2,470	no
0.30	10	2,470	no
0.30	10	2,539	yes
0.30	10	2,447	no
0.30	10	2,455	yes
0.30	10	2,385	no
0.30	10	2,503	no
0.30	10	2,535	no
0.30	10	2,444	no
0.30	10	2,446	no

Surface configuration:	undamaged		
Mean pressure [barg]:	2,432		
Gap opening, Y_i [mm]	**Z_i [mm]**	**P_{max} [barg]**	**Re-ignition**
0.30	15	2,429	no
0.30	15	2,435	yes
0.30	15	2,419	yes
0.30	15	2,430	yes
0.30	15	2,423	no
0.30	15	2,434	no
0.30	15	2,451	yes
0.30	15	2,435	yes
0.30	15	2,432	no
0.30	15	2,436	yes

Surface configuration:	undamaged		
Mean pressure [barg]:	2,508		
Gap opening, Y_i [mm]	Z_i [mm]	P_{max} [barg]	Re-ignition
0.30	20	2,516	yes
0.30	20	2,499	yes
0.30	20	2,497	yes
0.30	20	2,536	yes
0.30	20	2,520	yes
0.30	20	2,522	yes
0.30	20	2,489	yes
0.30	20	2,513	yes
0.30	20	2,476	no
0.30	20	2,510	yes

Surface configuration:	undamaged		
Mean pressure:	2,575		
Gap opening, Y_i [mm]	Z_i [mm]	P_{max} [barg]	Re-ignition
0.30	25	2,609	yes
0.30	25	2,589	yes
0.30	25	2,546	no
0.30	25	2,579	no
0.30	25	2,559	yes
0.30	25	2,604	no
0.30	25	2,612	yes
0.30	25	2,533	yes
0.30	25	2,518	no
0.30	25	2,596	no

D-3 Data from rusted flame gap surfaces

One month

Surface configuration:	B4		
MESG	0.30		
Mean pressure [barg]	2,574		
Explosion number	Z_i [mm]	P_{max} [barg]	Re-ignition
1	20	2,615	no
2	20	2,551	no
3	20	2,579	no
4	20	2,574	no
5	20	2,562	no
6	20	2,615	no
7	20	2,525	no

8	20	2,602	no
9	20	2,569	no
10	20	2,551	no

Surface configuration:	B5
MESG	0.29
Mean pressure [barg]	2,491

Explosion number	Z_i [mm]	P_{max} [barg]	Re-ignition
1	20	2,581	no
2	20	2,515	no
3	20	2,498	no
4	20	2,49	no
5	20	2,487	no
6	20	2,47	no
7	20	2,458	no
8	20	2,466	no
9	20	2,462	no
10	20	2,478	no

Surface configuration:	B6
MESG	0.28
Mean pressure [barg]	2,389

Explosion number	Z_i [mm]	P_{max} [barg]	Re-ignition
1	20	2,486	no
2	20	2,431	no
3	20	2,46	no
4	20	2,394	no
5	20	2,411	no
6	20	2,357	no
7	20	2,395	no
8	20	2,329	no
9	20	2,316	no
10	20	2,31	no

Surface configuration:	B8
MESG	0.29
Mean pressure [barg]	2,434

Explosion number	Z_i [mm]	P_{max} [barg]	Re-ignition
1	20	2,725	no
2	20	2,451	no
3	20	2,485	no
4	20	2,394	no
5	20	2,534	no
6	20	2,244	no
7	20	2,144	no

8	20	2,475	no
9	20	2,476	no
10	20	2,407	no

Surface configuration:	5		
MESG	0.25		
Mean pressure [barg]	2,370		
Explosion number	**Z_i [mm]**	**P_{max} [barg]**	**Re-ignition**
1	20	2,76	no
2	20	2,311	no
3	20	2,297	no
4	20	2,372	no
5	20	2,323	no
6	20	2,288	no
7	20	2,337	no
8	20	2,341	no
9	20	2,296	no
10	20	2,372	no

Surface configuration:	7		
MESG	0.35		
Mean pressure [barg]	2,334		
Explosion number	**Z_i [mm]**	**P_{max} [barg]**	**Re-ignition**
1	20	2,66	no
2	20	2,548	no
3	20	2,368	no
4	20	2,162	no
5	20	2,116	no
6	20	2,125	no
7	20	2,047	yes
8	20	2,446	yes
9	20	2,44	yes
10	20	2,423	yes

Two months

Surface configuration:	B1		
MESG	0.29		
Mean pressure [barg]	2,683		
Explosion number	**Z_i [mm]**	**P_{max} [barg]**	**Re-ignition**
1	20	2,872	no
2	20	2,592	no
3	20	2,52	no
4	20	2,486	no

5	20	2,435	no
6	20	2,774	no
7	20	2,789	no
8	20	2,836	no
9	20	2,777	no
10	20	2,752	no

Surface configuration:	B2		
MESG	0.30		
Mean pressure [barg]	2,905		
Explosion number	**Z_i [mm]**	**P_{max} [barg]**	**Re-ignition**
1	20	2,921	no
2	20	2,891	no
3	20	2,928	no
4	20	2,909	no
5	20	2,899	no
6	20	2,844	no
7	20	2,926	no
8	20	2,917	no
9	20	2,92	no
10	20	2,897	no

Surface configuration:	B3		
MESG	0.29		
Mean pressure [barg]	2,749		
Explosion number	**Z_i [mm]**	**P_{max} [barg]**	**Re-ignition**
1	20	2,794	no
2	20	2,761	no
3	20	2,773	no
4	20	2,788	no
5	20	2,714	no
6	20	2,739	no
7	20	2,741	no
8	20	2,718	no
9	20	2,725	no
10	20	2,734	no

Surface configuration:	B7		
MESG	0.30		
Mean pressure [barg]	2,865		
Explosion number	**Z_i [mm]**	**P_{max} [barg]**	**Re-ignition**
1	20	2,947	no
2	20	2,876	no
3	20	2,85	no

4	20	2,837	no
5	20	2,882	no
6	20	2,886	no
7	20	2,847	no
8	20	2,863	no
9	20	2,844	no
10	20	2,815	no

Surface configuration:	3		
MESG	0.25		
Mean pressure [barg]	2,926		
Explosion number	**Z_i [mm]**	**P_{max} [barg]**	**Re-ignition**
1	20	2,956	no
2	20	2,917	no
3	20	2,934	no
4	20	2,88	no
5	20	2,938	no
6	20	2,926	no
7	20	2,907	no
8	20	2,923	no
9	20	2,937	no
10	20	2,941	no

Surface configuration:	9		
MESG	0.35		
Mean pressure [barg]	2,773		
Explosion number	**Z_i [mm]**	**P_{max} [barg]**	**Re-ignition**
1	20	2,828	no
2	20	2,773	no
3	20	2,834	no
4	20	2,807	no
5	20	2,782	no
6	20	2,757	no
7	20	2,778	no
8	20	2,725	no
9	20	2,703	no
10	20	2,746	no

D-4 Data from finding the most favorable ignition point for re-ignitions through slits with multiple crosswise grooves

Surface configuration:	PH-7.2.3		
Mean pressure [barg]:	2,596		
Gap opening, Y_i [mm]	**Z_i [mm]**	**P_{max} [barg]**	**Re-ignition**
0.35	5	2,651	No
0.35	5	2,612	No
0.35	5	2,594	No
0.35	5	2,593	No
0.35	5	2,68	No
0.35	5	2,62	No
0.35	5	2,654	No
0.35	5	2,672	No
0.35	5	2,536	No
0.35	5	2,348	No

Surface configuration:	PH-7.2.3		
Mean pressure [barg]:	2,224		
Gap opening, Y_i [mm]	**Z_i [mm]**	**P_{max} [barg]**	**Re-ignition**
0.35	10	2,468	No
0.35	10	2,039	No
0.35	10	2,301	No
0.35	10	1,988	No
0.35	10	2,551	No
0.35	10	2,06	No
0.35	10	2,678	Yes
0.35	10	1,975	No
0.35	10	2,345	No
0.35	10	1,837	No

Surface configuration:	PH-7.2.3		
Mean pressure [barg]:	2,400		
Gap opening, Y_i [mm]	**Z_i [mm]**	**P_{max} [barg]**	**Re-ignition**
0.35	15	2,338	No
0.35	15	2,087	No
0.35	15	2,293	No
0.35	15	2,795	Yes
0.35	15	2,543	No
0.35	15	2,878	Yes
0.35	15	2,144	No
0.35	15	2,195	No
0.35	15	2,357	No
0.35	15	2,369	No

Surface configuration:	PH-7.2.3		
Mean pressure [barg]:	2,643		
Gap opening, Y_i [mm]	**Z_i [mm]**	**P_{max} [barg]**	**Re-ignition**
0.35	20	2,596	Yes
0.35	20	2,813	Yes
0.35	20	2,543	No
0.35	20	2,439	No
0.35	20	2,866	Yes
0.35	20	2,44	No
0.35	20	2,814	Yes
0.35	20	2,788	Yes
0.35	20	2,431	No
0.35	20	2,697	Yes

Surface configuration:	PH-7.2.3		
Mean pressure [barg]:	2,384		
Gap opening, Y_i [mm]	**Z_i [mm]**	**P_{max} [barg]**	**Re-ignition**
0.35	25	2,207	No
0.35	25	2,53	No
0.35	25	2,806	Yes
0.35	25	1,769	No
0.35	25	2,724	Yes
0.35	25	2,43	No
0.35	25	2,256	No
0.35	25	2,508	No
0.35	25	2,397	No
0.35	25	2,213	No

D-5 Data from finding MESG values of slits with multiple crosswise grooves

Surface configuration:	PH-7.2.3		
MESG [mm]	0.33		
Mean pressure [barg]	2,492		
Gap opening, Y_i [mm]	**Z_i [mm]**	**P_{max} [barg]**	**Re-ignition**
0.35	20	2,694	yes
0.34	20	2,323	no
0.34	20	2,319	no
0.34	20	2,402	yes
0.33	20	2,455	no
0.33	20	2,526	no
0.33	20	2,54	no
0.33	20	2,414	no
0.33	20	2,501	no
0.33	20	2,409	no
0.33	20	2,487	no
0.33	20	2,541	no
0.33	20	2,53	no
0.33	20	2,516	no

Surface configuration:	PH-7.1.3		
MESG [mm]	0.50		
Mean pressure [barg]	2,516		
Gap opening, Y_i [mm]	**Z_i [mm]**	**P_{max} [barg]**	**Re-ignition**
0.35	20	2,434	no
0.35	20	2,399	no
0.35	20	2,253	no
0.36	20	2,443	no
0.37	20	2,487	no
0.37	20	2,434	no
0.37	20	2,327	no
0.38	20	2,393	no
0.38	20	2,393	no
0.40	20	2,269	no
0.40	20	2,131	no
0.40	20	2,145	no
0.40	20	2,255	no
0.45	20	2,614	no
0.60	20	2,383	yes
0.55	20	2,253	yes
0.50	20	2,527	no
0.50	20	2,499	no
0.50	20	2,530	no
0.50	20	2,511	no
0.50	20	2,538	no

0.50	20	2,548	no
0.50	20	2,449	no
0.50	20	2,523	no
0.50	20	2,517	no
0.50	20	2,514	no

Surface configuration:	PH-7.2.2
MESG [mm]	0.32
Mean pressure [barg]	2,546

Gap opening, Y_i [mm]	**Z_i [mm]**	**P_{max} [barg]**	**Re-ignition**
0.35	20	2,462	no
0.38	20	2,438	yes
0.37	20	2,417	yes
0.36	20	2,471	yes
0.35	20	2,563	yes
0.34	20	2,559	yes
0.33	20	2,755	yes
0.32	20	2,564	no
0.32	20	2,551	no
0.32	20	2,546	no
0.32	20	2,539	no
0.32	20	2,498	no
0.32	20	2,531	no
0.32	20	2,574	no
0.32	20	2,511	no
0.32	20	2,601	no
0.32	20	2,542	No

Surface configuration:	PH-7.2.1
MESG [mm]	0.33
Mean pressure [barg]	2,234

Gap opening, Y_i [mm]	**Z_i [mm]**	**P_{max} [barg]**	**Re-ignition**
0.33	20	1,361	no
0.34	20	2,707	yes
0.33	20	2,102	no
0.33	20	2,231	no
0.33	20	2,184	no
0.33	20	2,117	no
0.33	20	2,466	no
0.33	20	2,339	no
0.33	20	2,034	no
0.33	20	2,166	no
0.33	20	2,223	no
0.33	20	2,482	no

Surface configuration:	PH-7.2.0,5		
MESG [mm]	0.34		
Mean pressure [barg]	2,622		
Gap opening, Y_i [mm]	**Z_i [mm]**	**P_{max} [barg]**	**Re-ignition**
0.33	20	2,352	no
0.34	20	2,644	no
0.34	20	2,454	no
0.35	20	2,422	no
0.36	20	2,51	no
0.37	20	2,593	no
0.38	20	2,429	no
0.40	20	2,511	no
0.40	20	2,474	no
0.45	20	2,426	no
0.45	20	2,291	no
0.50	20	2,289	no
0.55	20	2,552	yes
0.50	20	2,641	yes
0.40	20	2,662	yes
0.34	20	2,683	no
0.35	20	2,765	yes
0.34	20	2,667	no
0.34	20	2,569	no
0.34	20	2,641	no
0.34	20	2,613	no
0.34	20	2,588	no
0.34	20	2,545	no
0.34	20	2,649	no
0.34	20	2,683	no
0.34	20	2,596	no
0.34	20	2,664	no

Appendix E – Certificates

E-1 Charge amplifier

KISTLER
measure. analyze. innovate.

Kalibrierschein Ladung
Calibration Certificate Charge

Type **5015A0000** Serial No. **1683268**

Kalibriert durch Calibrated by		Datum Date
R. Büchele		19.05.2008
Referenzgeräte Reference Equipment	**Typ** Type	**Serien-Nr.** Serial-No.
Ladungskalibrator Charge Calibrator	5395A1	530626
Umgebungstemperatur Ambient Temperature °C		**Relative Feuchte** Relative Humidity %
24		40

Geräteeinstellungen
Instrument settings

HP Filter HP Filter	LP Filter LP Filter kHz	Ausgangsbereich FS Output Range FS V
DC (Long)	1,0	10

Messergebnisse Results of Measurement

Nullpunktabweichung ohne Filter Offset Voltage Filter off mV	Nullpunktabweichung mit Filter Offset Voltage Filter on mV	Measure Sprung Measure Jump mV	Drift Drift pC/s; mV/s
0,8	0,7	-0,1	0,00

Filter 30 kHz; obere Grenzfrequenz (-3 dB) Filter 30 kHz; upper cutoff frequency (-3 dB) kHz	Obere Grenzfrequenz bei voller Bandbreite (-3 dB) Upper cutoff frequency at full bandwidth (-3 dB) kHz
30,2	196

Bereichseinstellung Range setting pC	Eingangs-Ladung Input charge pC	Abweichung Spannungsausgang Voltage output error %	Abweichung Anzeige Readout error %
4,990	-4,990	-0,1	-0,1
9,990	-9,990	-0,1	-0,1
49,90	-49,90	0,0	0,0
99,90	-99,90	0,0	0,0
499,0	-499,0	0,0	0,0
999,0	-999,0	0,0	0,0
4'990	-4'990	0,0	0,0
9'990	-9'990	0,0	0,0
49'900	-49'900	0,0	0,0
99'900	-99'900	0,0	0,0
219'900	-219'900	0,0	0,0
1'099'000	-1'099'000	0,0	0,0
2'000'000	-2'000'000	0,0	0,0

Bestätigung Confirmation

Wir bestätigen, dass das oben identifizierte Gerät nach den vorgeschriebenen Verfahren geprüft wurde. Alle Messmittel sind auf nationale Normale rückverfolgbar. Kistler betreibt die SCS (Swiss Calibration Service) Kalibrierstelle Nr. 049, akkreditiert nach ISO 17025. Das Kistler Qualitätsmanagement System ist nach ISO 9001 zertifiziert.

We confirm that the device identified above was tested by the prescribed proppdures. All measuring devices are traceable to national standards. the SCS (Swiss Calibration Service) Calibration Laboratory No. 049 is operated by Kistler and accredited per ISO 17025. The Kistler Quality Management System is certified per ISO 9001.

Kistler Instrumente AG
Eulachstrasse 22
PO Box
CH-8408 Winterthur
Tel. +41 52 224 11 11
Fax +41 52 224 14 14
info@kistler.com
ZKB Winterthur 8C 732
Swift: ZKBKCHZZ80A
Account: 1132-0374.628
IBAN: CH67 0070 0113 2003 7462 8
VAT: 229 713
ISO 9001 certified
www.kistler.com

E-2 Pressure transducers

KISTLER
measure. analyze. innovate.

Kalibrierschein DRUCK
Calibration Certificate PRESSURE

Type **701A** Serial No. **1740583**

Kalibriert durch Calibrated by	Datum Date
U. Köhler	20.10.2008

Referenzgeräte Reference Equipment	Typ Type	Serien-Nr. Serial No.
Gebrauchsnormal Working Standard	Kistler 7005-350	634580
Ladungsverstärker Charge Amplifier	Kistler 5011A Kistler 5011A	572386 572385
Ladungskalibrator Charge Calibrator	Kistler 5395A	530633

Umgebungstemperatur Ambient Temperature °C	Relative Feuchte Relative Humidity %
23	41

Messergebnisse Results of Measurement

Kalibrierter Bereich Calibrated Range bar	Empfindlichkeit Sensitivity pC / bar	Linearität Linearity ≤ ± %FSO
0 ... 250	-80,60	0,11
0 ... 25	-79,49	0,04
0 ... 2,5	-79,22	0,04

Messverfahren Measurement Procedure: **Kontinuierliche Kalibrierung, Vergleichsverfahren** Continuous Calibration, Comparison Method

Bestätigung Confirmation

Die Geräte halten die Herstelltoleranzen gemäss Spezifikationen der Datenblätter ein. Wir bestätigen, dass das oben identifizierte Gerät nach den vorgeschriebenen Verfahren geprüft wurde. Alle Messmittel sind auf nationale Normale rückverfolgbar. Kistler betreibt die SCS (Swiss Calibration Service) Kalibrierstelle Nr. 049, akkreditiert nach ISO 17025. Das Kistler Qualitätsmanagement System ist nach ISO 9001 zertifiziert.

The equipment meets the manufacturing tolerances according to the specification data sheets. We confirm that the device identified above was tested by the prescribed procedures. All measuring devices are traceable to national standards. The SCS (Swiss Calibration Service) Calibration Laboratory No. 049 is operated by Kistler and accredited per ISO 17025. The Kistler Quality Management System is certificied per ISO 9001.

Kistler Instrumente AG
Eulachstrasse 22
PO Box
CH-8408 Wintherthur
Tel. +41 52 224 11 11
Fax +41 52 224 14 14
info@kistler.com
ZKB Winterthur BC 732
Swift: ZKBKCHZZ80A
Account: 1132-0374.628
IBAN: CH67 0070 0113 2003 7462 8
VAT: 229 713
ISO 9001 certified
www.kistler.com